

NASA CR 108506

N70-34526

THE COMBLINE FILTER AND PHASE-LOCK LOOP,
A NEW TECHNIQUE TO IMPROVE
FM TELEVISION RECEPTION

TR-7322.03-40

May 1970

F. M. Stuber
M. Y. Huang

Prepared for
NASA Manned Spacecraft Center
Houston, Texas

Under
Contract No. NAS9-10204

TRW
SYSTEMS GROUP

ONE SPACE PARK • REDONDO BEACH, CALIFORNIA

REPRODUCED BY
NATIONAL TECHNICAL
INFORMATION SERVICE
U.S. DEPARTMENT OF COMMERCE
SPRINGFIELD, VA. 22161

121

Errata

- 1) Page 4-28, Fig. 4-20, curve 2: A measured point is missing at the lower end of curve 2: output = -8.5 dB/input = -18.5 dB.
- 2) Page 5-4: eq. 5-3 should read

$$H_2(s) = \frac{K}{1 - Ke^{-s\tau}} \quad (5-3)$$

Approved: R. P. Liccini
R. P. Liccini
Section Head
Telecommunication Department

Approved: E. D. Dunford
E. D. Dunford
Manager
Telecommunication Department

Approved: R. R. Trapp
R. R. Trapp
Manager
Communication and Defense
Electronics Department

CONTENTS

1.	INTRODUCTION AND SUMMARY	1-1
2.	THEORETICAL BACKGROUND	2-1
3.	COMBLINE FILTERS	3-1
3.1	Introduction	3-1
3.2	Digital Comblime Filters	3-1
3.3	Analog Comblime Filters	3-3
3.3.1	Delay Lines	3-3
3.3.2	Additive Comblime Filter	3-7
3.3.3	Additive Comblime Filters with External Feedback	3-11
3.3.4	Additive-Subtractive Comblime Filter	3-16
3.4	General Results and Discussion	3-24
3.4.1	Noise Performance	3-24
3.4.2	Comblime Filtered Video Signals	3-26
4.	COMBLIME PHASE-LOCK LOOP	4-1
4.1	Introduction	4-1
4.2	Upconversion	4-1
4.3	Basic PLL System	4-1
4.3.1	Description	4-1
4.3.2	Comblime Subloop	4-3
4.3.3	Stability Criteria	4-18
4.3.4	Low Pass Filter Subloop	4-20
4.3.5	Modulation Error and Gain Requirements	4-21
4.3.6	Experimental Results and Discussion	4-24
5.	IMPROVED COMBLIME PLL SYSTEMS	5-1
5.1	Low Frequency Modulation Error Reduction	5-1
5.1.1	Miscellaneous Methods	5-1
5.1.2	Preemphasis	5-2
5.2	Automatic Frequency Control	5-2
5.3	Predistortion and Postdetection Filtering	5-3
APPENDIX A.	ANALYSIS AND CHARACTERISTICS OF THE DIGITAL FILTER	A-1
APPENDIX B.	COMPUTER PROGRAMS	B-1

ILLUSTRATIONS

1-1	Multiloop PLL with Comblin Filter Loop	1-4
2-1	Black and White Pattern	2-2
2-2	Measured Video Spectrum of Black and White Test	2-4
2-3	Diagonal Bar Spectrum in High Frequency Region Detail	2-5
2-4	Diagonal Bar Spectrum in Low Frequency Region Detail	2-5
2-5	Analysr Displays of 2 in. Black Bar Spectra (in the vicinity of 520 kHz)	2-7
2-6	Analysr Displays of 2 in. Black Bar Spectra (in the vicinity of 100 kHz)	2-9
2-7	Amplitude Spectrum of a Stationary TV Signal	2-11
3-1	Generalized Sampler Configuration (Four Single-Section RC Filters	3-2
3-2	Low Pass Response of 63.1 μ sec LC Network Delay Line	3-4
3-3	Low Pass Response of 63 μ sec Glass Delay Line	3-5
3-4	Frequency Response of 63 μ sec Delay Module	3-5
3-5	Combined Delay Lines Block Diagram	3-7
3-6	Additive Delay Line Comblin Filter	3-8
3-7	Comblin Filter Amplitude Characteristic	3-9
3-8	Comblin Filter Phase Characteristic	3-9
3-9	Comblin Peak Response and Valley Response vs K	3-10
3-10	Amplitude vs Normalized Frequency for 10 Harmonic of Comb Filter	3-12
3-11	Relative Comb Amplitudes of CLF Spectrum vs Frequency	3-12
3-12	Additive Comblin Filter with External Feedback	3-14
3-13	Amplitude Response of a CLF with External Feedback	3-15
3-14	Phase Response of a CLF with External Feedback	3-15
3-15	Subtractive Comblin Filter	3-18
3-16	Additive-Subtractive Comblin Filter	3-18
3-17	Amplitude Response vs Frequency for Additive-Subtractive Comb Filter	3-19
3-18	PVR vs K for Additive and Additive-Subtractive CLF	3-21
3-19	Amplitude vs Frequency for Additive-Subtractive with a Negative Feedback Loop	3-21
3-20	PVR vs G in PLL for Additive-Subtractive CLF	3-23
3-21	Square Wave Plus Noise Test	3-25
3-22	Square Wave Plus Noise on Monitor	3-27

ILLUSTRATIONS (Continued)

3-23	Horizontal and Vertical Bar Test	3-28
4-1	50 MHz to 235 MHz Upconverter Block Diagram	4-2
4-2	Upconverter Transfer Characteristics	4-2
4-3	Basic PLL System Block Diagram	4-3
4-4	Phase Equivalent Circuit of the Comblines Subloop	4-4
4-5	Amplitude vs Normalized Frequency for Fundamental of Comb Filter PLL	4-5
4-6	Amplitude vs Normalized Frequency for 100th Harmonic of Comb Filter PLL	4-5
4-7	Relative Amplitude of Combs in Phase-Lock Loop	4-6
4-8	Envelope 3-dB Bandwidth vs G in Phase-Lock Loop	4-8
4-9	Half Width and Peak Shifts of Combs in Phase-Lock Loop vs Low Pass Cutoff Frequency	4-8
4-10	Half Widths and Peak Shifts of Combs in Phase-Lock Loop vs Comb Number	4-9
4-11	First Peak-to-Valley Ratio vs K in Phase-Lock Loop	4-9
4-12	Noise Bandwidth Reduction vs K, G	4-10
4-13a	Amplitude vs Time	4-11
4-13b	Amplitude vs Time for $n = 0$	4-16
4-13c	Response to Horizontal Half-White, Half-Black Picture (10 black lines followed by 10 white lines)	4-16
4-13d	Response to Vertical Half-White, Half-Black Picture	4-17
4-14a	$A_d(s)$	4-19
4-14b	$A_s(s)$	4-19
4-15	Low Pass Filter Subloop	4-20
4-16	Amplitude vs Frequency	4-22
4-17	Response of Comblines Phase-Lock Loop to Swept Modulator Input (Envelope 3 dB Cutoff at 723 kHz)	4-25
4-18	Expanded View of Figure 4-17 from 100 to 220 kHz (Peak-to-Valley Ratio at 100 kHz is 16 dB)	4-25
4-19	Expanded View of Figure 4-17 from 1 to 1.1 MHz (PVR at 1 MHz is 10 dB)	4-26
4-20	SNR of 95.11 kHz Signal vs Input CNR Narrowband, Additive Noise	4-28
5-1	Inverse Comblines Filter	5-3
5-2	Amplitude Response of Inverse Comblines Filter	5-4

1. INTRODUCTION AND SUMMARY

Under Contract No. NAS9-10204 with NASA MSC, TRW Systems performed a 6-month study on the use of "comblines" filters to improve television signal reception. The potential merits of using these filters for improving TV signal quality was based on previous theoretical work, which established that a television signal has a large portion of its energy at multiples of the line-scanning frequency with little energy in between; that is, that the energy spectrum is roughly analogous to the teeth of a comb. It was reasoned that, if a filter could be constructed consisting of passbands and stopbands congruent with the comb shape of the TV signal, the noise-filled empty space could be filtered out and the energy-filled portion passed through, with a subsequent improvement in the signal-to-noise ratio (SNR).

It was further reasoned that, if a combline filter were used as the filter in a phase-lock loop demodulator, the effective loop noise bandwidth would be reduced and the threshold would be improved. In other words, the loop would operate more efficiently and the demodulator would produce usable signals at input SNR several dB below that of a PLL demodulator without the combline filter.

The purpose of the program, therefore, was to study and implement combline filters, to analyze their effectiveness, to develop a combline filter phase-lock loop combination, and to test its merits in the laboratory. Various techniques to realize combline filters were investigated and extensive studies prompted implementations of an analog scheme that is based on a filter loop with delayed feedback. Experimental and analytical studies revealed and explained the effectiveness of these filters in rejecting noise between the TV signal bands. Furthermore, a PLL demodulator with the combline filter as the loop filter was built and analyzed extensively and the analysis indicated significant output SNR and threshold improvement. This was subsequently demonstrated experimentally for tone-modulated signals.

In more detail, the results of this program were as follows:

- 1) Both digital and analog type filters were investigated. It was determined that digital filters offered considerable flexibility for establishing the shape of the pass-

bands, but that the complexity and cost of implementing experimental models prohibited such an effort during this study. All further effort was concentrated on analog type filters.

2) Exhaustive analyses and computer studies were made on analog combline filter techniques to:

- Establish the best design for given delay line constraints
- Predict performance and dependence on the filter parameters for adjusting the filter response to a TV spectrum.

A tradeoff was predicted between the peak-to-valley ratio (ratio of passband response to stop-band response) and the filter bandwidth. The fundamental limits were determined to be the delay line response.

3) A study was made on delay techniques and available delay lines suitable for analog combline filters.

Among those investigated, passive LC delay lines provided the highest dynamic range, but were found to have limited bandwidth. Glass delay line modules appeared to be the most promising with limited but adequate dynamic range and sufficient bandwidth. A conceptual design was established to combine the advantages of LC and glass delay lines.

4) An analog combline filter was designed and bread-boarded. This filter was adjustable for a wide variety of response characteristics and was primarily intended as a baseband signal processor to:

- Confirm the analytical results
- Study the effect of combline filtering on various signals, in particular TV
- Establish qualitative verification of previous theoretical studies on TV signals.

- 5) The effectiveness of the combine filter in signal-to-noise ratio improvement was demonstrated. Some unexpected distortion problems on TV signals were discovered, but are explainable in terms of previous theoretical studies on TV spectra. Recommendations and conceptual circuit designs were made to overcome this problem.
- 6) A combine filter suitable for integration in a phase-lock loop was designed and implemented. A comprehensive study was made on the combine PLL to:
- Predict performance and parameter dependence
 - Establish stability criteria
 - Perform tradeoff studies for best designs and systems to be implemented or recommended.

It was found that high loop gain and high peak-to-valley ratio are incompatible. Thus, there is a tradeoff between loop noise and modulation error that can be optimized.

- 7) A multiloop PLL with a combine filter loop (Figure 1-1) was designed and implemented to:
- Demonstrate its feasibility as a demodulator of carriers modulated with TV and similar signals
 - Study and optimize loop parameters and components experimentally
 - Obtain experimental evidence of better threshold sensitivity and improved signal-to-noise ratio above threshold.

A threshold improvement of 16 dB and a signal-to-noise ratio improvement above threshold of 7 dB was experienced in the comparison of the

experimental combine PLL with a first-order PLL when measured for tone modulation and narrowband additive RF noise. The expected tracking problems were encountered for TV signals due to low loop gain requirements, but methods for improvement were conceived and implemented. In summary, it can be stated that, despite the problems encountered, a combine phase-lock loop was shown to provide significant sensitivity improvement below and above threshold. It should be mentioned that the present hardware is in an experimental stage and that several parameters and components such as the IF stages (gain control, AFC, bandwidth) have not been fully optimized due to time and fund limits. However, results in this report point the direction in which to further improve this promising concept.

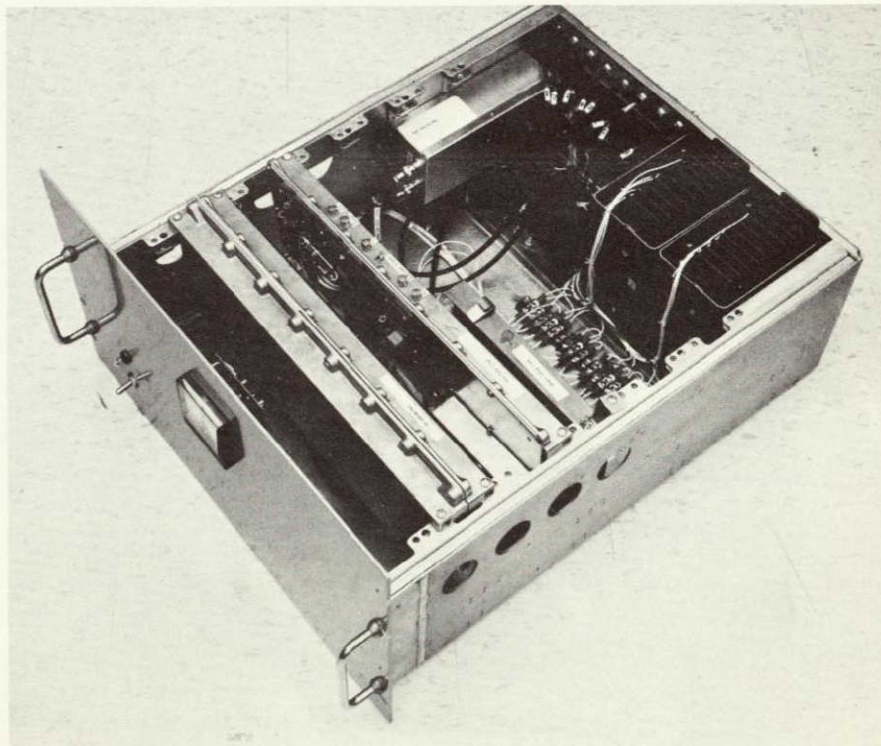


Figure 1-1. Multiloop PLL with Combine Filter Loop

74677 70

2. THEORETICAL BACKGROUND

The nature of the TV signal waveform has been analyzed quite thoroughly by others, and our study takes as its starting point the results of this previous work.

A television signal was modeled and analyzed by L. E. Franks in 1965¹ and earlier, in 1934, by Pierre Mertz and Frank Gray². Using typical picture material parameters, Franks observed that the video spectral components were concentrated near multiples of the line scan and frame scan rates. This conclusion was basically in agreement with that determined earlier by Mertz and Gray. More recently Carden, Osborne, and Davis³ of the University of New Mexico performed an analysis of the Apollo TV signals for NASA/MSO that utilized the model established by Franks. According to them, the video signal, assuming linear scanning produced at the output of a camera, is given by

$$E_o(t) = v'(t) + S(t) \quad (2-1)$$

where

$v'(t)$ = the total video signal

$S(t)$ = the synchronization signal

The total video signal, however, is composed of three other functions: the video signal $V(t)$, the horizontal blanking signal $B_h(t)$, and the vertical blanking signal $B_v(t)$. This information introduced into (2-1) yields the expression obtained by Franks¹

$$E_o(t) = V(t) B_h(t) B_v(t) + S(t) \quad (2-2)$$

¹L. E. Franks, "A Model for the Random Video Process," Bell Systems Technical Journal, December 1965, pp. 609-630.

²P. Mertz and F. Gray, "A Theory of Scanning and Its Relation to the Characteristics of the Transmitted Signal in Telephotography and Television," BSTJ, July 1934.

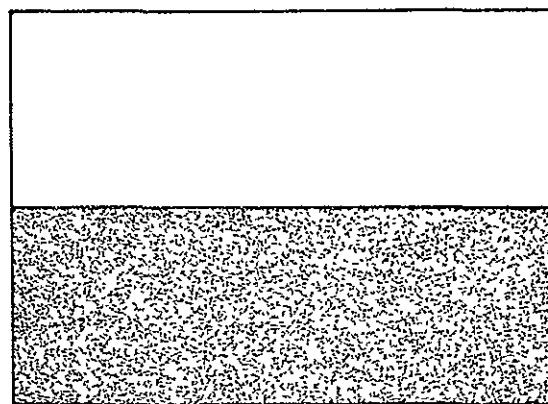
³F. Carden, W. Osborne, and G. Davis, "Advanced Study of Video Signal Processing in Low Signal-to-Noise Environment," NASA Research Grant NGR-32-003-037, December 1967.

Since the blanking signal, $B_v(t)$, represents a pulse train with a very high duty cycle and a narrow spectrum, it may be neglected without any significant effect on the spectrum of $E_o(t)$. With this approximation (2-2) becomes

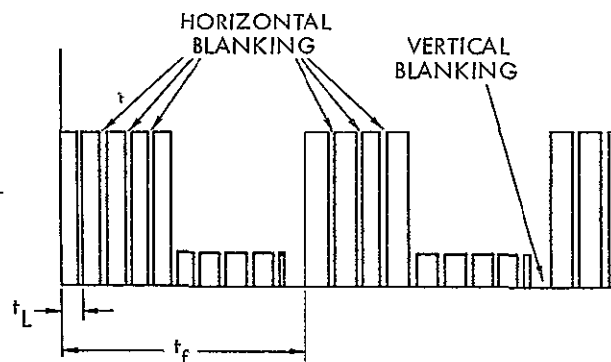
$$E_o(t) = V(t) B_\ell(t) + S(t) \quad (2-3)$$

The cited analysis³ proceeds to establish the desired expression for the spectrum of the composite video signal resulting from scanning the still image shown in Figure 2-1. The result is a double power series of the form

$$V'(t) = \sum_{n=-\infty}^{\infty} \sum_{m=-\infty}^{\infty} v(m) B_\ell(n) e^{j\omega_f(nN+m)t} \quad (2-4)$$



BLACK AND WHITE TEST PATTERN



TIME DOMAIN VIDEO OUTPUT FOR ABOVE IMAGE

Figure 2-1. Black and White Pattern

where

$v'(t)$ = total video signal

$$v(m) = 1/t_f \int_0^{t_f} v(t) e^{-j m \omega_f t} dt$$

= the Fourier components of the periodic video signal averaged over 1 frame time

$B_\ell(n)$ = the Fourier components of the horizontal blanking signal

$\omega_f = 2\pi f_f$ = the frame frequency

m and n = integer values of the Fourier series

$N = w/\omega_f$ = number of lines in the scanning pattern.

$V(t)$ is a square wave of 50 percent duty cycle with its line period equal to t_ℓ and frame period equal to t_f . The Fourier transform, $V(m)$ for this function can be shown to be

$$V(m) = \frac{t_f}{m\pi} e^{-\frac{j m \pi}{2}} \sin \frac{m\pi}{2}$$

and the absolute value for this function is Equation (23) from Reference 3

$$|V(m)| = \left| \frac{\frac{t_f}{2} \left(\sin \frac{m\pi}{2} \right)}{\frac{m\pi}{2}} \right| \quad (2-5)$$

The transform of the blanking signal of Figure 2-1 is

$$B_\ell(n) = \frac{\tau e}{t_\ell} e^{-\frac{j n \pi \tau}{t_\ell}} \frac{\left(\sin \frac{\pi n \tau}{t_\ell} \right)}{\frac{\pi n \tau}{t_\ell}}$$

where

$$\tau = t_\ell - t_r$$

= time to horizontally blank

and the absolute value of this function, Equation (24) of Reference 3, is

$$|B_{\ell}(n)| = \left| \frac{\tau}{t_{\ell}} \frac{\sin\left(\frac{n\tau\pi}{t_{\ell}}\right)}{\frac{n\pi\tau}{t_{\ell}}} \right| \quad (2-6)$$

A plot of the products of (2-5) and (2-6) versus frequency is the amplitude spectrum of the composite video signal produced by the black and white pattern. This is reproduced in Figure 2-2. This plot was compared with the actual spectrum produced by scanning a black and white test pattern. The spectrum was measured by NASA and the agreement between the measured and calculated spectrum is quite good.

The plot in Figure 2-2 does not show the components about the frame frequency harmonics because such detail is impossible to achieve on the frequency scale used. However, this detail has been plotted in Figures 2-3 and 2-4 for the TV spectrum of a diagonal bar, which is another case of interest. It should be noted that the synchronizing signals

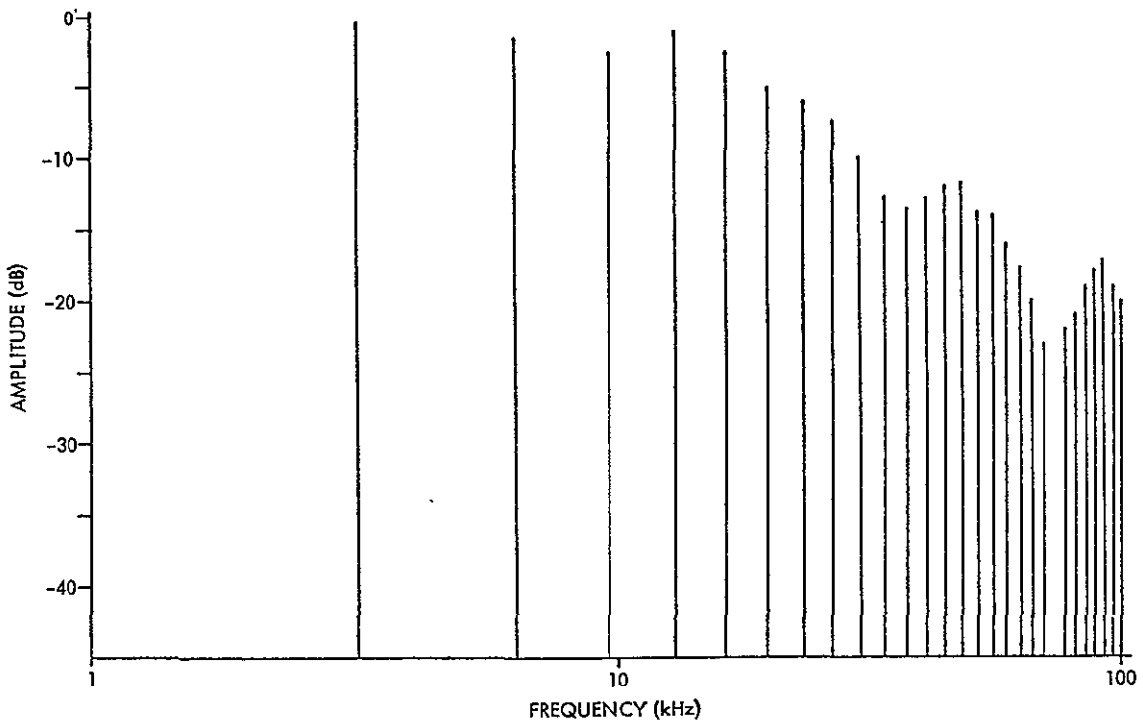


Figure 2-2. Measured Video Spectrum of Black and White Test

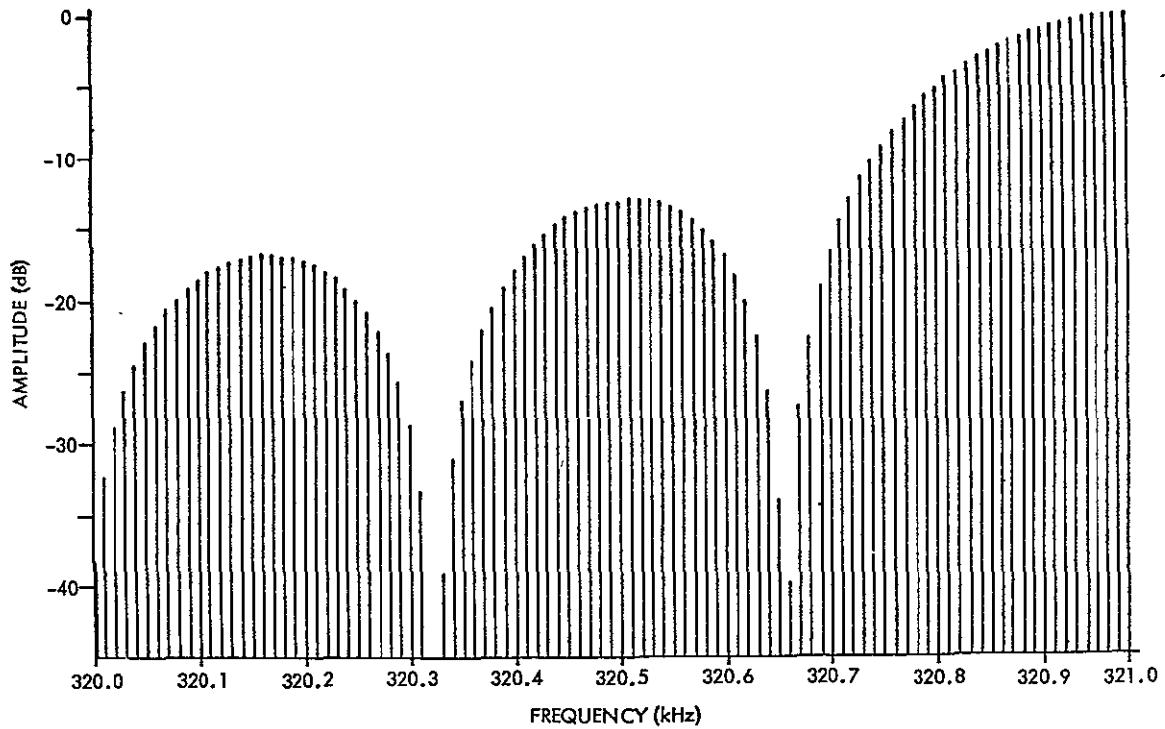


Figure 2-3. Diagonal Bar Spectrum in High Frequency Region Detail

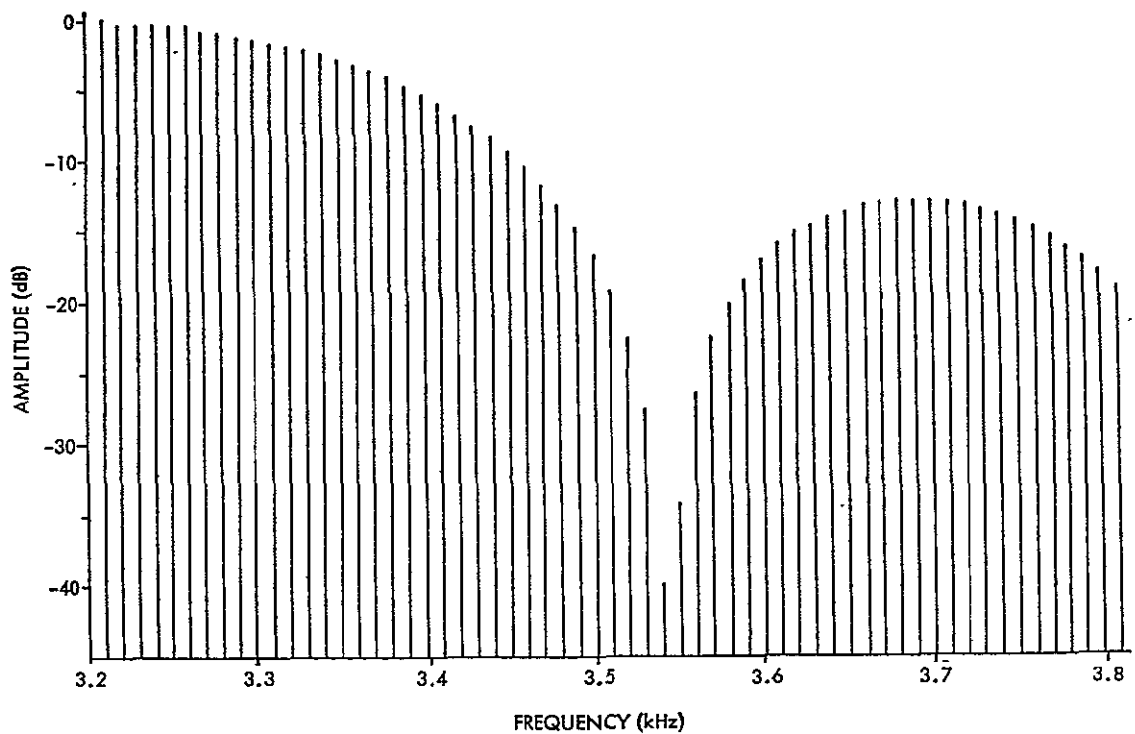
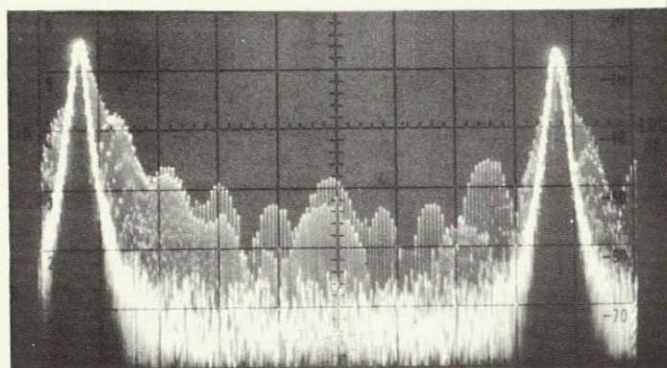


Figure 2-4. Diagonal Bar Spectrum in Low Frequency Region Detail

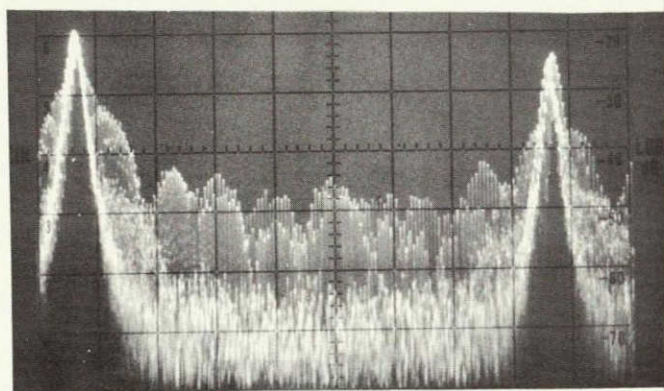
have not been considered in calculating this case. This accounts for the absence of strong components at the line rate (especially in Figure 2-4). However, since they are additive, their spectra simply add and give rise to harmonics at multiples of f_L . It turns out that the total spectrum, in addition to being confined to harmonics of frame frequency f_f , is concentrated in the band about multiples of $f = 1/t_\ell + \Delta t$, where Δt is the time delay of subsequent pulses due to the slant of the bar and is indirectly proportioned to the angle α of the bar with the horizontal. If $\Delta t = 0$, i.e., if the bar is vertical, the peaks are at the harmonics of the line frequency. For small $\Delta t \neq 0$, however, the first peak is very near the line frequency; at higher harmonics of f , the peaks occur farther away from the line frequency, the distance being indirectly proportional to α . Bars at different angles have peaks at different locations. It can be concluded, therefore, that the more "horizontal" information the image contains, the more energy appears in the valleys between the line frequency harmonics of the total video spectrum.

To gain a qualitative appreciation of these findings, the actual spectrum of a 2-inch wide black bar on a white background was measured. The output of a TV camera was displayed on a spectrum analyzer. Figures 2-5 and 2-6 show the results. Figure 2-5 is taken in the vicinity of 520 kHz and Figure 2-6 in the vicinity of 100 kHz.

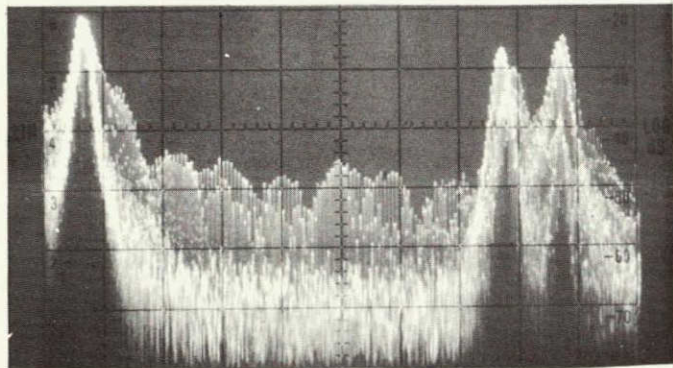
Figure 2-7 presents the spectral content of a TV signal at baseband. Clearly, the higher harmonics appear spread out. The spectrum in the valleys is due to horizontal picture information. Figure 2-7 also reveals another important property of TV spectra which is that the amplitude of the spectrum rolls off rather rapidly: about -10 dB at 100 kHz and at least -40 dB at 1 MHz.



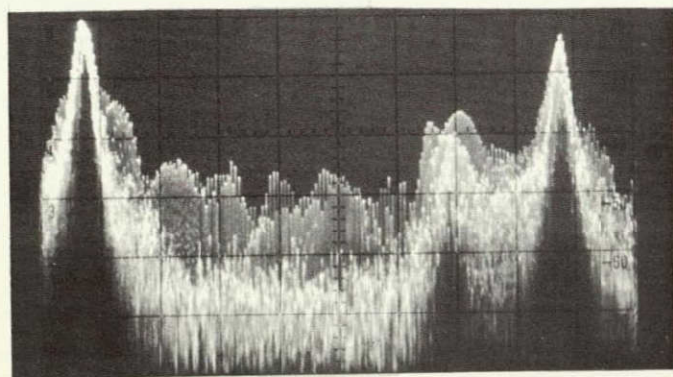
- a) Camera lens covered. Shown are two spectral comb peaks at harmonics of f_L due to synchronizing and blanking signals. Horizontal scale 2 kHz/div., scan time 0.5 sec.



- b) Vertical bar, $\alpha = 90^\circ$. Horizontal scale factor 2 kHz/div. Image spectrum is confined to multiples of f_L .

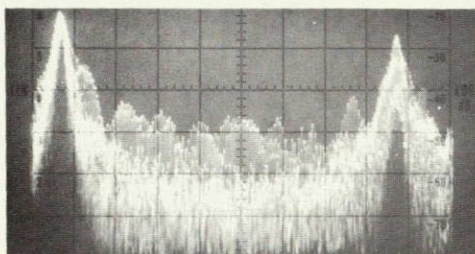


- c) $\alpha = 40^\circ$. Second peak from right is due to image. Horizontal 2 kHz/div.

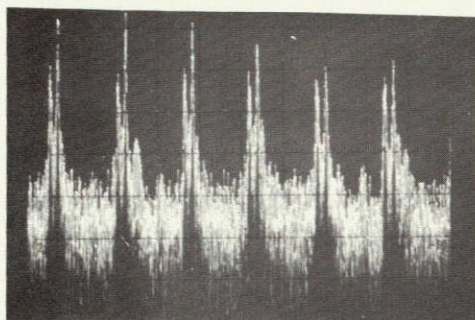


- d) $\alpha = 22^\circ$. Horizontal 2 kHz/div.

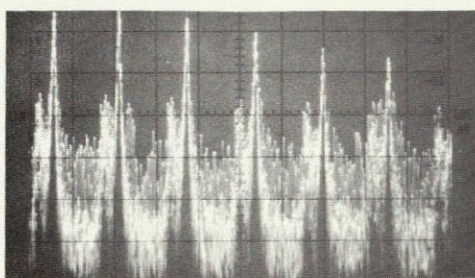
Figure 2-5. Analyser Displays of 2 in. Black Bar Spectra (in the vicinity of 520 kHz)



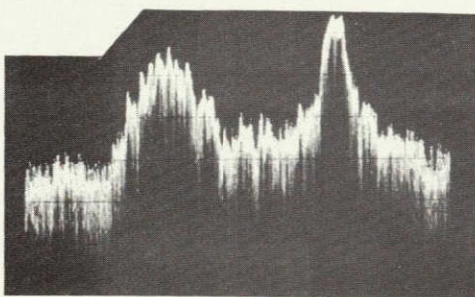
e) Horizontal bar, $\alpha = 0$. Horizontal 2 kHz/div.



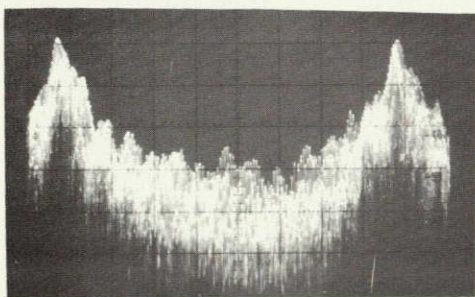
f) Same as c) but horizontal 10 kHz/div.



g) Same as d) but horizontal 10 kHz/div.

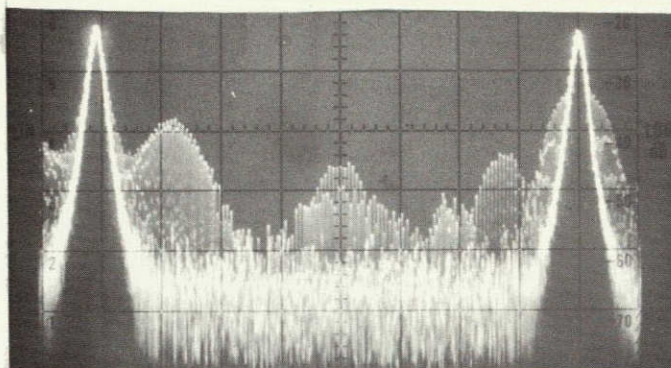


h) Same as c) but horizontal 0.5 kHz/div. Note comb structure around multiples of f_f .

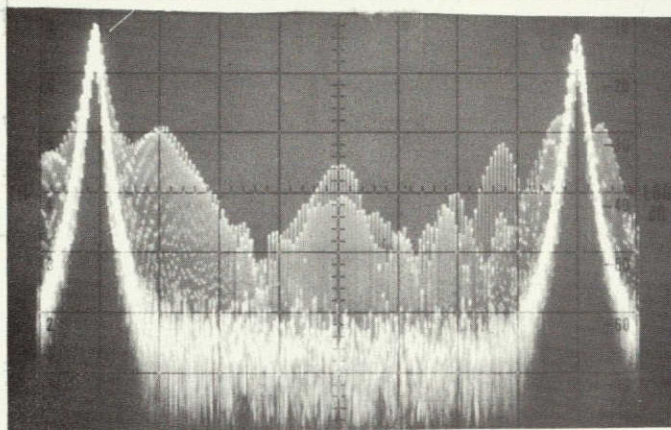


i) Spectrum of general picture. Horizontal 2 kHz/div.

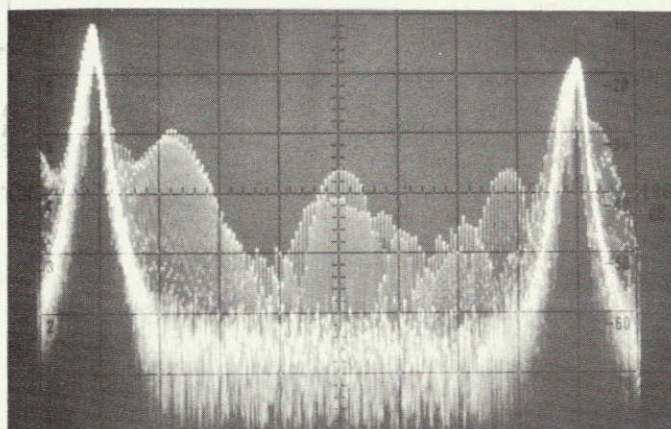
Figure 2-5. Analyser Displays of 2 in. Black Bar Spectra (in the vicinity of 520 kHz) (Continued)



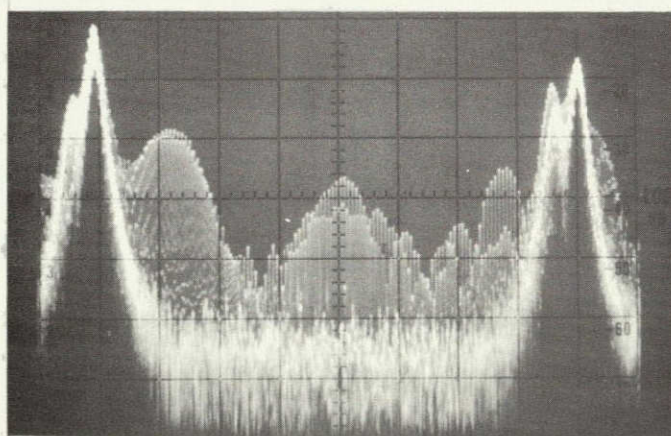
a) Lens covered



b) $\alpha = 90^\circ$

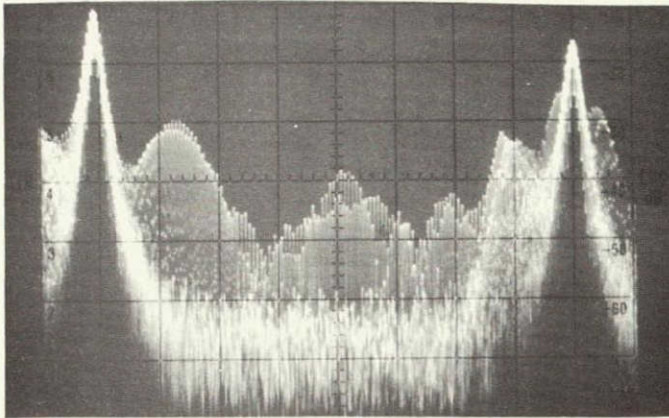


c) $\alpha = 40^\circ$

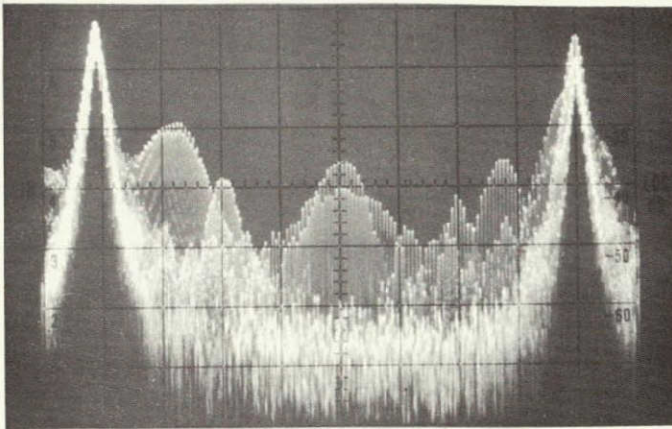


d) $\alpha = 22^\circ$

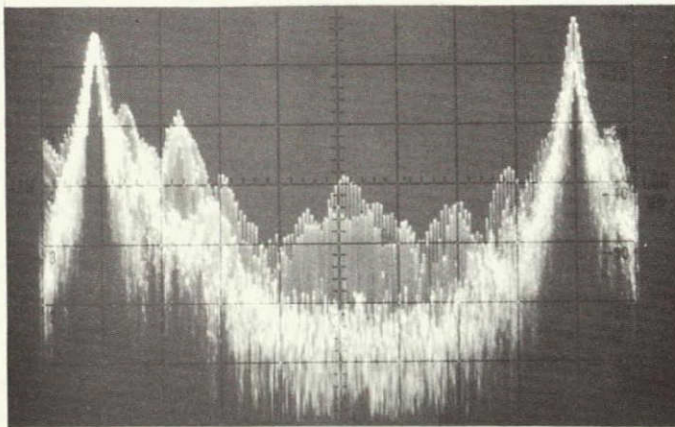
Figure 2-6. Analyser Displays of 2 in. Black Bar Spectra
(in the vicinity of 100 kHz)



e) $\alpha = 13^{\circ}$

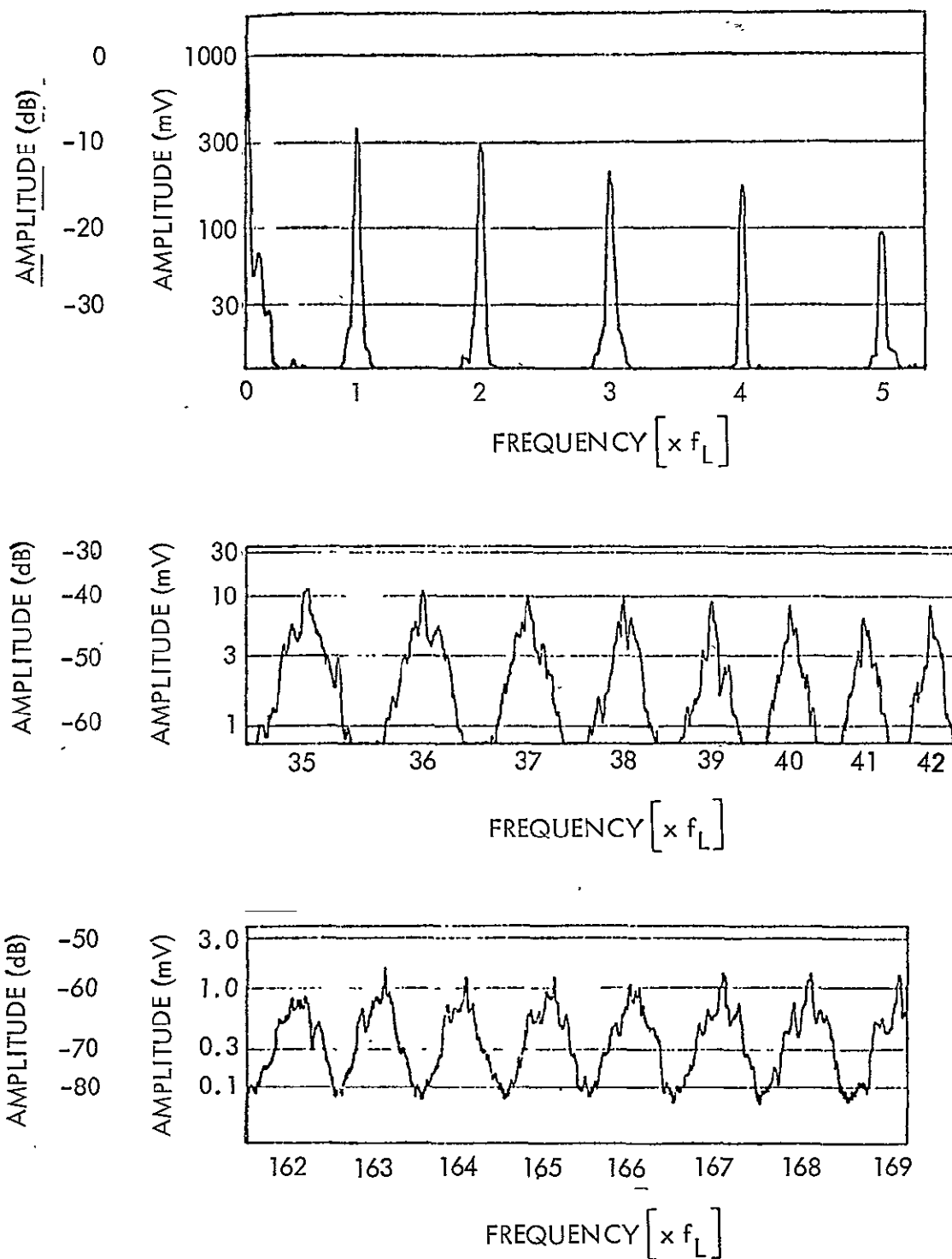


f) $\alpha = 0^{\circ}$



g) General Picture

Figure 2-6. Analyser Displays of 2 in. Black Bar Spectra
(in the vicinity of 100 kHz) (Continued)



NOTE: FROM D. G. FINK, TELEVISION ENGINEERING HANDBOOK,
McGRAW-HILL, 1957, pp. 10-25.

Figure 2-7. Amplitude Spectrum of a Stationary TV Signal

3. COMBLINE FILTERS

3.1 INTRODUCTION

Digital and analog methods of implementing filters with comb-like amplitude responses were considered. Digital filters were found to offer a great deal of flexibility as far as the shape of the passbands are concerned but since it is very difficult to determine the optimal shape of the filter response with respect to noise filtering, distortion, and loop tracking error, their complexities ruled out any hardware implementation in this initial project. The hardware effort was therefore concentrated on analog filters. These are based on a feedback loop which is relatively easy to implement except for the delay lines which are the crucial components.

Our study results on digital combline filters are summarized in 3.2. The remainder of this section is given over to the analog combline filter.

3.2 DIGITAL COMBLINE FILTERS

The following is based on a generalized study which is presented in Appendix A. Two approaches, both utilizing digital bandpass filters (DBF), can be used to synthesize a comb-like filtering structure. The first approach (DBF_1) is to use the DBF shown in Figure 3-1 to generate all the TV combines.* The second approach (DBF_2) is to use one DBF per TV spectrum combline. Since most of the energy inherent in a TV signal resides in the first 200 combines, the DBF_2 approach would necessitate the use of about 200 DBF's similar to that shown in Figure 3-1 operating in parallel.

As stated previously, the general aim of the combline filter is to produce a comb structure that adapts to the TV baseband comb structure. Another way of expressing this is to say that the Q ($Q = f_c/f_{3\text{dB}}$)** of the i th comb of the filter should approximately equal the Q of the i th TV spectrum comb. One of the salient features of the digital synthesis of a comb is this method's ability to produce responses with very large Q 's.

*Note that DBF_1 actually requires 200 R-C networks similar to the four shown in Figure 3-1.

**Note that f_c is just the center frequency of any one of the combs.

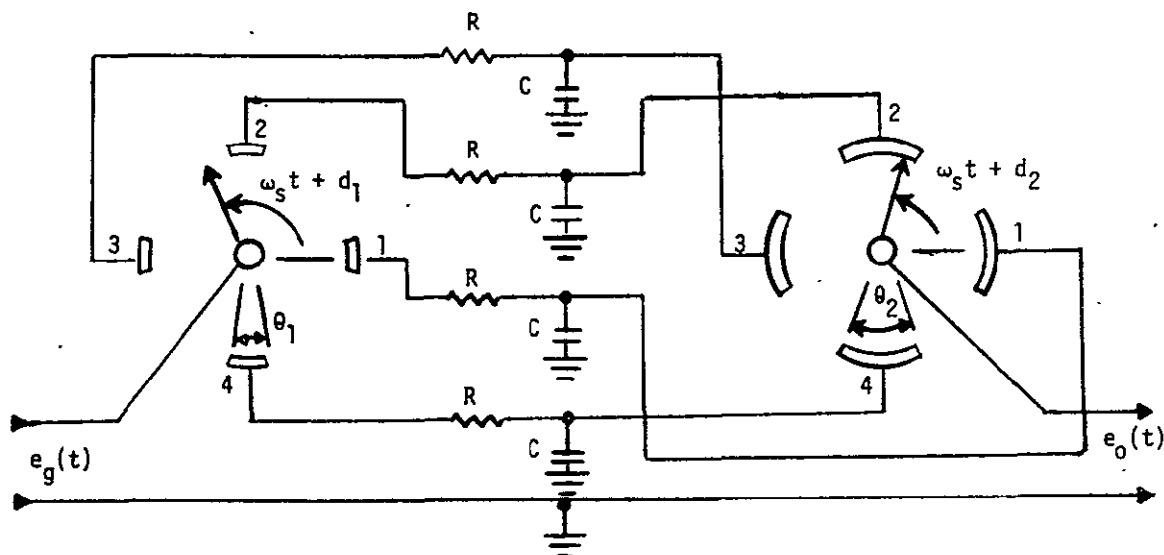


Figure 3-1. Generalized Sampler Configuration (Four Single-Section RC Filters)

The results obtained in the study indicate that for DBF_1 , the Q of the n th comb is equal to n times the Q of the first comb; whereas, for DBF_2 , the Q of the n th comb is a function of the number of filter sections in the n th sampler. This is interpreted to mean that the Q 's for the comb response of DBF_2 are variable while for DBF_1 they are fixed. Table 3-1 shows the approximate Q for three TV combines and the nearest Q obtainable with DBF_1 , DBF_2 , and also with an analog filter. Obviously, DBF_1 cannot satisfy the first criterion since the comb structure of the filter is incompatible with that of the TV signal.

Table 3-1. Relative Comb Q 's for Three TV Line Harmonics

Frequency	TV Harmonic	Q of DBF_1	Q of DBF_2	Analog
f_h	16	200	16	16
$36 f_h$	108	7200	108	108
$162 f_h$	324	32,400	324	324

A second consideration is the cost of implementing each method. Approximately the same number of components is needed to implement the analog method that is required to implement just one DBF of the DBF₂ method. This means that it would take many more components to realize the DBF₂ method than the analog method and therefore that the cost and complexity of implementing DBF₂ would greatly exceed that of the analog method.

However, there are considerations favorable to the use of DBF₂. These are:

- The digital approach is conducive to microminiaturization since there are no delay elements which can limit size reduction
- The digital approach is less sensitive to gain and temperature changes
- The digital method does not require the use of a delay line.

3.3 ANALOG COMBLINE FILTERS

The analog combline filters discussed are all based on a feedback system whose feedback path contains a delay line with a time delay equal to the line scanning rate, i. e., 63.5 μ sec. The properties that are most important in the present application are wide bandwidth (4 MHz or better) and high dynamic range. These are very stringent requirements and have only recently been met by state-of-the-art models. A review of the most promising delay lines available to date is included in the discussion below.

3.3.1 Delay Lines

3.3.1.1 Passive LC Delay Lines

An ESC Electronics LC network delay line (Figure 3-2), which we were able to borrow temporarily, was found to have a time delay of 63 μ sec, a bandwidth of 1.3 MHz, and an insertion loss of 13 dB. The advantage of this line is its stability and essentially unlimited dynamic range. However, the bandwidth is very limited and a large effort went into designing schemes to achieve combline filters with appreciable bandwidth.

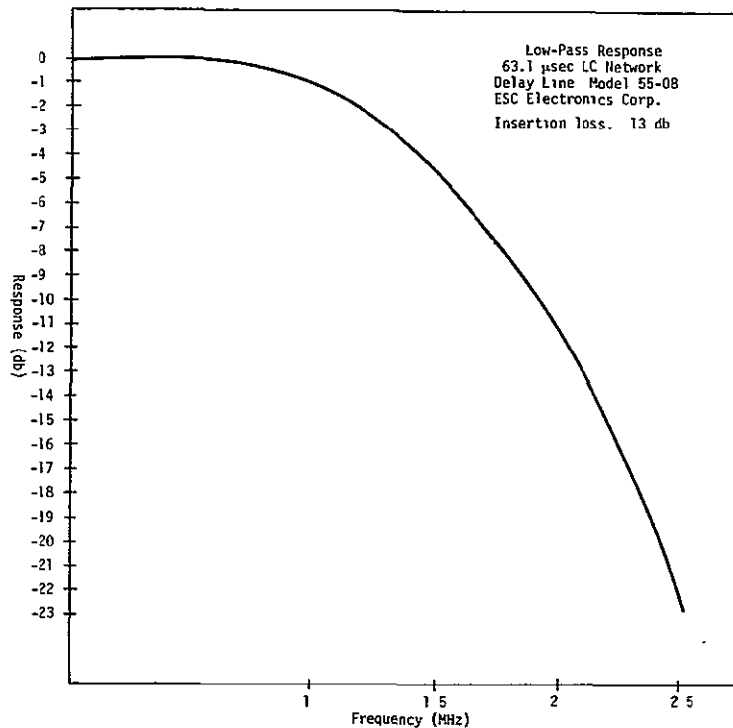


Figure 3-2. Low Pass Response of 63.1 μ sec LC Network Delay Line

Three LC lines were subsequently ordered from ESC; two with a 31.500 μ sec delay to be used in an additive-subtractive combline filter scheme and a 63.100 μ sec line. They are reported to have bandwidths of 4 and 2 MHz, respectively.

3.3.1.2 Corning Glass Delay Line

A Corning glass delay line was tested and found to have a 63.3 μ sec delay. The input signal is amplitude modulated and detected to give a passband response from 20 Hz to 4.5 MHz (Figure 3-3). Although this line had an acceptable bandwidth, it was found to be noisy and to have a very limited dynamic range (\approx 25 dB).

A newer version of the same lines was obtained 17 April 1970. It has a bandwidth of 7 MHz, a signal-to-noise ratio of at least 50 dB, and a linearity of 1.5% (Figure 3-4). This line appears to meet the requirements for implementing the necessary combline filters. According to the manufacturer, a line with the same specifications but with only half the time delay is also available.

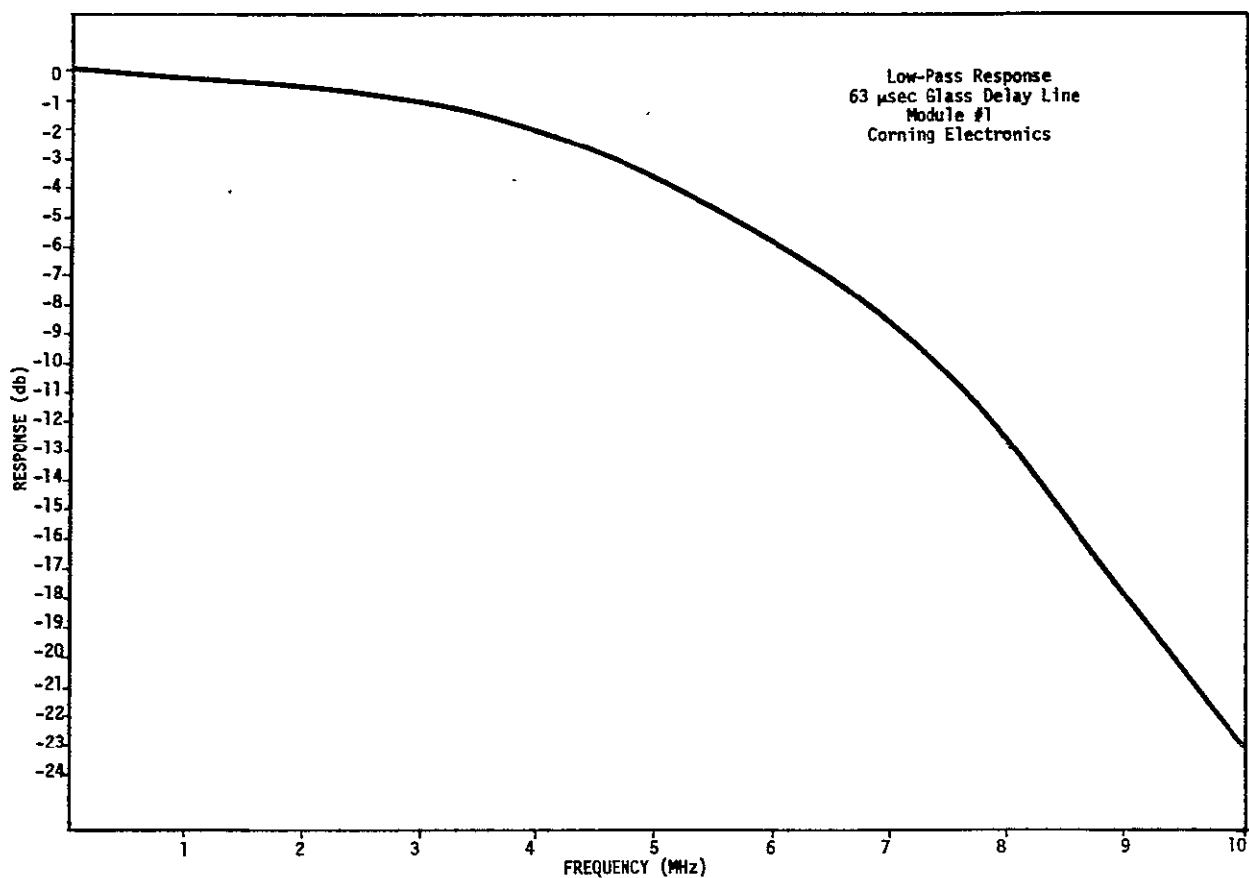


Figure 3-3. Low Pass Response of 63 μ sec Glass Delay Line

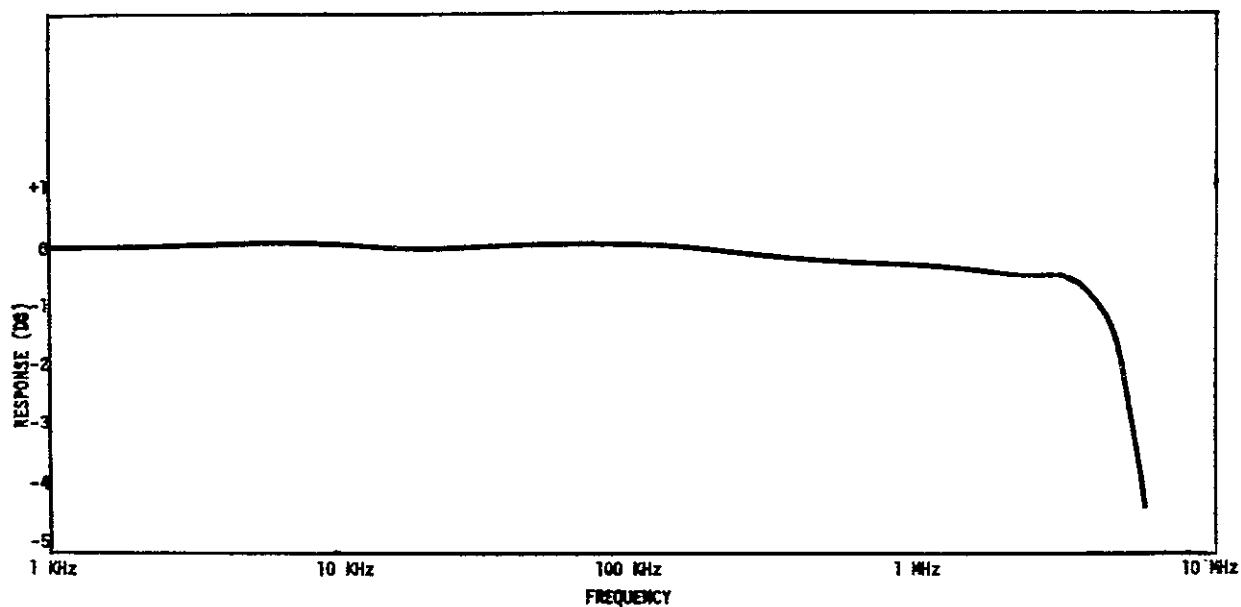


Figure 3-4. Frequency Response of 63 μ sec Delay Module

3.3.1.3 Magnetic Disk Delay Line

One method for producing a wideband, large dynamic range, video delay line is to record the video information on a memory, hold it for 63.5 μ sec, and then return it to the circuit. A magnetic disk delay line which can meet the desired specification is not available off-the-shelf and would have to be developed. However, we have investigated the performance of a magnetic disk delay line for a previous project and the information obtained indicates that such a delay line can be built with a 5 MHz bandwidth. The peak signal power to rms noise ratio achieved with such a device was 42 dB. Additionally, the time delay can be stabilized to 0.4 nsec for a 63.3 μ sec delay.

3.3.1.4 Bucket Brigade Capacitor Storage Delay Line

A paper on "Integrated MOS and Bipolar Analog Delay Lines Using a Bucket-Brigade Capacitor Storage" was submitted to the IEEE International Solid-State Circuits Conference, 18-20 February 1970, by F.L.T. Sangster. Additional information was requested from the author who replied that the specifications of interest (63 μ sec, 3 MHz bandwidth or better, 40 dB dynamic range) are about the limit that is realizable at present. However, the work is in a purely experimental stage and is expected to go beyond these values in the future.

3.3.1.5 Paralleling LC and Glass Delay Lines

An effort was made to improve the bandwidth and dynamic range of earlier delay line models. The scheme used (Figure 3-5) makes use of the fact that the dynamic range of the TV spectrum drops from around 40 dB at low frequencies to below 20 dB above 1 MHz. Advantage is taken of the high dynamic range of the LC line and the wide bandwidth of the glass line. An implementation resulted in a delay line with the desired characteristics and low ripple at the interface of the two paths. However, it was found that this ripple was magnified in the combline loop due to positive feedback. Since better delay lines became available, this method was not pursued any further.

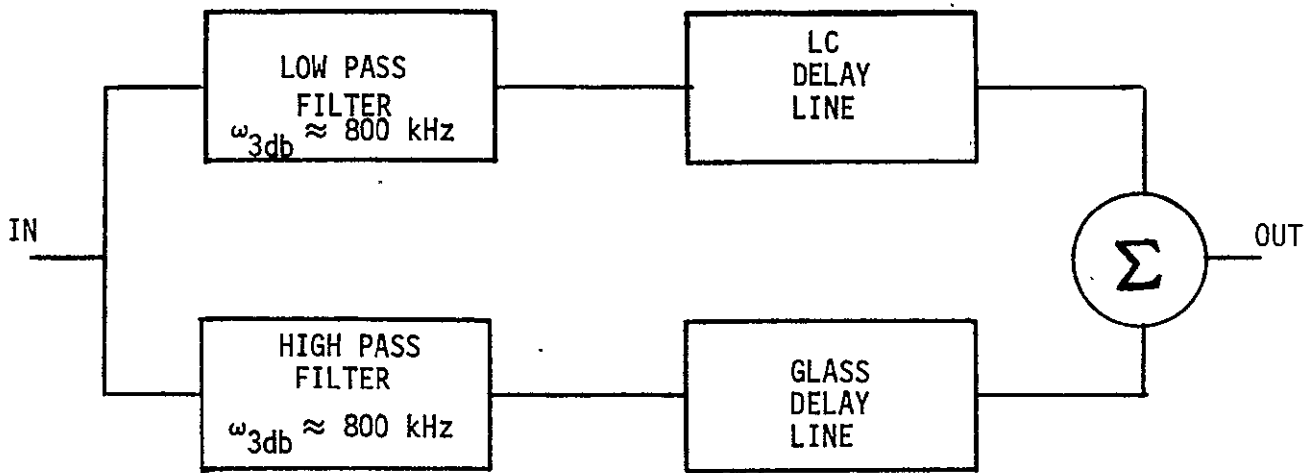


Figure 3-5. Combined Delay Lines Block Diagram

3.3.2 Additive Comblines Filter

A basic additive delay line comblines filter (CLF) is shown in Figure 3-6.¹ The feedback element $d(s)$ represents an ideal delay line (infinite bandwidth) with a transfer function of

$$d(s) = e^{-s\tau} \quad (3-1)$$

$k(s)$ is a low pass filter with gain K and 3 dB cutoff frequency f_o and a transfer function of

$$k(s) = \frac{K\omega_o}{s + \omega_o} \quad (3-2)$$

This filter is not essential for the circuit to have a comblines response. It is intended to give an additional degree of freedom in determining the shape of the comb structure. It may also be used to account for constraints due to limited delay line bandwidths.

Consider first the case for $\omega_o = \infty$. The transfer function becomes

$$H(s) = \frac{E_o(s)}{E_{in}(s)} = |H(s)| e^{j\phi} = \frac{K}{1 - Ke^{-s\tau}} \quad (3-3)$$

and the amplitude response is

¹J.A. Develet, "A High Sensitivity Television (TV) Receiver," TRW Systems Proprietary Report No. 7100.2-25, 28 October 1968.

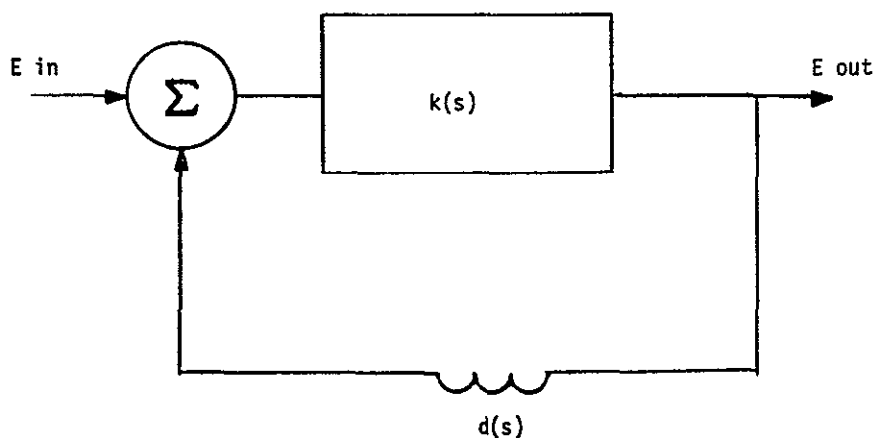


Figure 3-6. Additive Delay Line Combline Filter

$$|H(j\omega)| = \frac{K}{(1 - 2K \cos \omega\tau + K^2)^{1/2}} \quad (3-4)$$

Plots of this function are shown in Figures 3-7 and 3-8. The amplitude response in Figure 3-7 has even symmetry about 0 and the phase response in Figure 3-8 has odd symmetry about 0.

To find the comb peaks P and valleys V, we use

$$P = \frac{K}{1 - K} \quad \text{and} \quad V = \frac{K}{1 + K}$$

as sketched in Figure 3-9. The peak-to-valley ratio (PVR) is

$$PVR = \frac{1 + K}{1 - K} \quad (3-5)$$

This is tabulated for some values of interest as follows:

<u>K</u>	<u>Peak</u>	<u>Valley</u>	<u>PVR (dB)</u>
0.9	9	0.473	25.6
0.95	19	0.488	31.8
0.99	99	0.497	46.0
0.995	199	0.498	52.0

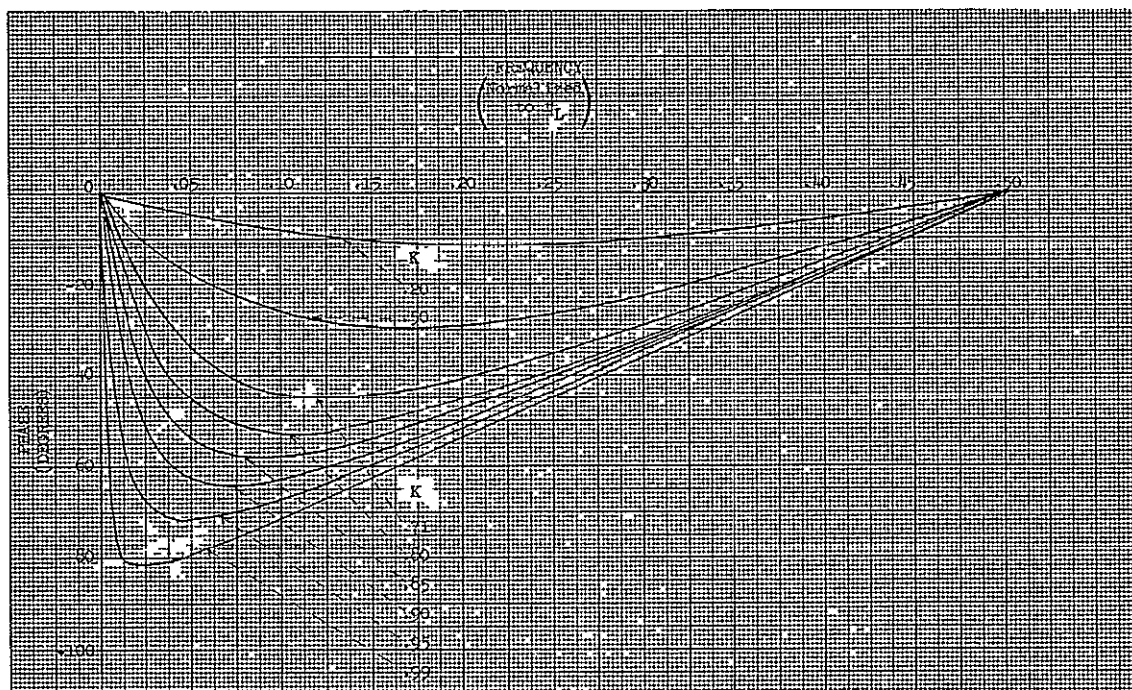
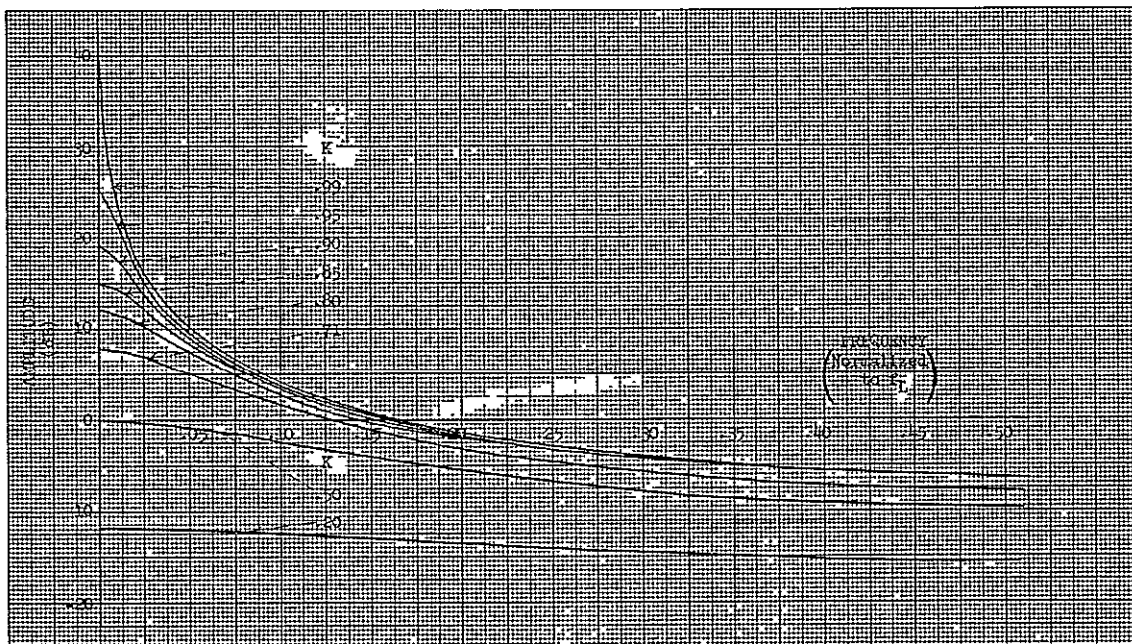


Figure 3-8. Combline Filter Phase Characteristic

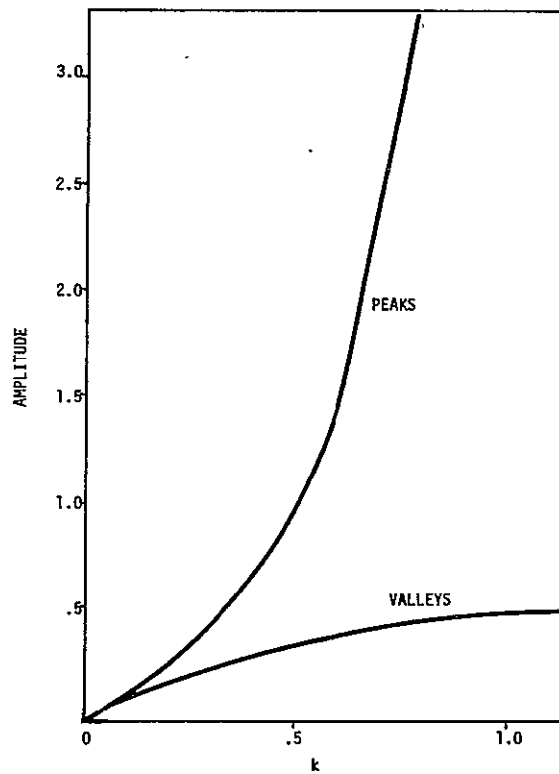


Figure 3-9. Combine Peak Response and Valley Response vs K

Obviously, PVR is fundamentally limited by K and increases rapidly as K approaches 1 at the cost of increased valley level.

The frequency response for a finite ω_0 is found from (3-1), (3-2), and (3-3) and is given by

$$H(s) = \frac{K\omega_0}{s + \omega_0 - K\omega_0 e^{-s\tau}}$$

or

$$H(j\omega) = \frac{K}{1 - K \cos \omega\tau + j \left(\frac{\omega}{\omega_0} + K \sin \omega\tau \right)} \quad (3-6)$$

The amplitude response is found to be

$$|H(j\omega)| = \frac{K}{\left(1 + K^2 - 2K \cos \omega\tau + \frac{\omega^2}{\omega_0^2} + \frac{\omega}{\omega_0} K \sin \omega\tau \right)^{1/2}} \quad (3-7)$$

This is evaluated numerically and plotted in Figure 3-10 versus the normalized frequency $\omega\tau$ in the vicinity of the 10th comb (note scale changes). Figure 3-11 shows a plot of the comb envelope.

The results of this analysis can be summarized as follows:

- The comb width increases for decreasing filter gain and for decreasing low pass cutoff ω_0 .
- The comb peak amplitude increases for increasing K and ω_0 .
- A small shift of the peak of the nth comb from the nth line harmonic is observed. The shift increases with n.
- The comb envelope cutoff increases for increasing ω_0 but decreasing K.

As mentioned earlier, ω_0 introduces a degree of freedom as it allows for independent control of the comb Q factors that may be adjusted to a particular signal spectrum. The peak shift which is due to ω_0 may be partially compensated by slightly increasing the time delay τ .

In order to verify the computer results, the performance of a comb-line filter produced in the lab was compared with the calculations. The results are tabulated in Table 3-2 for two values of loop gain K. The agreement is fairly good, and verifies the dependence of the peak to valley ratio on K and the tendency of the comb peaks to increase with K.

3.3.3 Additive Combline Filters with External Feedback

A combline filter was built to study (separately from the phase-lock loop (PLL) effort) several unique problems that may arise as a result of filtering a TV signal with a combline filter. It offers the same potential for tradeoff studies between PVR, comb Q factors, and bandwidth as a PLL, and has the advantage over a PLL of avoiding the complications of the RF portion. In addition, it is analytically identical to a PLL with a combline loop filter and therefore offers the possibility of optimizing PLL loop parameters.

Since a low pass filter in the combline filter loop may have to account for the bandwidth limitations of the delay line, it is desirable to have some additional means for controlling the comb Q factors. Such a possibility is illustrated in Figure 3-12. It consists of a combline filter

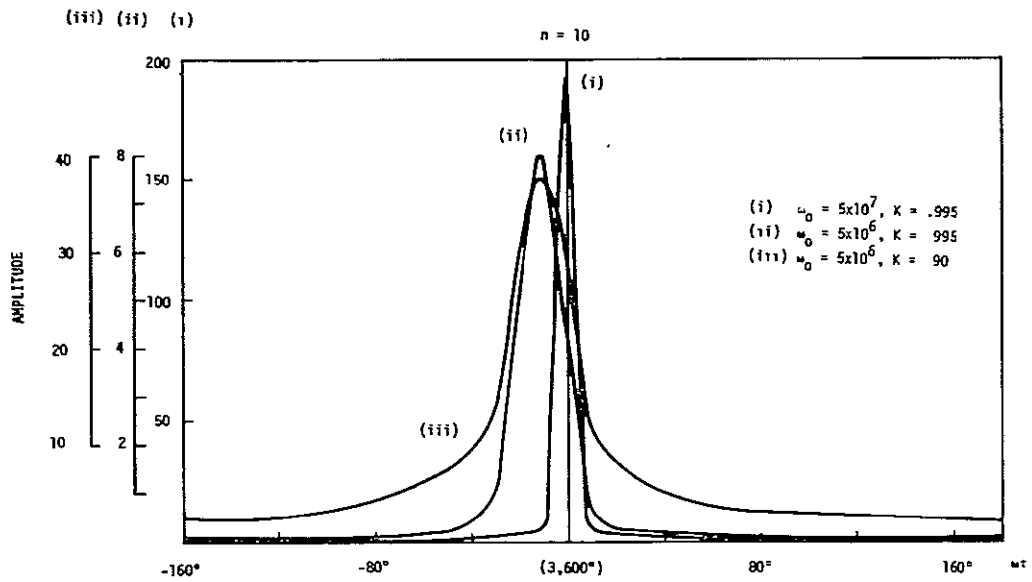


Figure 3-10. Amplitude vs Normalized Frequency for 10th Harmonic of Comb Filter

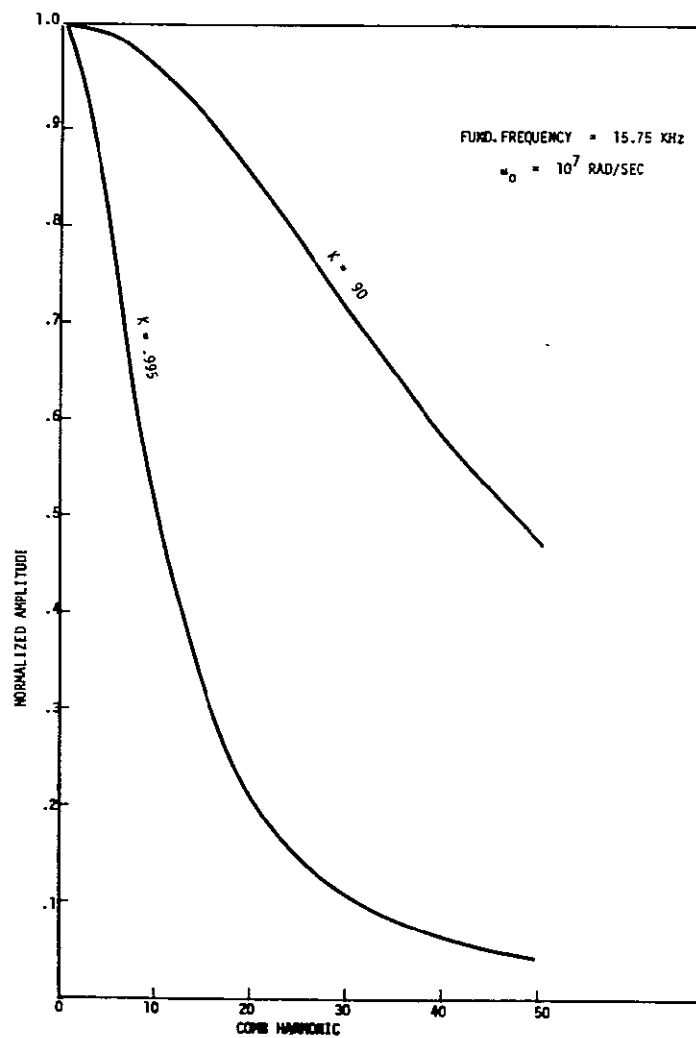


Figure 3-11. Relative Comb Amplitudes of CLF Spectrum vs Frequency

Table 3-2. Comparison of Measured and Calculated
Comblne Filter Response

a) $K = 0.95$ $f_0 = 1 \text{ MHz}$ $1/\tau = 15,850 \text{ kHz}$							
No. of Combs	Fre- quency (kHz)	Measured			Calculated		
		Response (dB)	PVR (dB)	Comb Width (Hz)	Response (dB)	PVR (dB)	Comb Width (Hz)
1	15.82	0	30	396	0	31.8	≈ 300
2	31.63	0			-0.06		
4	63.26	-0.5			-0.3		
6	94.91	-0.12			-0.7		
8	126.62	-2.1			-1.25		
10	158.28	-2.2			-1.9		
32	505.99	-6.3			-10.0		
64	1013.20	-14.0			-19.0		
b) $K = 0.9$ $f_0 = 1 \text{ MHz}$ $1/\tau = 15,850 \text{ kHz}$							
No. of Combs	Fre- quency (kHz)	Measured			Calculated		
		Response (dB)	PVR (dB)	Comb Width (Hz)	Response (dB)	PVR (dB)	Comb Width (Hz)
1	15.82	0	26.5	593	0	25.5	≈ 570
2	31.63	-0.4			-0.03		
4	63.26	-0.8			-0.16		
6	94.91	-1.1			-0.37		
8	126.62	-1.5			-0.65		
10	158.28	-1.8			-1.0		
32	505.99	-5.0			-6.8		
64	1013.20	-11.0			-14.0		

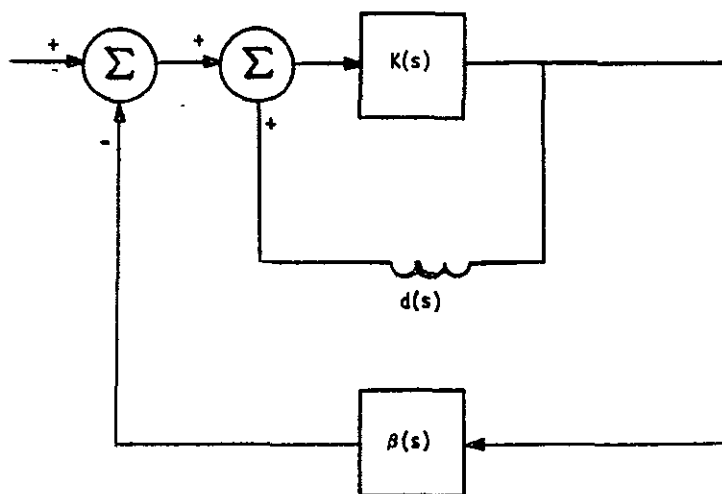


Figure 3-12. Additive Combine Filter with External Feedback

loop with an external negative feedback loop that contains a filter. Note that the analysis pertaining to the case where the feedback loop does not contain a filter is of prime interest in the development of the basic phase-lock loop and will be discussed in Section 4.3. The response of the filter in Figure 3-12 becomes

$$J(s) = \frac{V_o(s)}{V_i(s)} = \frac{\beta H(s)}{1 + \beta H(s)} \quad (3-8)$$

where

$H(s)$ = equation (3-5)

β = degree of negative feedback

The amplitude and phase response of (3-8) for $K = 0.95$ are shown in Figures 3-13 and 3-14 for various values of β . The amplitude curves in Figure 3-13 have even symmetry about 0 and the phase curves in Figure 3-14 have odd symmetry about 0. Both sets of curves are periodic with period τ .

The 3 dB bandwidth of the combs and the peak amplitudes are functions of K and β . Thus, if the proper frequency variations of K and β are used, it is possible to achieve the proper comb width while maintaining uniform peak response over the desired baseband bandwidth.

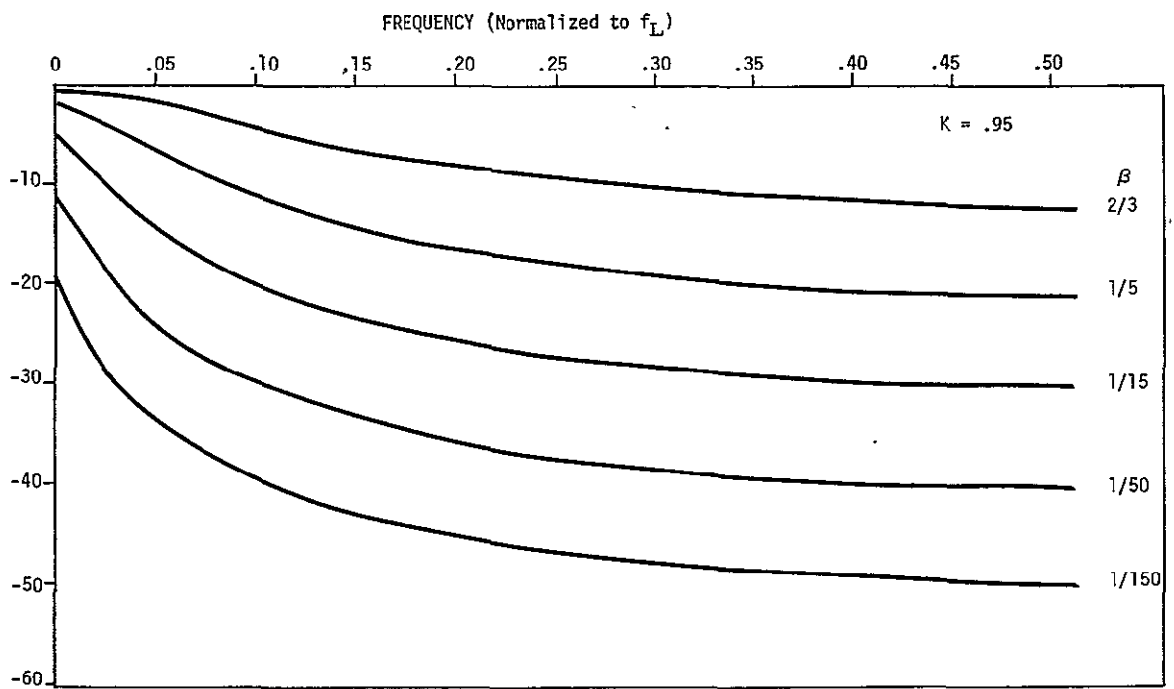


Figure 3-13. Amplitude Response of a CLF with External Feedback

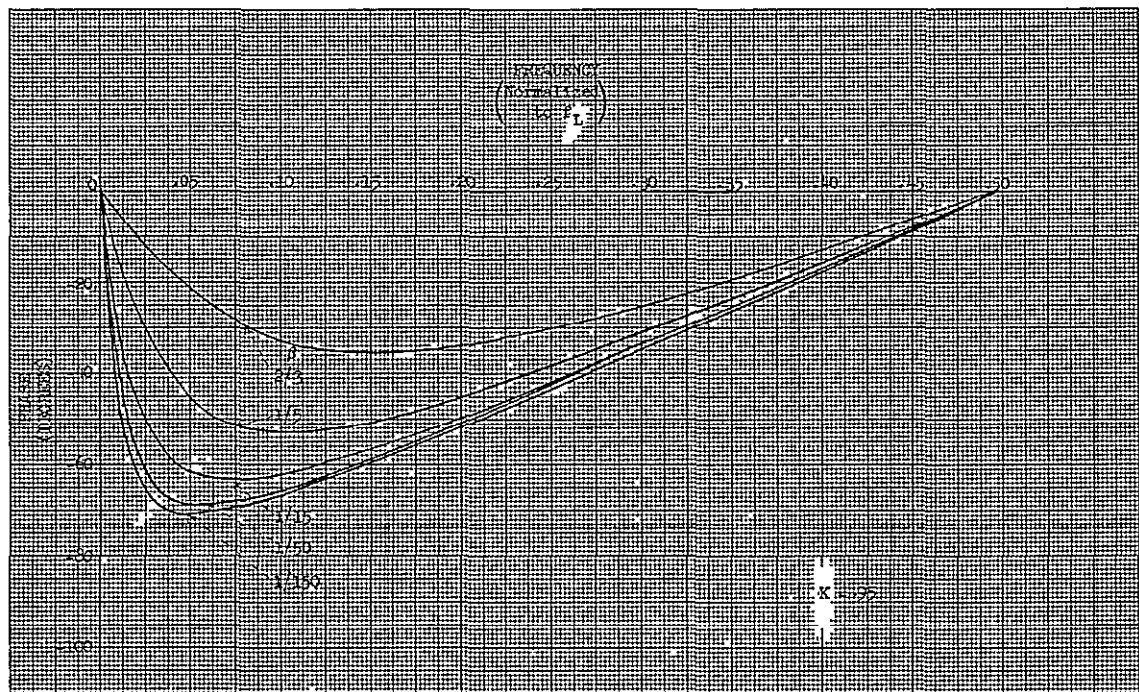


Figure 3-14. Phase Response of a CLF with External Feedback

The combline loop, operated by itself, produces a combline structure like the filter discussed in Section 3.3.2. For example, if K is arbitrarily set to 0.95 the voltage gain at the comb peaks is +25 dB and the attenuation in the valley is -6 dB.

The complete filter of Figure 3-12 was operated in two modes over a bandwidth of about 2 MHz. The first mode arises with a high pass β filter and a low pass K filter. Table 3-3 shows the comb structure obtained.

In this mode, the bandwidth of the individual combs was increased at higher frequencies. It is noteworthy again that a tradeoff between bandwidth and PVR is unavoidable.

The second mode is based on unity feedback. The structure of this mode is shown in Table 3-4. A high and uniform PVR is maintained over the band of interest. The combs are narrow and decrease significantly at higher frequencies.

3.3.4 Additive-Subtractive Combline Filter

An alternate technique for realizing a combline filter is based on combining additive and subtractive comb filters which may result in improved bandwidth. A subtractive comb filter is obtained with the circuit in Figure 3-15. This is similar to the additive circuit and gives rise to the same combline response except that the peaks are shifted by half the peak separation.

It appeared that "short" delay lines with time delays of $\tau/2$ are available with about twice the bandwidth compared to the long lines with $\tau = 63 \mu\text{sec}$. Under these circumstances, the circuit in Figure 3-16 may result in a filter with improved bandwidth. The respective transfer functions are

$$H_1(s) = \frac{K\omega_0}{s + \omega_0 - K\omega_0 e^{-s\tau}} \quad (3-9)$$

and

$$H_2(s) = \frac{K\omega_0}{s + \omega_0 + K\omega_0 e^{-s\tau}} \quad (3-10)$$

Table 3-3. Mode 1 Comb Structure

Frequency at Peak (kHz)	Peak-to- Valley Ratio (dB)	3 dB Bandwidth (kHz)
15.18	18.0	0.86
157.60	8.5	2.11
458.51	8.0	4.20
901.05	7.0	5.58
1107.32	6.5	6.03

Table 3-4. Mode 2 Comb Structure

Frequency at Peak (kHz)	Peak-to- Valley Ratio (dB)	3 dB Bandwidth (kHz)
15.85	24.5	0.58
158.31	24.5	0.50
459.16	23.0	0.60
918.34	20.0	0.80
1789.23	17.0	1.20

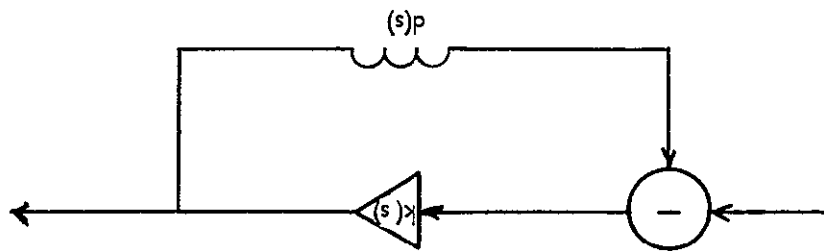


Figure 3-15. Subtractive Comblines Filter

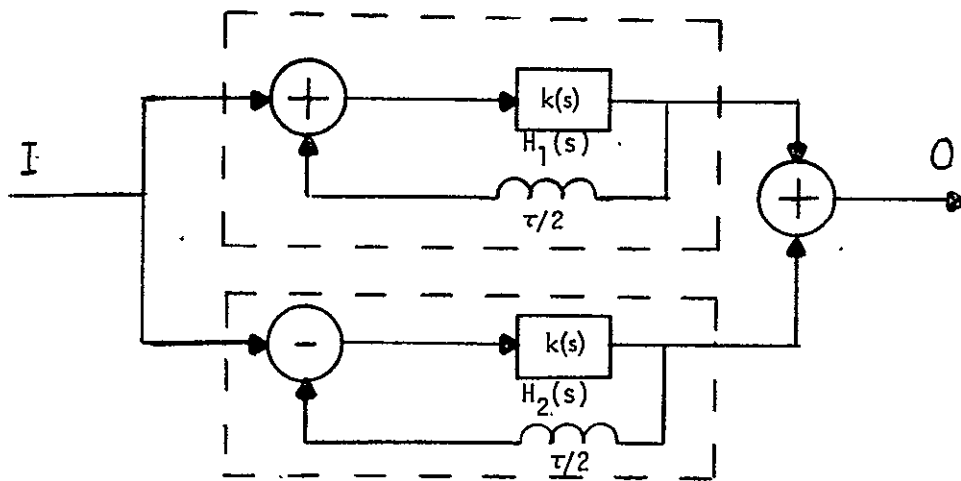


Figure 3-16. Additive-Subtractive Comblines Filter

The total transfer function is

$$H(s) = \frac{0}{1} = H_1(s) + H_2(s) \quad (3-11)$$

$|H_1(j\omega)|$, $|H_2(j\omega)|$, and $|H(j\omega)|$ are plotted in Figure 3-17. The peaks for $|H(j\omega)|$ are approximately equal to the peaks for $|H_1(j\omega)|$ and $|H_2(j\omega)|$, but the valleys are greatly increased by the summation of $|H_1(j\omega)|$ and $|H_2(j\omega)|$. In fact, for this particular example, the peak-to-valley ratio is decreased by about half for $H(\omega)$ because the valleys are twice as high. This can be more easily seen in the simplified case $(\omega_0 = \infty)^*$.

$$H_1(s) = \frac{K}{1 - K e^{-s\tau/2}} \quad (3-12)$$

$$H_2(s) = \frac{K}{1 + K e^{-s\tau/2}} \quad (3-13)$$

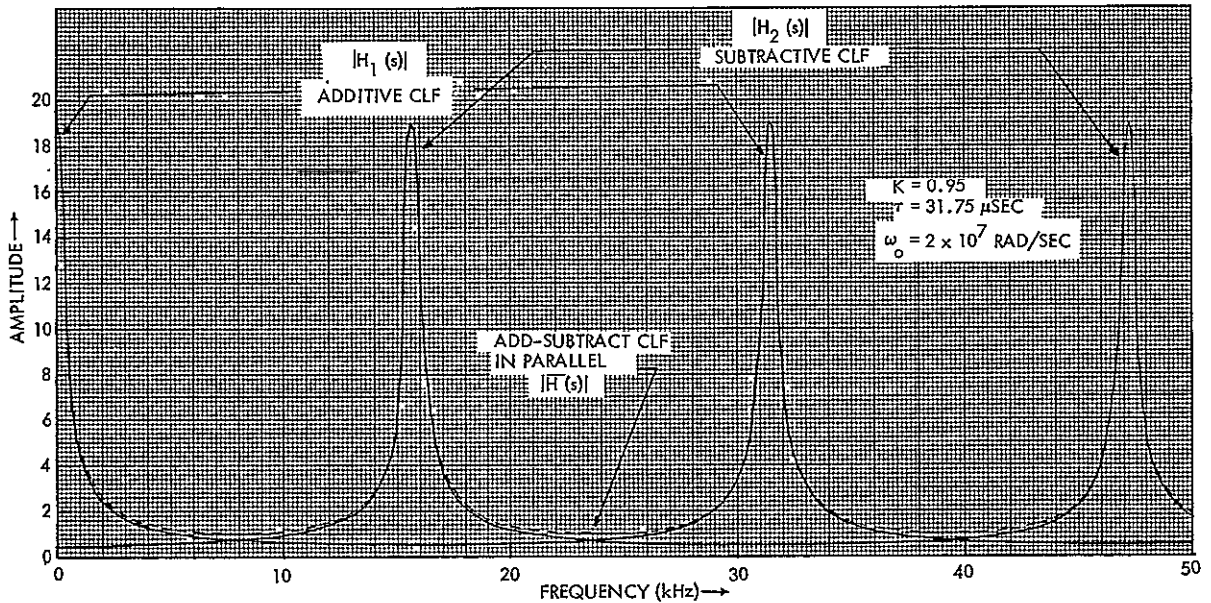


Figure 3-17. Amplitude Response vs Frequency for Additive-Subtractive Comb Filter

*The first peak and valley is left almost unchanged regardless of the actual value of ω_0 if $\omega_0 \gg 1$.

$$H(s) = \frac{K}{1 - Ke^{-s\tau/2}} + \frac{K}{1 + Ke^{-s\tau/2}} = \frac{2K}{1 - K^2 e^{-s\tau}} \quad (3-14)$$

Note that the peaks and valleys occur at multiples of π (no shift). The maximum occurs when $e^{-s\tau} = 1$ and the minimum when $e^{-s\tau} = -1$, so the peak values $P = 2K/1-K^2$ and the valleys $V = 2K/1+K^2$

$$PVR = \frac{1+K^2}{1-K^2}, \quad K \leq 1$$

One can compare this result with the PVR for the simple additive combline which was $1+K/1-K$. From these two equations, it can be seen that the PVR is decreased by the additive-subtractive scheme since $K < 1$ (i.e., $K^2 < K$). Curves comparing the peaks and valleys for these two cases are shown in Figure 3-18. Lower peak-to-valley ratios imply that the equivalent noise bandwidth is larger. For the infinite bandwidth case, it can be shown that the equivalent bandwidth for a comb filter with delay $\tau/2$ is twice that for a comb filter with delay τ . If one then had an additive-subtractive comb filter (time delay = $\tau/2$) of the same envelope bandwidth as an additive comb filter (time delay = τ), one would expect the equivalent noise bandwidth of the former to be approximately twice the noise bandwidth of the latter.

Suppose the additive-subtractive filter of Figure 3-16 is placed in a negative feedback loop (or a phase-lock loop) with open loop gain $G = 0.5$. The amplitude response at low frequencies is shown in Figure 3-19 and compared with an additive filter (time delay = τ). Notice that the peaks of the additive-subtractive filter are slightly higher than the peaks for the additive filter, but the valleys for the former are much greater than that for the latter. This can be seen from the equations when $\omega_0 = \infty$.

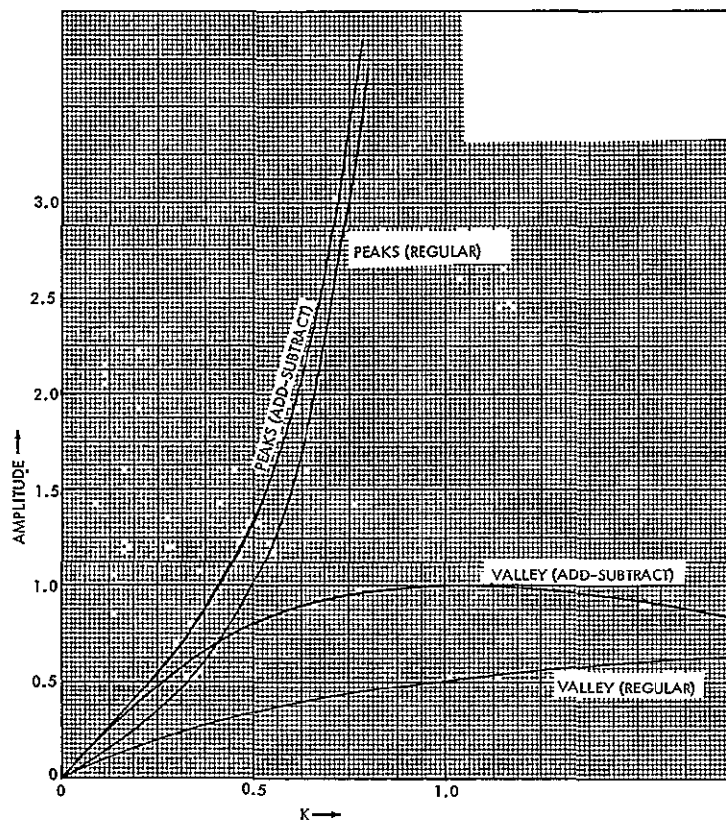


Figure 3-18. PVR vs K for Additive and Additive-Subtractive CLF

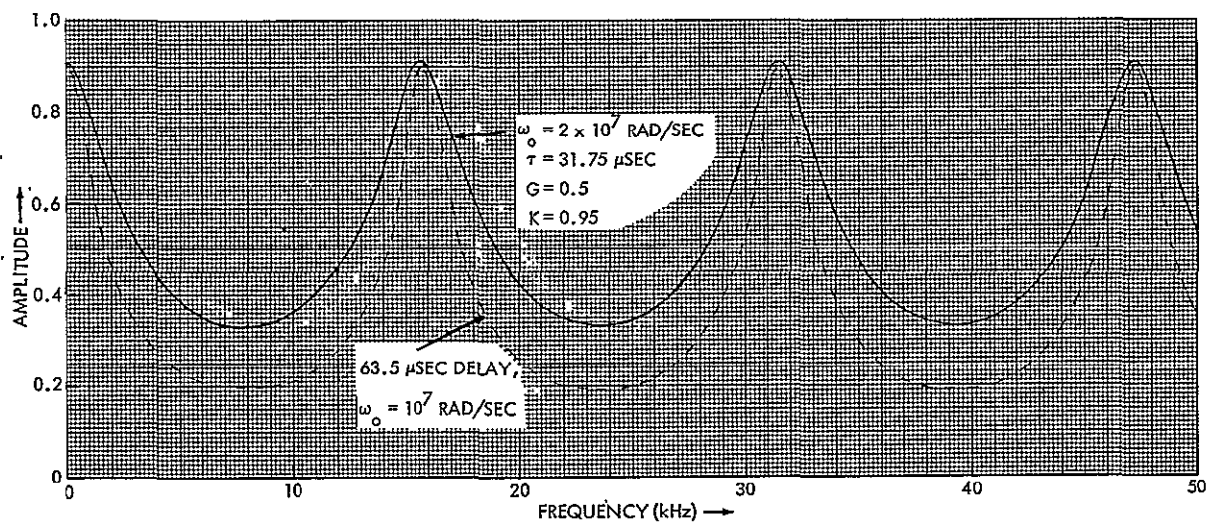


Figure 3-19. Amplitude vs Frequency for Additive-Subtractive with a Negative Feedback Loop

Since

$$\begin{aligned}\frac{0}{I} &= \frac{GH(s)}{1 + GH(s)} = \frac{2 KG}{1 + 2 KG - K^2 e^{-s\tau}} \\ P &= \frac{2 KG}{1 + 2 KG - K^2} \\ V &= \frac{2 KG}{1 + 2 KG + K^2} \\ PVR &= \frac{1 + 2 KG + K^2}{1 + 2 KG - K^2}\end{aligned}\tag{3-15}$$

This equation should be compared with the PVR for the additive (time delay = τ) case

$$(PVR)_{\tau} = \frac{1 + GK + K}{1 + GK - K}$$

Curves showing the PVR dependence on K and G are plotted in Figure 3-20. Comparisons can also be made between $(PVR)_{+}$ for an additive-subtractive loop and $(PVR)_{\tau}$. For a stable minor loop ($K < 1$), one sees that the $(PVR)_{+}$ is several dB worse. Now suppose that a delay line of delay τ and bandwidth f_0 and delay lines of delay $\tau/2$ and bandwidth $2f_0$ are available. (Such an assumption was quite reasonable for earlier delay line models, see 3.3.1.) With this in mind, consider the following methods to obtain a required comb filter.

- a) Additive comb filter with delay = 63.5 μ sec.
- b) Additive-subtractive comb filter with delay = 31.75 μ sec.
- c) Additive comb filter with two 31.75 μ sec delay lines in series to produce a 63.5 μ sec delay.

Suppose a given peak-to-valley ratio is required. One can then find values of K and G which would produce this PVR from Figure 3-20. Looking at the bandwidth vs K, G curves, one can then determine the bandwidths in the phase-lock loop. Suppose that a 63.5 μ sec delay line with a bandwidth of 1.3 MHz and two 31.75 μ sec delay lines with bandwidths of 2.6 MHz are available and that a peak-to-valley ratio of 10 dB is

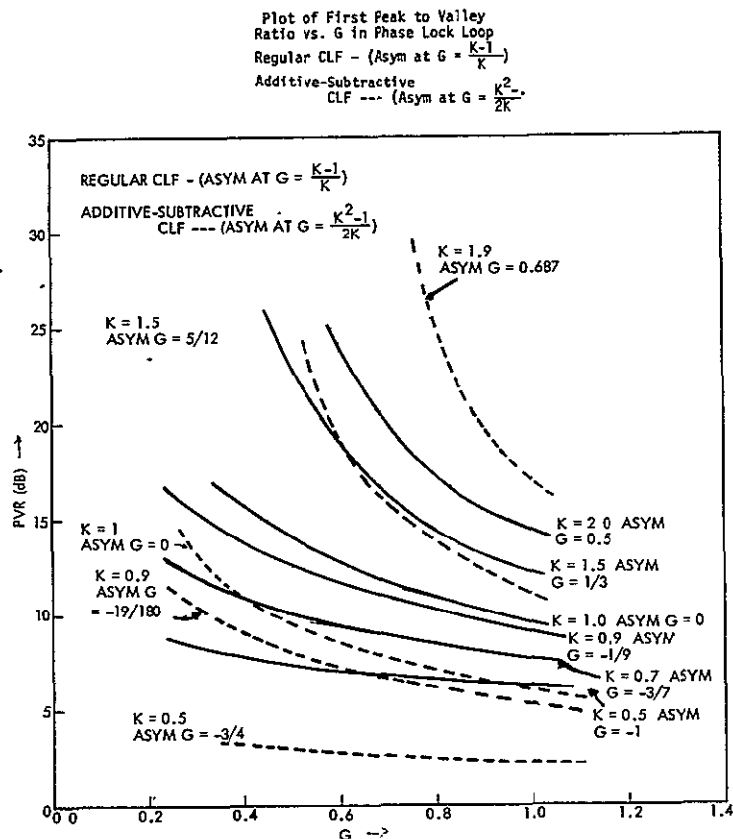


Figure 3-20. PVR vs G in PLL for
Additive-Subtractive CLF

required. (Since the additive-subtractive filters are the sum of two comb filters, the bandwidth curves for the single additive filter are approximately the same as that for the additive-subtractive filter. In practice, however, the additive-subtractive line is slightly wider than a single line of the same width.) Let K be 1. The bandwidth in the phase-lock loop is:

Method	Delay (μ sec)	Delay Line Bandwidth (MHz)	K	G	Bandwidths in PLL for 10 dB PVR (MHz)
a)	63.5	1.3	1	0.9	1.6
b)	31.75	2.6	1	0.45	1.9
c)	31.75	1.67*	1	0.9	2.06

*The bandwidth is found by the formula $f_0' = f_0 \sqrt{2-1} = (2.6 \text{ MHz})\sqrt{2-1}$ which is true for amplifiers, but was verified for delay lines by actual measurements.

Under the above assumptions, while the additive-subtractive comb-line filter offers some bandwidth advantages over the single additive comb filter, the scheme of stacking two short delay lines in series still offers the greater advantage in bandwidths, peak-to-valley ratios, and simplicity of implementation.

As indicated, the above assumptions were appropriate for earlier delay line models. However, no bandwidth advantages seem to be realizable with recent $\tau/2$ glass delay lines over τ lines. Thus, method a) would definitely be preferable over b) and c).

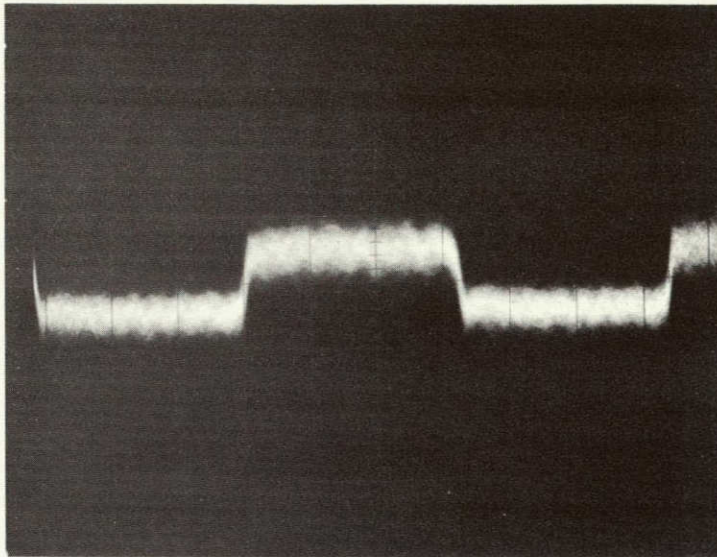
3.4 GENERAL RESULTS AND DISCUSSION

3.4.1 Noise Performance

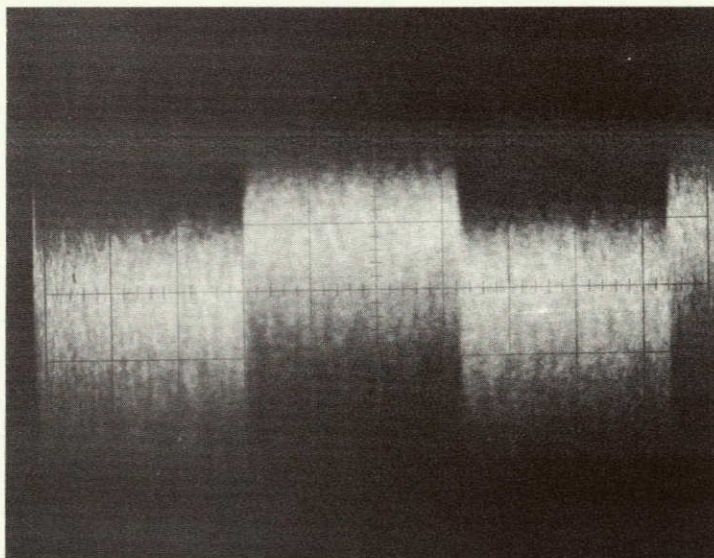
Because of the combline characteristic of the combline filters, various problems with respect to noise filtering that are unique to this filter have to be considered and are elaborated in this section.

The total noise power at the output of the combline is reduced with respect to the input noise power according to the noise bandwidth reduction calculated in Section 4.3. A qualitative estimate of the noise reduction performance was obtained by observing the effect of the device on the output signal-plus-noise waveforms as displayed on an oscilloscope. The results of this test performed with the Mode 2 filter (see 3.3.3) are shown in Figure 3-21. One trace represents the unprocessed output of a square wave of approximately 31.5 kHz (the frequency was adjusted so that the spectral impulses of this wave coincided with the comb-peaks of the filters). The other trace shows the filtered output, subject to a SNR improvement of 13 dB with respect to the other trace. Clearly, this observation verifies a significant reduction in noise power.

SNR is defined as the ratio of total signal power to total noise power. However, if measured at the output of the combline, this quantity needs some explanation. The output noise has the characteristic of the combline transfer function because it is, like any input signal, subjected to the line-to-line correlation on which the filter is based. (The filter transfer function and the filter correlation function are related by a Fourier transform.) Thus, the noise is suppressed in the valleys, retained or



With CLF



Without CLF

Figure 3-21. Square Wave Plus Noise Test

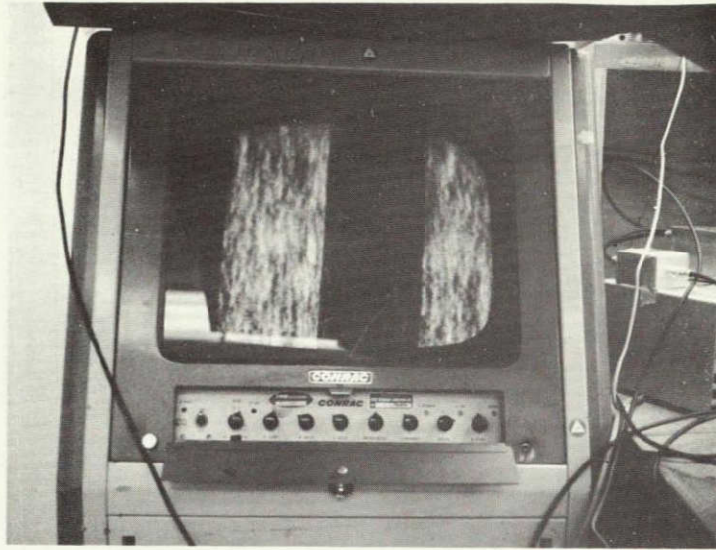
enhanced in the combs, and the signal-to-peak noise ratio is not altered if the signal is located at a comb peak (this point was verified experimentally). However, a combline filter with a certain SNR is not expected to result in a subjective improvement of, say, TV picture quality, equal to that of a filter with an output of equal signal-to-noise ratio but flat noise spectrum. This fact was also pointed out by L. E. Franks (Reference 1). Needless to say, the SNR improvement decreases if the signal is not 100 percent correlated, i. e., if it does not occur at a comb peak. Measurements indicated that a tone at a comb valley would result in a SNR degradation of 8 dB for the filter operating in Mode 2.

Another phenomenon affecting the subjective noise performance of a combline filter may be tentatively explained in terms of the memory inherent to the filter (see Appendix B and consider the impulse response). Horizontal regions are stored in the delay line and "played back" during subsequent horizontal lines. This has the effect of smearing out the short horizontal streaks, characteristic of a noisy TV picture, into the vertical. This effect is illustrated in Figure 3-22 which shows the monitor display of a vertical bar with additive noise with and without combline filtering.

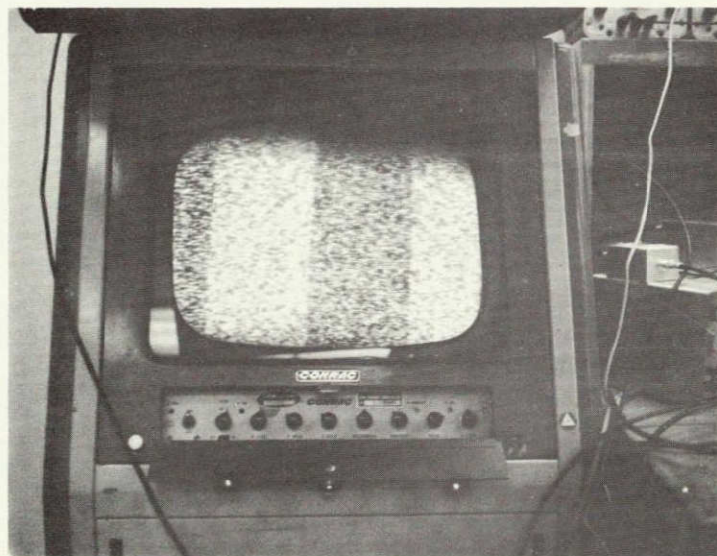
3.4.2 Comblined Filtered Video Signals

To begin the discussion on the effects of a combline filter on a video signal, let us consider the video signal due to the image of a vertical black bar. Referring back to Section 2, we recall that the spectrum of this signal is confined to harmonics of the line frequency. Since a combline filter with a uniform peak response processes these frequency components uniformly (they are equally attenuated or amplified and the phase shift is zero) the signal should remain undistorted. This is illustrated in Figure 3-23 which shows a TV monitor display of this type of signal.

Now consider a nonvertical bar whose spectrum has strong peaks at unequal intervals from the filter comb peaks. Since the filter phase and amplitude response is nonuniform at these points (e. g., see Figures 3-13 and 3-14), we suspect that the signal emerges distorted. To gain a qualitative appreciation for this point, the signal processed by the Mode 2 filter of a horizontal black bar was displayed on a monitor. This result is also shown in Figure 3-23.



With CLF



Without CLF

Figure 3-22. Square Wave Plus Noise on Monitor

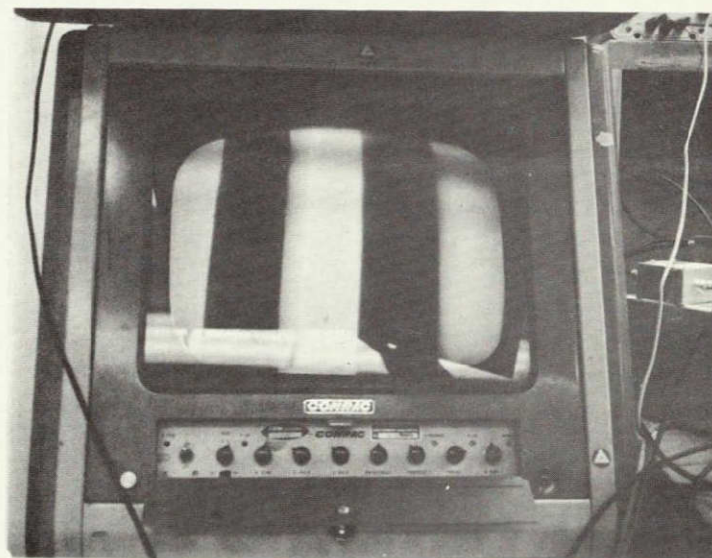
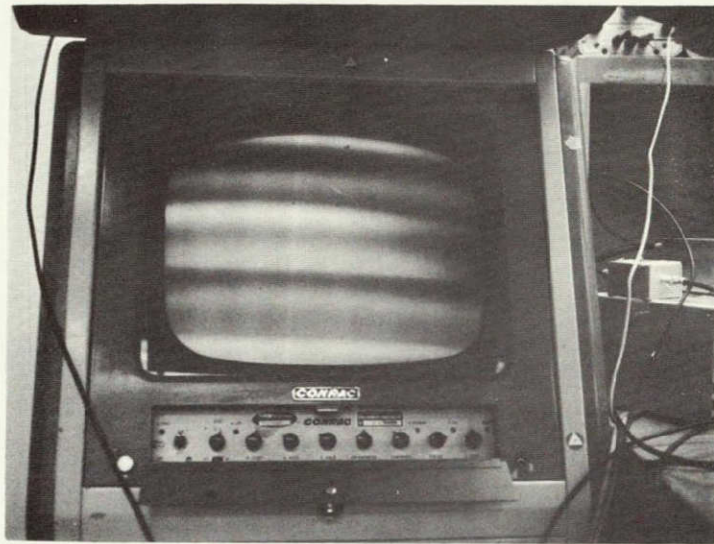


Figure 3-23. Horizontal and Vertical Bar Test
With CLF

An alternate explanation for these distortion phenomena may follow the time domain considerations set forth at the end of 3.4.1.

In an attempt to minimize these effects, the latter signal was processed with the Mode 1 filter which has wider combs. The resulting picture was indeed less distorted. However, since the PVR was smaller, noise filtering was insignificant. This resulted in an overall picture quality that was not noticeably improved.

In conclusion, the key results of this section are summarized as follows:

- Mode 1 causes minimal picture distortion. The SNR improvement is small, and insignificant picture improvement is achieved.
- Mode 2 causes severe distortion of the horizontal picture content. Significant SNR improvement and modest picture improvement result.
- There is no distortion (in either mode) for picture material that is 100 percent correlated at the line frequency, i. e. , whose spectrum coincides with the line harmonics. Significant picture quality improvement is obtained.
- In both modes, noise "smearing effects" occur that may subjectively degrade the picture.

The inherent efficiency of a combline filter in filtering noise between passbands certainly seems to make it attractive for processing video material. However, the noise smearing effect and particularly the signal distortion are severe drawbacks. We conclude that a combline filter does not offer substantial picture improvement if used as a baseband processor. If used as a PLL loop filter, however, most of the difficulties can be overcome and parts of Section 4 are devoted to this question.

4. COMBLINE PHASE-LOCK LOOP

4.1 INTRODUCTION

In the previous section, the comblin filter was shown to be very effective in improving the signal-to-noise ratio of signals with repetitive spectra. Placed in a phase-lock loop as a loop filter, it should effectively reduce the loop-noise-bandwidth. Thus the loop threshold sensitivity should increase.

The purpose of this section is to demonstrate that a phase-lock loop with a comblin loop filter is feasible and that threshold extension is achievable with such a loop. Included is an analysis of the loop transfer functions to assess the dependence of important loop characteristics on the loop parameters. A basic PLL is then implemented using an analog comblin filter. Various experiments are reported to evaluate loop performance.

4.2 UPCONVERSION

Two reasons prompted the decision to operate the PLL at a frequency of approximately 240 MHz.

- Previous experience at this frequency and existing hardware made it possible to get early experimental results.
- Higher sensitivity can be achieved with a VCO at 240 MHz than at 50 MHz.

Figure 4-1 shows a block diagram of the circuit used to upconvert the incoming signal at 50 MHz. An analysis of the spurious frequencies showed that 185 MHz is the best mixer frequency. The circuit contains AGC and a limiter stage and the response curve is plotted in Figure 4-2.

4.3 BASIC PLL SYSTEM

4.3.1 Description

Figure 4-3 shows the basic concept. The receiver consists of two subloops. One is a low pass loop of the conventional first or second order type. This loop is required to track the carrier and low frequency modulation if the comblin filter does not have dc response. The bandwidth

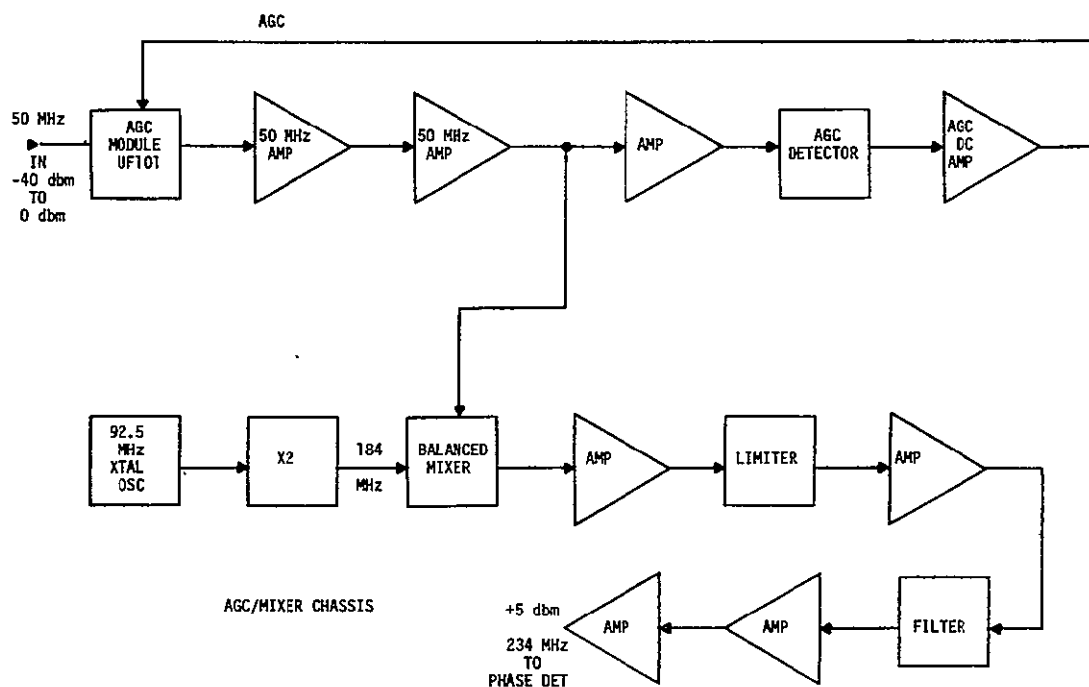


Figure 4-1. 50 MHz to 235 MHz Upconverter Block Diagram

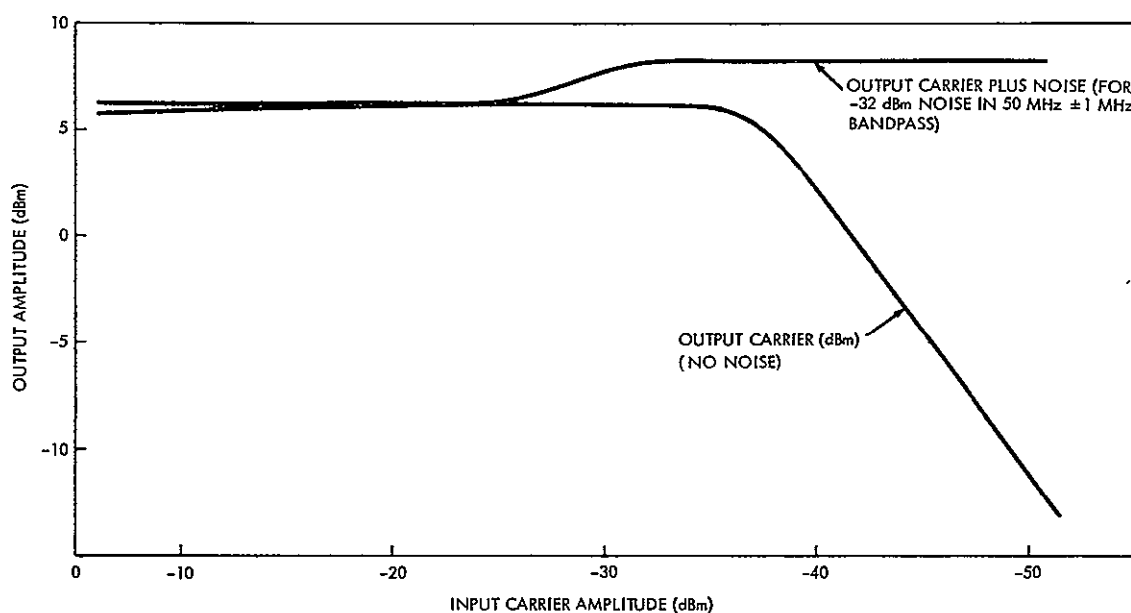


Figure 4-2. Upconverter Transfer Characteristics

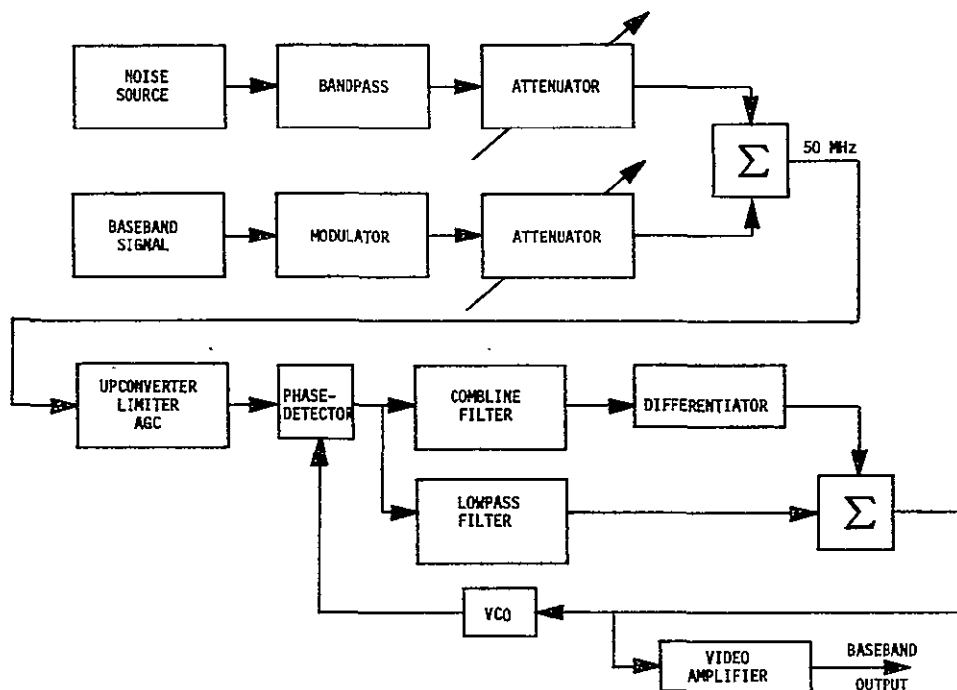


Figure 4-3. Basic PLL System Block Diagram

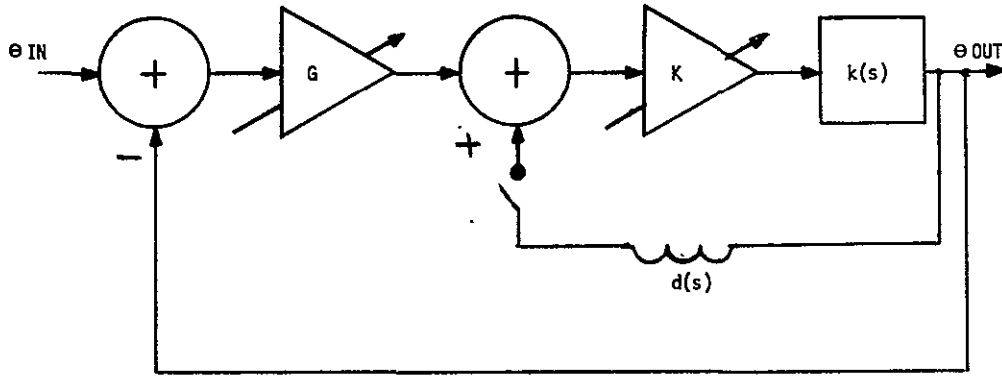
depends on the width of the frequency band to be tracked and other requirements that will be discussed in 4.3.4.

The second loop contains a combline filter tuned to the line repetition frequency. Various comb filters were discussed in detail in Section 3. The differentiator in this loop is added for stability reasons (see 4.3.3) and for compensating the $1/s$ of the VCO to ensure constant loop gain.

We assume that the differentiator just cancels the integrator and that a basic combline filter is used. The phase equivalent circuit of the combline loop is given by Figure 4-4, where G is the total open-loop gain due to the differentiator, VCO, phase detector, and any additional amplification or attenuation.

4.3.2 Comblne Subloop

Analytically, the combline subloop depicted in Figure 4-4 is a special case of the combline filter with external feedback as discussed in 3.3.3. In the present case, the β feedback network has unity transfer function. Some of the results of 3.3.3 are, therefore, applicable here, and vice versa. What follows in this section is a more detailed analysis of the transfer functions for this special case.



$$d(s) = e^{-s\tau}$$

$$k(s) = \frac{\omega_0}{s + \omega_0}$$

ω_0 = low pass 3 db cutoff

τ = line period

K = comb filter gain

G = open loop gain

Figure 4-4. Phase Equivalent Circuit of the Comblines Subloop

4.3.2.1 Frequency Domain Analysis

The transfer function for the comblines subloop is given by

$$H(j\omega) = \frac{GK}{1 + GK - K \cos \omega\tau + j \left(\frac{\omega}{\omega_0} + K \sin \omega\tau \right)} \quad (4-1)$$

The amplitude characteristic $|H(j\omega)|$, determined numerically, is plotted in Figure 4-5 around the first comb and in Figure 4-6 around the 100th comb. It is seen that the comb shape and the peak-to-valley ratio (PVR) are functions of G , ω_0 and K of the comblines loop.

Another important parameter determined by G , K , and ω_0 is the comb envelope rolloff.

A number of computer programs have been written (see Appendix B) to study these characteristics in detail. Figure 4-7 depicts a plot of relative comb peak amplitude versus comb harmonics and demonstrates

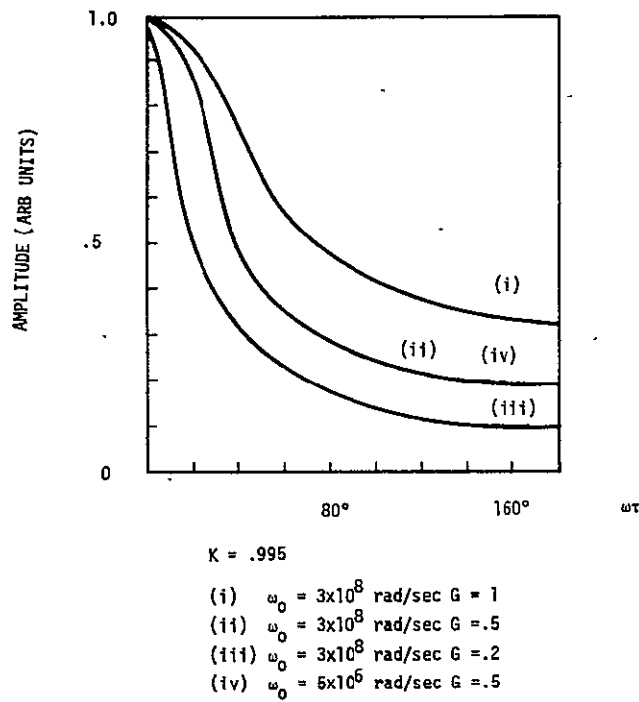


Figure 4-5. Amplitude vs Normalized Frequency for Fundamental of Comb Filter PLL

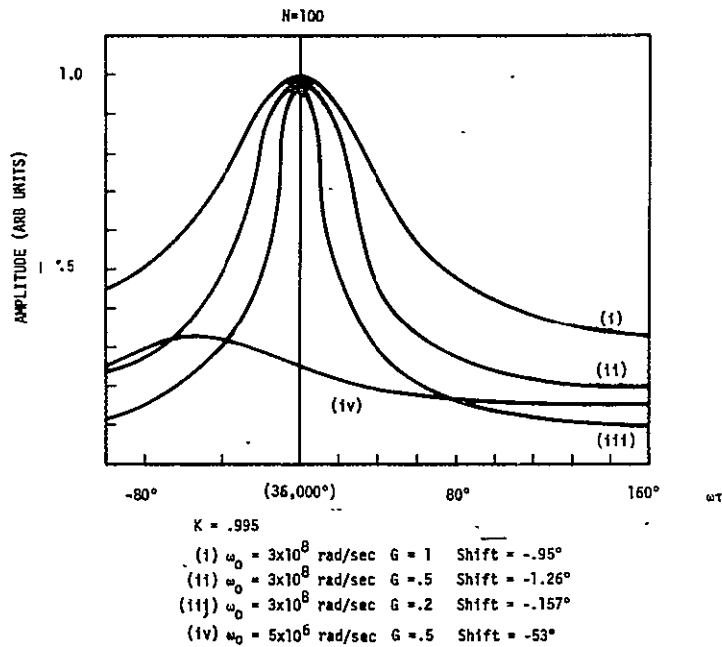


FIGURE 4-6. PLOT OF AMPLITUDE VS. NORMALIZED FREQUENCY FOR 100TH HARMONIC OF COMB FILTER PLL

Figure 4-6. Amplitude vs Normalized Frequency for 100th Harmonic of Comb Filter PLL

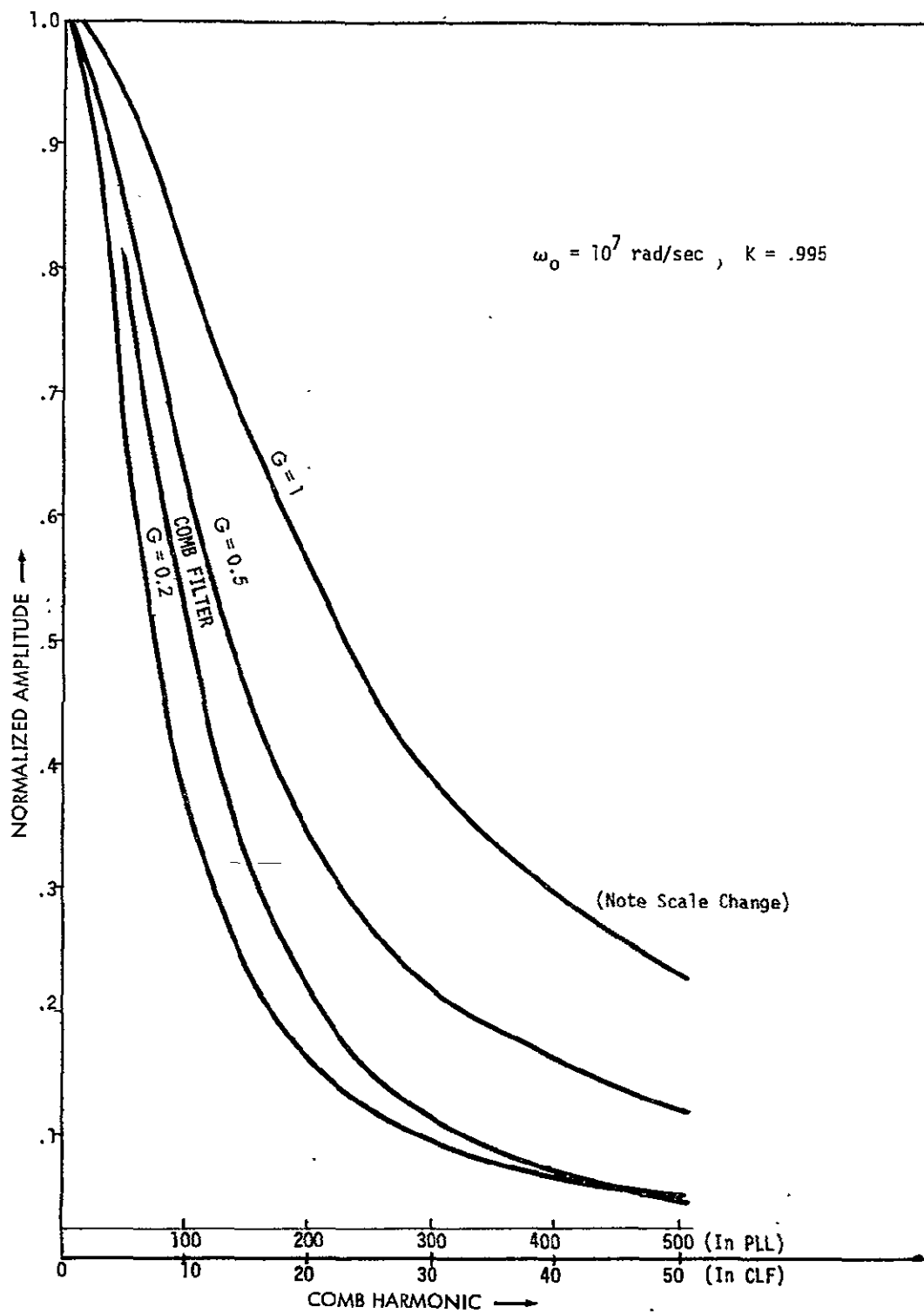


Figure 4-7. Relative Amplitude of Combs in Phase-Lock Loop

the fact that the envelope bandwidth increases with increasing open loop gain G . (The comb peak envelope of the corresponding combline filter by itself is also included for comparison.) For proper combinations of G and K , the envelope bandwidth of the PLL may become wider than ω_0 . Thus the negative feedback has the effect of widening the comb filter response.

This effect is explored in more detail in Figure 4-8, which shows plots of the envelope 3 dB bandwidth versus the open loop gain G . It is evident that the bandwidth drops sharply for small G values.

Figures 4-9 and 4-10 show the effects of various parameters on the comb Q factor and the shift of the comb peaks.

Figure 4-11 shows a plot of PVR versus K for various values of G . PVR is an important quality, since it is readily measurable and permits an easy estimate of the noise bandwidth reduction to be expected. Generally, the higher PVR, the better the noise reduction. PVR increases with K , but is reduced for increasing open-loop gain G .

Figure 4-12 depicts a plot of the noise bandwidth reduction (NR) versus K . Since mean-square loop noise error is reduced in proportion to loop noise bandwidth and if the modulation error remains fixed, the receiver threshold should increase in proportion to the noise bandwidth reduction. Figure 4-12 gives, therefore, a direct indication of the threshold improvement to be expected.

The preceding analysis leads to several interesting conclusions. It is evident from Figures 4-10 and 4-11 that a tradeoff between the bandwidth of the comb structure and NR is unavoidable since increasing G increases the bandwidth, but decreases NR. Similar adverse tendencies are true for the minor loop gain K , except when G is large enough. For this case, increasing K improves both the bandwidth and NR.

The choice of G , K , and ω_0 may be limited because of delay line bandwidth limitations (ω_0 fixed). Moreover, the comb Q factors may have to be adjusted to the signal spectrum (lower Q 's at higher frequencies). Figures 4-8 and 4-9 indicate how the comb shapes are determined by K , G , and ω_0 . Note that, for large ω_0 , the Q factors (or widths at half

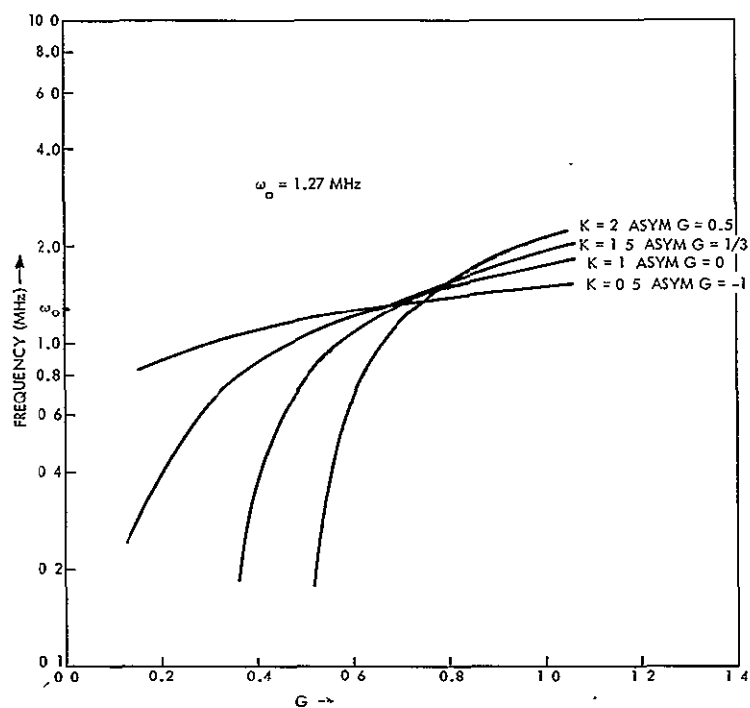


Figure 4-8. Envelope 3-dB Bandwidth vs G in Phase-Lock Loop

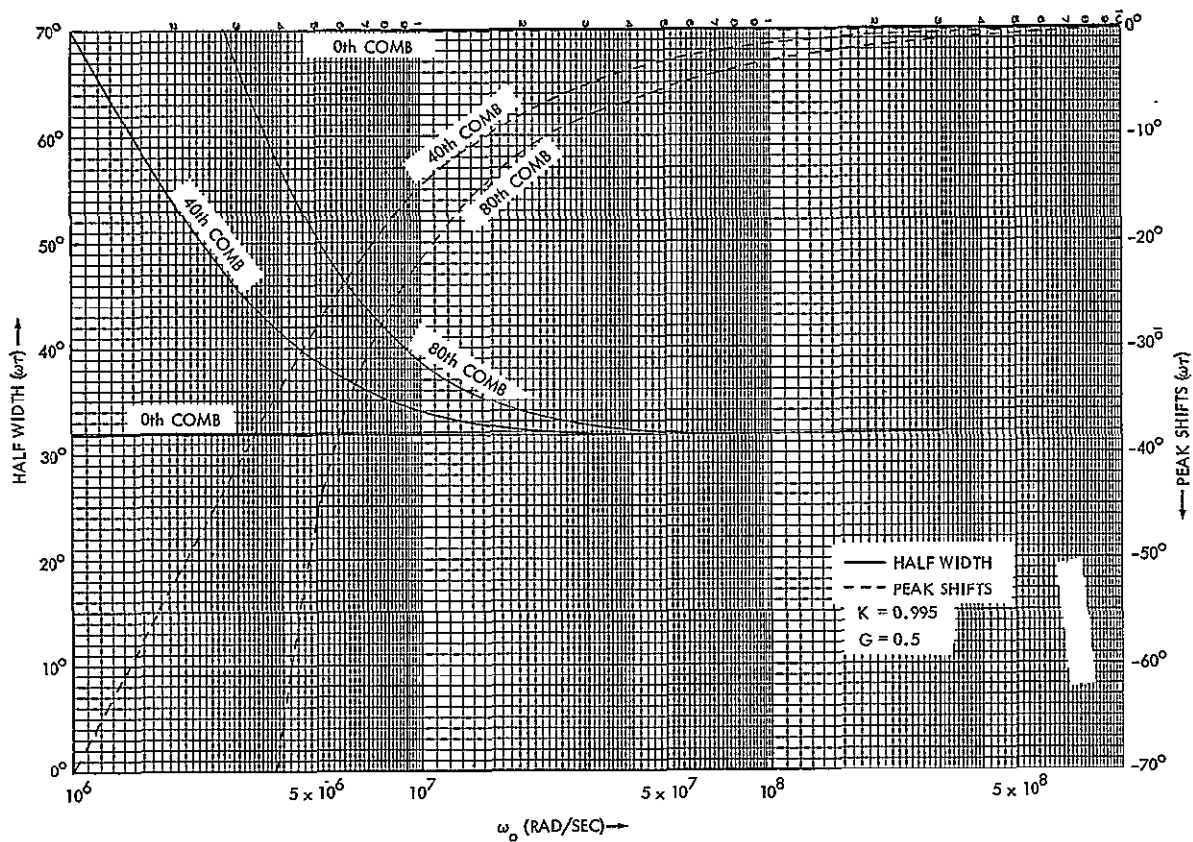


Figure 4-9. Half Width and Peak Shifts of Combs in Phase-Lock Loop vs Low Pass Cutoff Frequency, ω_0

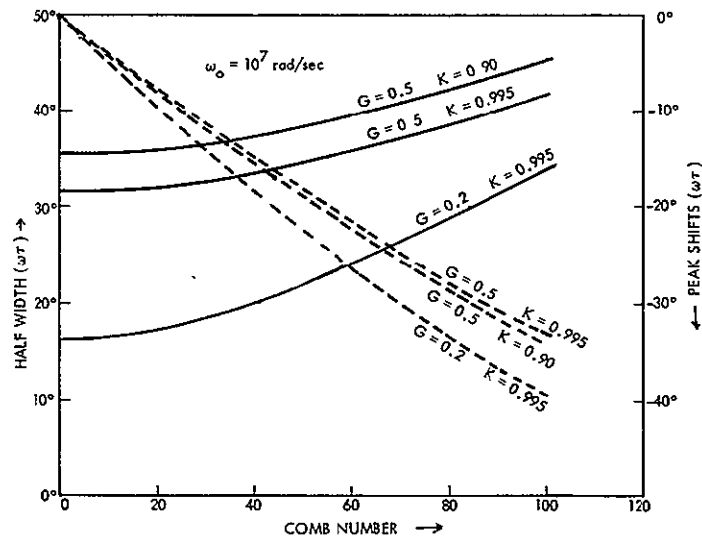


Figure 4-10. Half Widths and Peak Shifts of Combs in Phase-Lock Loop vs Comb Number

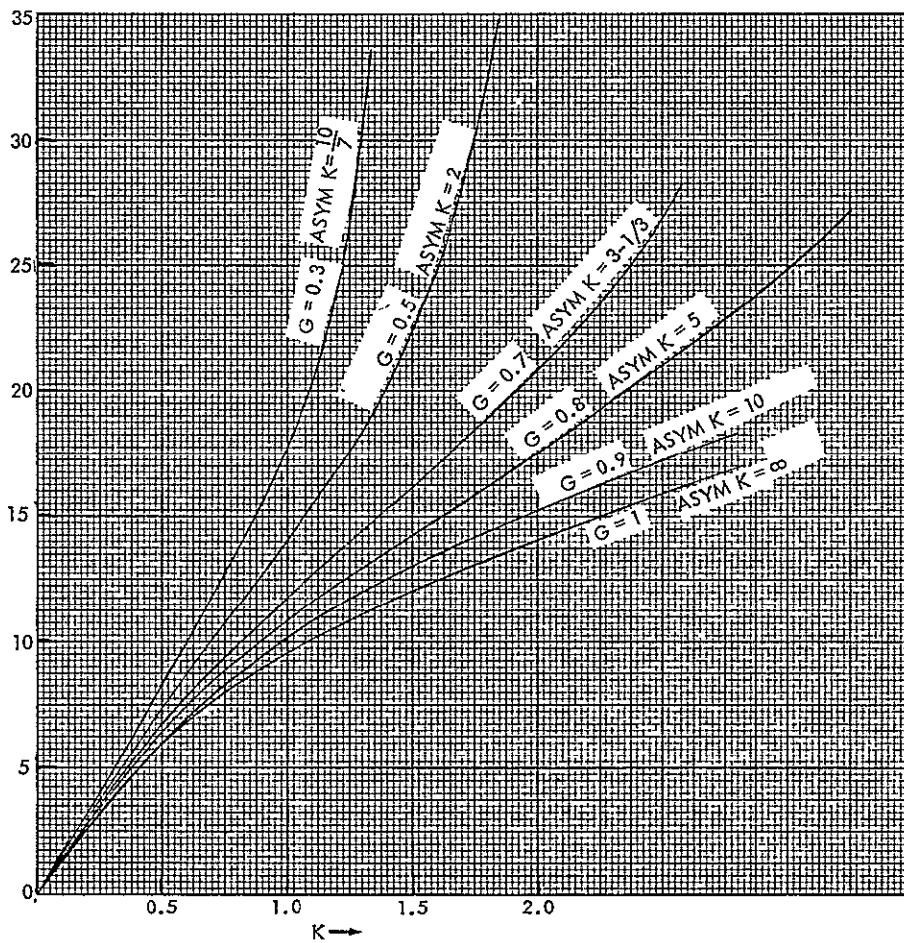


Figure 4-11. First Peak-to-Valley Ratio vs K in Phase-Lock Loop

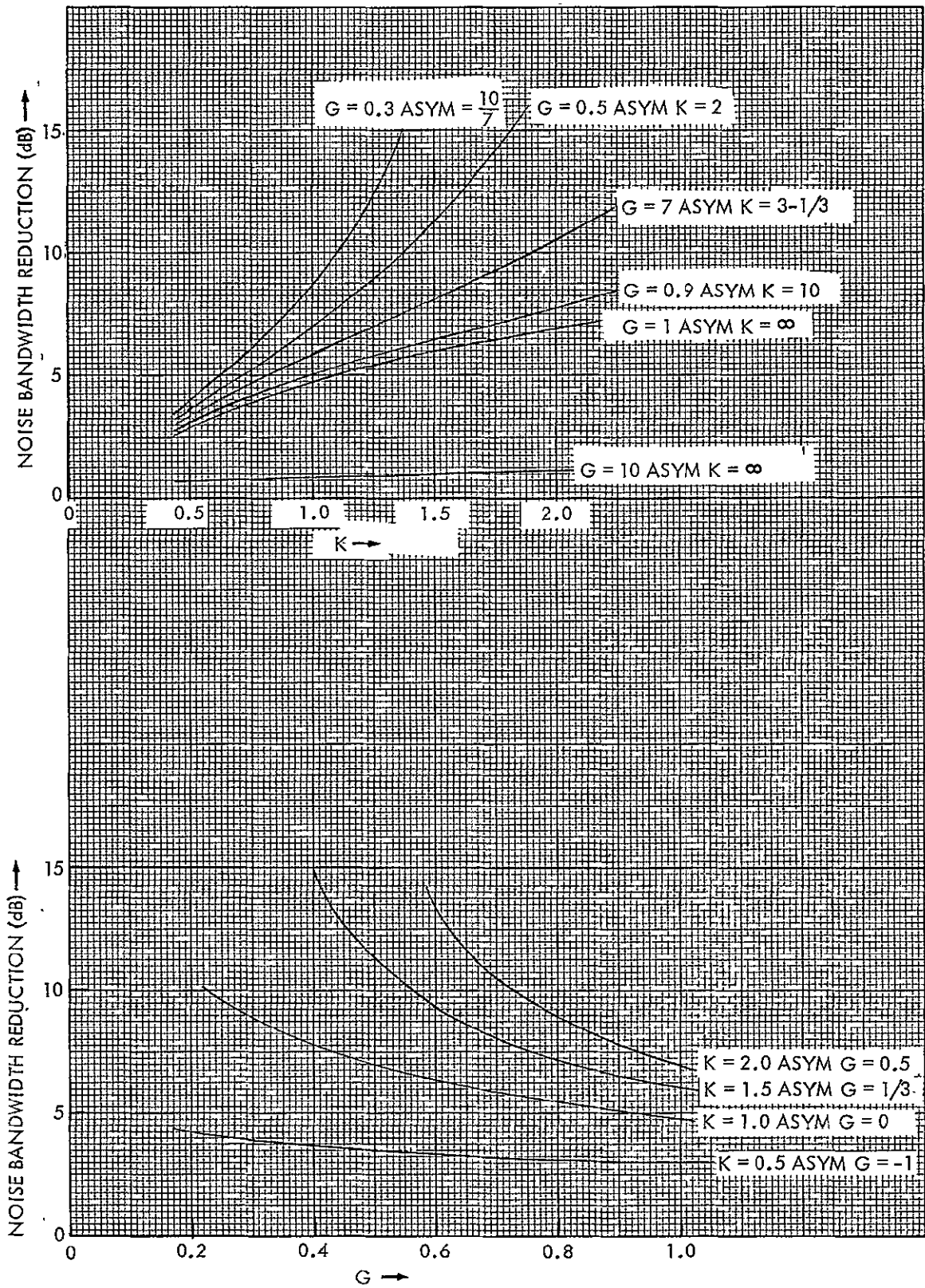


Figure 4-12. Noise Bandwidth Reduction vs K, G

height) approach the same value for all combs. For smaller ω_0 , the Q's decrease at rates that are faster for higher-order combs. This is desirable since the comb width of the TV spectrum increases at higher frequency.

It should be mentioned at this point that G depends on the amplitude of the input RF signal into the phase detector. Thus, if the RF signal is fading, G decreases and the PVR increases. This results in more effective noise filtering which is desirable, but the error due to modulation may increase. These effects have to be considered when optimizing the various loop gains unless RF signal variations are effectively eliminated.

Of special interest is the question of analytically optimizing the open-loop gain G with respect to the total (noise and modulation) error, which is generally accepted as determining threshold. The problem can be summarized briefly as follows:

Large G decreases the error due to modulation. However, the effective noise bandwidth increases due to decreasing PVR. This results in a larger noise error. Small gain, on the other hand, reduces the noise bandwidth and thus improves the noise error. But the modulation error increases.

These effects of G on threshold have been observed experimentally. No attempts have been made to optimize G, however. Further study appears necessary to optimally design the loop gains and to operate the PLL with minimum threshold.

4.3.2.2 Time Domain Analysis

This section contains a study of the combine loop impulse response and related topics. The effects of ω_0 , τ , and G on the time domain behavior are evaluated. ω_0 is found to affect mainly the horizontal resolution: the larger ω_0 , the better the resolution. G similarly affects both the horizontal and the vertical resolution.

The impulse response is first calculated because it describes, as does the transfer function, the input-output relation of the system. Moreover, it allows for easy determination of the response of the system

to an arbitrary excitation (which is Laplace transformable) by simple convolution of its impulse response and the excitation function.

The impulse response $h(t)$ is obtained by taking the inverse Laplace transform of the transfer function $H(s)$ given by (4-1). $H(s)$ is repeated here for convenience and brought into a more convenient form for transformation.

$$H(s) = \frac{A}{B + \frac{S}{\omega_o} - Ke^{-s\tau}} \quad (4-2)$$

where

$$A = GK$$

$$B = 1 + A$$

$$H(s) = \frac{A}{B + \frac{S}{\omega_o}} \left[\frac{1}{1 - \frac{K}{B + \frac{S}{\omega_o}} e^{-s\tau}} \right] \quad (4-3)$$

Since

$$\left| \frac{K}{B + \frac{S}{\omega_o}} \right| < 1 \text{ and } |e^{-s\tau}| \leq 1$$

one may expand the term in brackets by a power series,

$$\begin{aligned} \left[\frac{1}{1 - \frac{1}{B + \frac{S}{\omega_o}} e^{-s\tau}} \right] &= 1 + \left(\frac{K}{B + \frac{S}{\omega_o}} \right) e^{-s\tau} + \left(\frac{K}{B + \frac{S}{\omega_o}} \right)^2 e^{-2s\tau} + \dots \\ &= \sum_{n=0}^{\infty} \left(\frac{K}{B + \frac{S}{\omega_o}} \right)^n e^{-ns\tau} \end{aligned} \quad (4-4)$$

so that (4-3) becomes

$$\begin{aligned}
 H(s) &= \frac{A}{B + \frac{S}{\omega_o}} \left[\sum_{n=0}^{\infty} \left(\frac{K}{B + \frac{S}{\omega_o}} \right)^n e^{-ns\tau} \right] = \sum_{n=0}^{\infty} AK^n \frac{e^{-ns\tau}}{\left(B + \frac{S}{\omega_o} \right)^{n+1}} \\
 &= \sum_{n=0}^{\infty} AK^n \omega_o^{n+1} \left(\frac{e^{-ns\tau}}{(B\omega_o + S)^{n+1}} \right) \quad (4-5)
 \end{aligned}$$

The inverse Laplace transform of the quantity in brackets is well known; the exponential term becomes a time delay term, and the $\frac{1}{(B\omega_o + S)^{n+1}}$ term becomes $\frac{1}{n!} (t^n \exp(-B\omega_o t))$. The impulse response can now be written

$$h(t) = L^{-1} [H(s)] = \sum_{n=0}^{\infty} h_n(t) \quad (4-6)$$

where

$$h_n(t) = \begin{cases} 0, & t < n\tau \\ \frac{AK^n \omega_o^{n+1}}{n!} (t - n\tau)^n \exp[-B\omega_o(t - n\tau)], & t \geq n\tau \end{cases} \quad (4-7a)$$

Before investigating these equations, suppose that we have a system with infinite bandwidth, i. e., $\omega_o = \infty$. It can be shown that the individual terms $h_n(t)$ become $h_n(t) \propto \delta(t - n\tau)$ so that the impulse response is

$$h(t) \propto \sum_{n=0}^{\infty} \delta(t - n\tau)$$

Thus the impulse response consists of an impulse train. This may be visualized by assuming that the incoming impulse is fed back, delayed by τ , appears at the output, and is fed back again, etc. (It should be noted in passing that this response is much like that of a tapped delay line.)

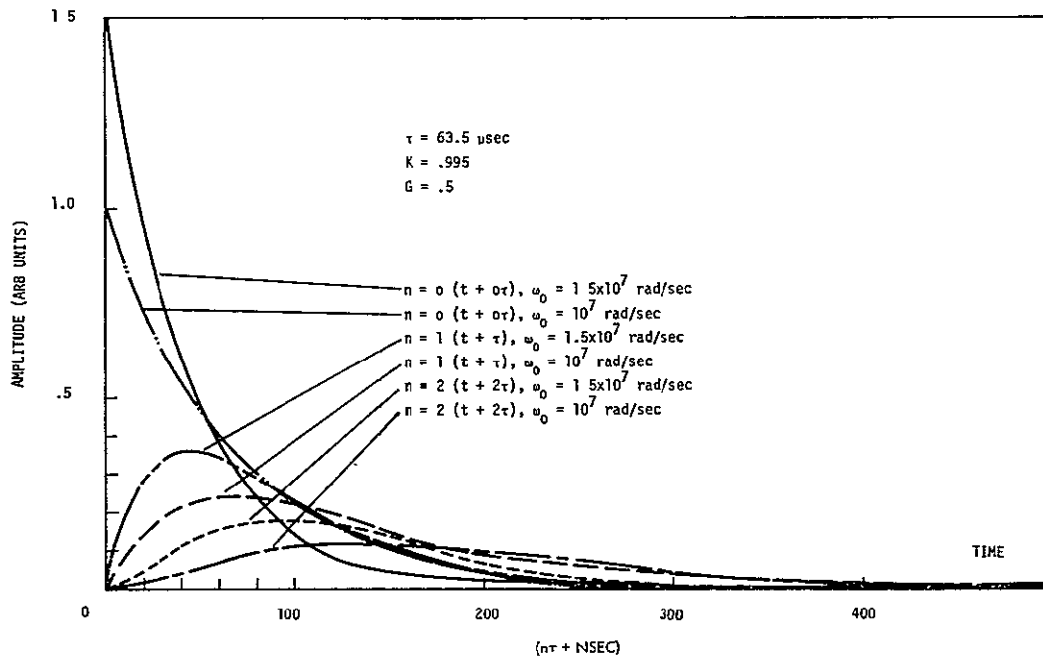
If the system contains a low pass filter, i.e., if $\omega_0 \neq \infty$, we must consider (4-6) and (4-7). The terms $h_n(t)$ are plotted in Figure 4-13a for various parameters on the same time scale (in actuality, they are shifted by $n\tau$). It is apparent that $h_n(t)$ has a peak at a time somewhat greater than $n\tau$ and drops off rapidly thereafter such that

$$h_n(t) \text{ at } t = (n+1)\tau \approx 0 \text{ and } h(t) \approx h_n(t) \quad (4-7b)$$

where $n3n\tau \leq t \leq (n+1)\tau$

Therefore, it can be concluded that the complete impulse response of (4-6) is approximately a pulse train with pulses having the general characteristic shown in Figure 4-13a, and where subsequent pulses are delayed by τ .

Suppose, for example, that the TV signal due to a short thin black bar on the i th scan line is to be processed (assuming that such an image gives rise to a single rectangular pulse). Recalling that the combline filter response is obtained by convolving its impulse response with the excitation, it is clear that the response to the TV pulse is a pulse train, subsequent pulses being delayed by τ and having amplitudes and widths



PLOT OF AMPLITUDE VS. TIME OF COMB LINE FILTER IN
PHASE LOCK LOOP

Figure 4-13a.. Amplitude vs Time

proportional to the impulse response pulses (and to the TV pulse). The practical consequence is that the n th response pulse arrives while scanning the $(i + n)$ th line. In short, the image appears smeared out horizontally by an amount proportional to the "size" of the n th response pulse, which is, therefore, a direct indication of the horizontal resolution.

Some measure of the size of h_n can be obtained by taking the following integral:

$$I = \int_0^{\infty} h_n(t) dt = \left(\frac{A}{n!} K^n \omega_o^{n+1} \right) \left(\frac{n!}{(B \omega_o)^{n+1}} \right) = G \left(\frac{K}{1+GK} \right)^{n+1} \quad (4-7c)$$

It is expected that the smaller this integral, for $n > 1$ the better the resolution. It is seen that I decreases for increasing n (since the term in parenthesis is smaller than 1) and increasing G . The influence of K is less pronounced for higher n . Interestingly enough, I does not depend on ω_o , but no significant physical meaning could be attached to this fact.

Another interesting observation can be made by computing the peaks of $h_n(t)$, which can be shown to occur at

$$t_{\max} = \frac{n}{(1+GK)\omega_o}$$

Note that t_{\max} depends on n . In terms of our example, this means that the smearing is not vertical but slightly diagonal. The effect can be corrected by changing the time delay τ slightly, and was observed experimentally.

Again recalling the convolution process, the shape of $h_n(t)$ for $n = 0$ can be shown to be largely responsible for vertical resolution. Figure 4-13b shows the effect of G and ω_o on $h_0(t)$. The larger ω_o and G , the narrower h_0 , which results in better horizontal resolution.

The time response was calculated for two examples. The first is for the signal of a horizontal black bar of 10 lines width. The image gives rise to a pulse train with a duration $t = 10 t_f$ and a duty cycle of t_f . The convolution of this signal with the impulse response is shown in Figure 4-13c for different G 's. The larger the G , the faster the response, i.e., the

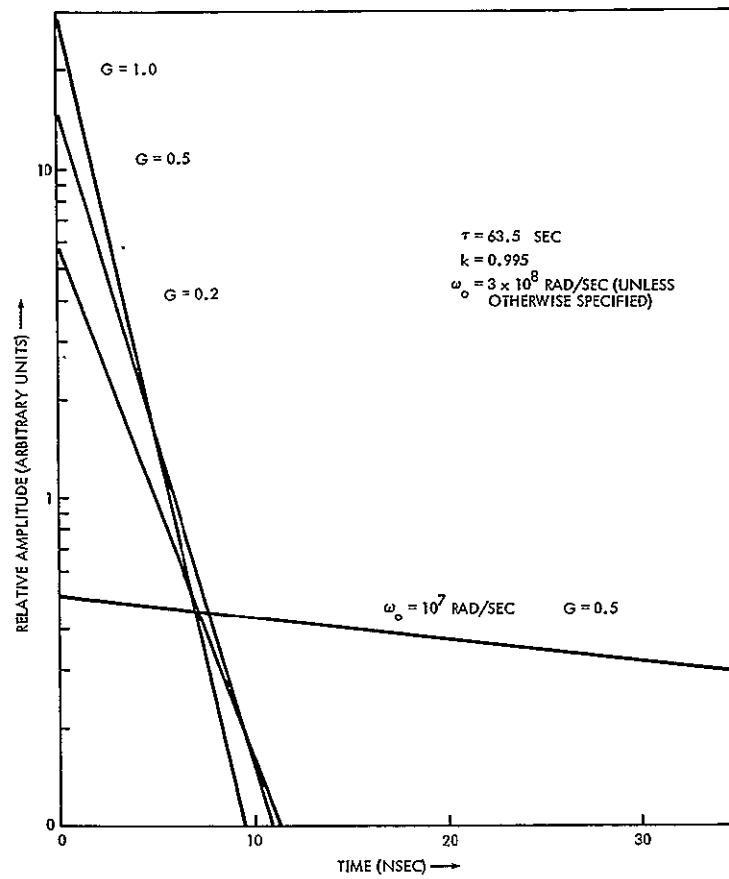


Figure 4-13b. Amplitude vs Time for $n = 0$

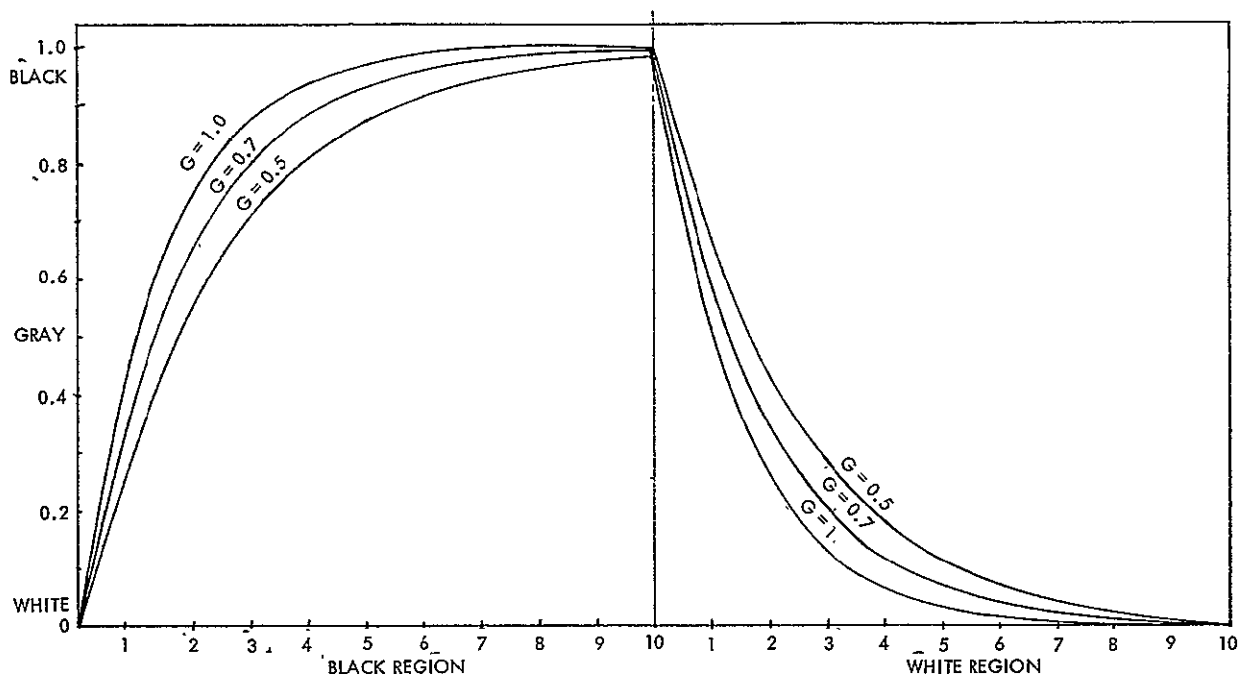


Figure 4-13c. Response to Horizontal Half-White, Half-Black Picture (10 black lines followed by 10 white lines)

fewer gray lines and the better the horizontal resolution. This is compatible with the previous observations.

The second example is for a vertical half-black, half-white image. The corresponding signal is a pulse train with a pulse width of $t_\ell/2$ and a duty cycle of t_ℓ . The combline filter time response is shown in Figure 4-13d, where it is seen that G determines the vertical resolution in much the same way as the horizontal resolution.

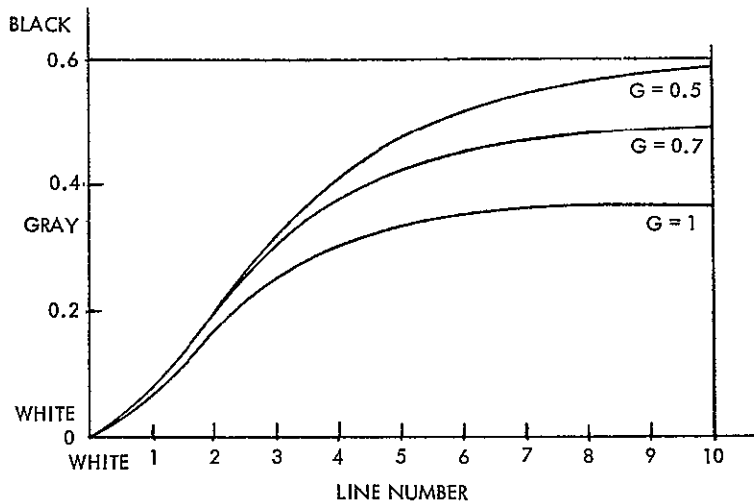


Figure 4-13d. Response to Vertical Half-White, Half-Black Picture

The relationship between the time and frequency responses may be further explored by considering an ideal comb response. Suppose that such a response is given by a pulse train with a duty cycle $1/\tau$ and a pulse width $1/T$. The time response is then given by the inverse Fourier transform, i.e., an impulse train having the characteristic of a sinc function. Now consider the step response, which is obtained by integrating the impulse response. For $t \rightarrow \infty$, the response amplitude approaches some constant value. However, for finite τ , there may be some ringing effect. For fixed τ , the "overshoot" is proportional to $1/T$ and the rise time is proportional to T . Thus, if T is large, i.e., if the comb width is small, the rise time is long, and the ringing effect is minimal because the overshoot is small. However, if the comb width is wide (small T), there is a large overshoot and a fast rise time. Perhaps the considerations may

also be used to explain the distortion effects visible in Figure 3-23. Notice that the immediate response to the horizontal black bar is white (fast rise time) but returns to gray (overshoot) and white again. A similar effect can be seen in the bottom picture of Figure 3-23, where the gray bar at the upper end of the picture is due to the frame blanking.

4.3.3 Stability Criteria

This section presents a stability analysis for the basic combline PLL. Referring to Figure 4-4, the loop containing only the combline filter was analyzed with and without the differentiator.

The Nyquist criterion was employed to investigate stability. Although the Bode diagram permits straightforward design procedures, it could not be used effectively because the circuit is a multiloop system containing nonminimum phase elements and a minor loop that is unstable under certain conditions. If corresponding transfer functions are put into a form suitable for stability analysis, the denominator may be written in the form

$$D = 1 + A(s)$$

where, for the system with the differentiator,

$$A(s) = A_d(s) = \frac{s}{\omega_o} - Ke^{-s\tau} + GK \quad (4-8)$$

and

$$A(s) = A_s(s) = \frac{s^2}{GK \omega_o} + \frac{s}{GK} - \frac{s}{G} e^{-s\tau} \quad (4-9)$$

for the system without the differentiator. The condition for stability is that the polar plot of $A(s)$ does not encircle the $(-1, j0)$ point. Sketches for these plots are shown in Figures 4-14a and 4-14b. Neither plot encircles the $(-1, 0)$ point, i. e., both systems are stable for the parameters used.

It turns out that the zeros of the imaginary part of $A_s(s)$ do not exist for $K < 1$ except at the origin. If $K \geq 1$, the locus crosses the

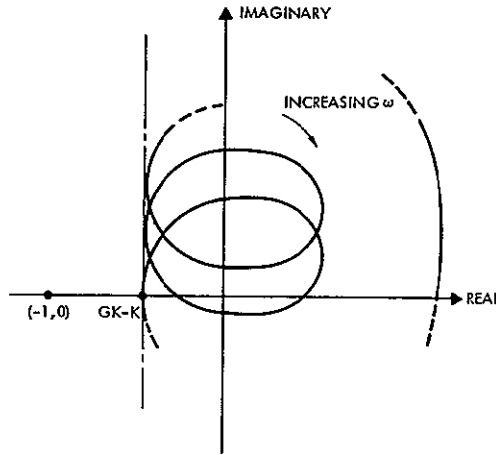


Figure 4-14a. $A_d(s)$

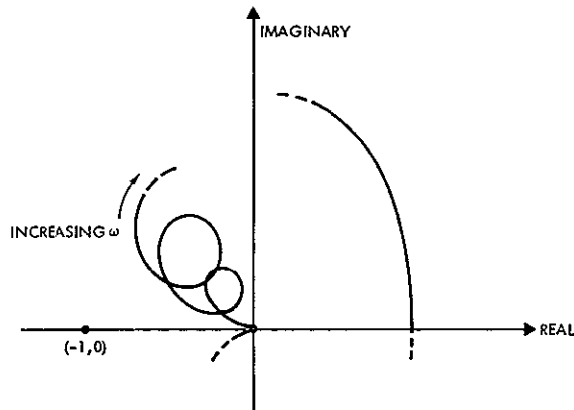


Figure 4-14b. $A_s(s)$

negative real axis and may encircle the $(-1,0)$ point for certain parameter values (G , τ , and ω_0). Thus the system is only conditionally stable, becoming unstable for some values of $K \geq 1$.

For the other case, a stability condition in closed form is easily available from the locus of $A_d(s)$.

$$G > 1 - \frac{1}{K} \quad (4-10)$$

This is plotted in Figure 4-15, where the marked region indicates the stability range. It can be seen that the system is stable even if the minor loop is unstable (i. e., $K > 1$). This is of practical importance, since the combine filter loop may have to be operated at high gain in

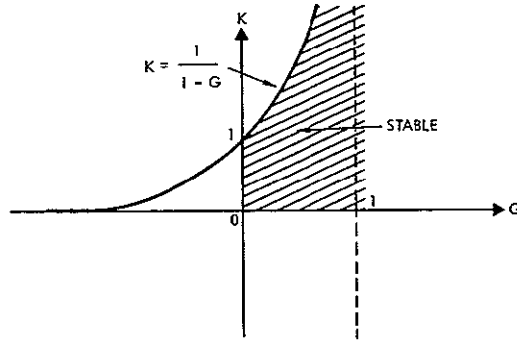


Figure 4-15. Stability Condition for the Phase-Lock Loop

order to achieve high peak-to-valley ratio of the combs. Thus the lead element is, indeed, desirable from a stability point of view.

Stability conditions can also be derived from the impulse response of the PLL.

For stability, the integral J of $h(t)$ over the infinite range has to be finite. Thus

$$J = \int_{t=0}^{\infty} \sum_{n=0}^{\infty} h_n(t) = \sum_{n=0}^{\infty} \int_{t=0}^{\infty} h_n(t) = \sum_{n=0}^{\infty} I$$

where I is given by (4-7c). Therefore

$$J = \sum_{n=0}^{\infty} G \left(\frac{K}{1 + GK} \right)^{n+1} = \frac{GK}{1 - K + GK} \quad (4-11)$$

This integral is finite if $1 + GK - K > 0$ or $K < \frac{1}{1-G}$. This is the same condition as previously obtained by the Nyquist method.

4.3.4 Low Pass Filter Subloop

The most desirable delay lines presently available do not have dc response. Combline filters using them, therefore, have no significant gain below the first comb at f_L . This makes ineffective the tracking of low-frequency components due to modulation, doppler shift, and frequency drift. The possibility of dc coupling the filter forward path

and increasing the PLL open-loop gain was tried, but found to be impractical. Even if a delay line were available with dc response, the tracking would probably be poor because of the narrow low pass response. One possibility is to add a separate feedback with a low pass characteristic around the combline filter. However, adding a separate loop with dc response was considered to be the best choice. It is especially convenient during the experimental phase, because combline characteristics can be modified without altering the carrier acquisition and holding properties significantly.

A potential interference problem between a high-gain, low-pass filter and the combline filter was of some concern. It was evaluated by calculating the combined transfer function of the combline filter and a low pass of the standard form

$$F(s) = \frac{s\tau_2 + 1}{s\tau_1} \quad (4-12)$$

giving rise to a second-order loop response. The amplitude response of the PLL is shown in Figure 4-16. Also shown is the response of the second-order PLL that would result from the low pass filter alone. It is seen that no significant interference problems seem to occur, and that the low pass filter can be designed independently. Similar results were found for low pass filters with higher gains, i.e., resulting in closed-loop response somewhat below f_L . Thus a low pass filter in parallel with a combline filter appears to be a satisfactory method for providing the proper low-frequency response of the combline PLL.

Severe interference problems were predicted and verified experimentally for low pass filters whose closed-loop responses exceeded f_L . More will be said about this problem in Section 5.

4.3.5 Modulation Error and Gain Requirements

In this section, we deal with the loop gain required to keep the loop error due to modulation below certain limits. First, we investigate loop

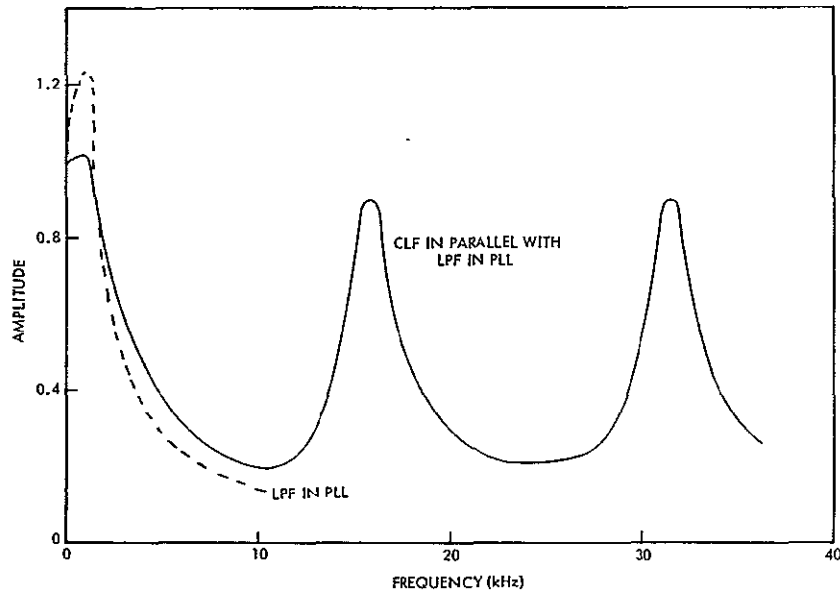


Figure 4-16. Amplitude vs Frequency

behavior in the presence of a sinusoidal modulator input.

$S(t) = A_m \cos \omega_m t$. The modulated signal becomes

$$C(t) = A_c \sin [\omega_c t + \theta_i(t)]$$

where

$$\theta_i(t) = \frac{\Delta\omega}{\omega_m} \cos \omega_m t \text{ is the input phase to the PLL}$$

$$\Delta\omega = 2\pi f_d A_m = \beta \omega_m \text{ is the peak frequency deviation.}$$

β is the modulation index, and f_d the frequency deviation constant.

The phase error may be calculated simply as the steady-state frequency response of the loop

$$\theta_e(t) = M \frac{\Delta\omega}{\omega_m} \cos (\omega_m t + \phi)$$

where M is the magnitude of the loop frequency response, and ϕ is the phase shift. M can be written in terms of the total open-loop gain G_T (including integrator, loop filter, attenuator, differentiator, etc.)

$$M = \frac{1}{1 + G_T}$$

Consider the first comb at 15 kHz where the TV peak signal spectrum is at a maximum. Suppose we want to determine G_T to keep the maximum error below a value of 0.2 radians (this value was found practical in previous PLL projects) for a given peak frequency deviation (prescribed by NASA). For $\Delta\omega = 1.1$ MHz, we obtain

$$G_T = \frac{\theta_i}{\theta_e} - 1 = \frac{1.1 \times 10^6}{15 \times 10^3} \frac{1}{0.2} - 1$$

$$G_T = 330 \approx 50 \text{ dB}$$

Suppose the combline filter has a peak gain of 30 dB at the first comb. It would then be possible to track the signal with a gain G (due to the other loop elements) of 20 dB. From Figure 4-11, we can estimate roughly that for this case the peak-to-valley ratio (PVR) would drop to a few dB, assuming that $K = 1$.

If we want to preserve PVR, G must be decreased. But with $G < 1$, which is required for high PVR, more comb-filter gain would be necessary. Unfortunately, this is practically impossible with the present configurations and delay lines since the best comb filter peak gains that could be achieved over the desired bandwidth are between 20 and 30 dB.

In summary, if the open-loop gain is kept small to achieve high PVR and effective noise filtering, the forward gain achievable with presently available combline filters is insufficient to yield the total gain G_T required for tracking the prescribed deviation. A compromise is possible but of little interest: G could be increased, resulting in a degradation of peak-to-valley ratio and ineffective noise filtering. Several possibilities to overcome this drawback of the combline PLL are discussed in Section 5.

4.3.6 Experimental Results and Discussion

Several tests were performed to verify some of the preceding analyses and to evaluate the performance of the device in terms of its ability to improve the demodulated output. These were:

- Evaluation of the comb structure obtainable in a combine PLL
- Evaluation of the ability to demodulate a TV modulated FM signal in terms of tracking and picture quality
- Signal plus noise waveform tests
- Signal-to-noise ratio tests.

These tests are described in the following sections.

4.3.6.1 Comb Structure

The PLL described in 4.3.1 was implemented with LC and Corning Glass delay lines. The filter of the low pass subloop was designed for a closed-loop response of about 10 kHz and optimal damping.

Figures 4-17, 4-18, and 4-19 show the response of a loop (with the LC delay line) to a swept modulator input. A uniform comb structure was obtained. Upon varying the open-loop gain G and keeping K at some fixed value, the following results were achieved:

<u>Peak-to-Valley Ratio (PVR)</u> <u>(dB)</u>	<u>Envelope 3 dB Bandwidth ω_{3dB}</u> <u>in Phase-Lock Loop (MHz)</u>
10.5	1.23
15	1.06
20	1.01
35	0.86

The maximum PVR obtainable was about 45 dB.

The above bandwidths can best be appreciated by comparison with the bandwidths obtainable with a combine filter by itself. Theory predicts that the bandwidth of a combine filter is increased when inserted in a PLL. The tabulation below shows some peak-to-valley ratios of a combine filter and the corresponding 3 dB bandwidth as measured on a filter that is based on the same delay line as the above PLL.

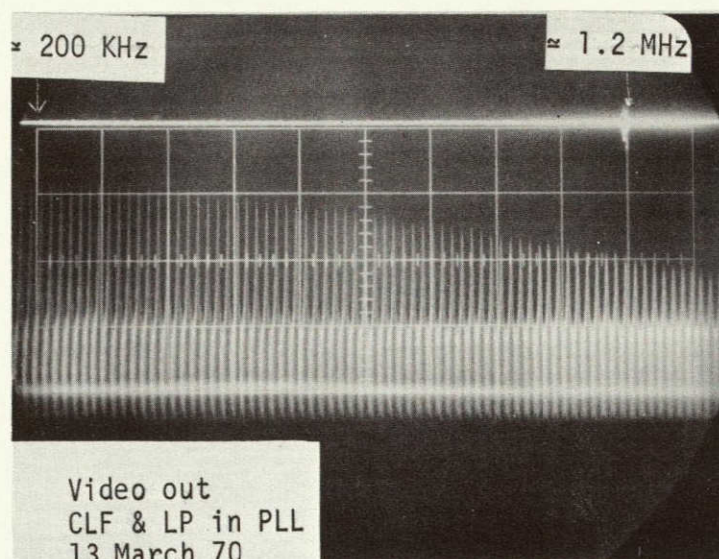


Figure 4-17. Response of Comblin Phase-Lock Loop to Swept Modulator Input (Envelope 3 dB Cutoff at 723 kHz)

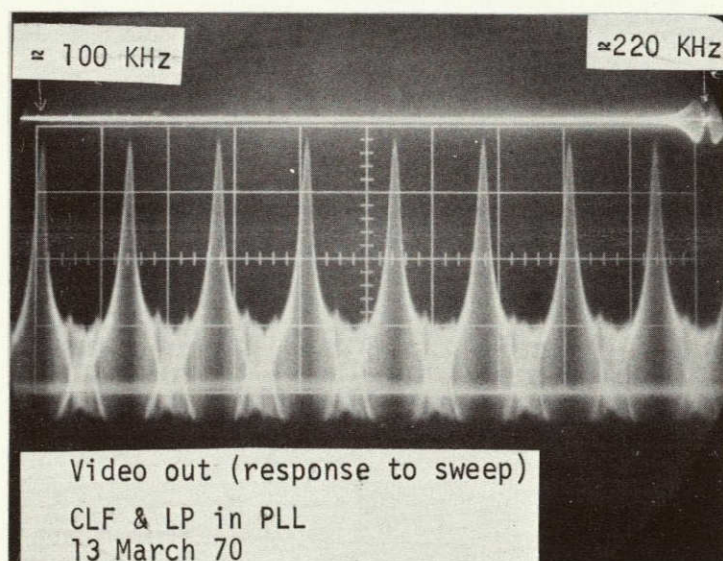


Figure 4-18. Expanded View of Figure 4-17 from 100 to 220 kHz (Peak-to-Valley Ratio at 100 kHz is 16 dB)

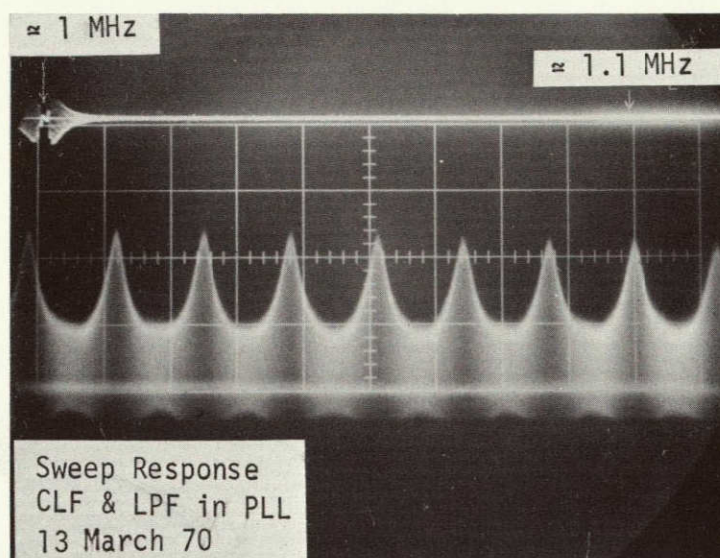


Figure 4-19. Expanded View of Figure 4-17 from 1 to 1.1 MHz (PVR at 1 MHz is 10 dB)

<u>PVR (dB)</u>	<u>ω_{3dB} (MHz)</u>
26.5	0.400
32	0.160
38.3	0.080

A conservative estimate indicates a more than five-fold improvement in bandwidth for PVR = 35 dB.

Using the new improved Corning Glass delay line made it possible to extend a 17 dB PVR response to 2.0 MHz.

4.3.6.2 Tracking and Picture Quality

An FM signal modulated with a TV signal was demodulated with the PLL. The results can be summarized as follows:

- 1) The output signals gave distorted pictures when displayed on a monitor. This problem is solely a result of combline filtering and was discussed in 3.3.3. In fact, TV signals processed in the baseband loop (3.3.4) and in the PLL were equally distorted if both loops had the same combline characteristics.

- 2) The loop gain achievable with high PVR was insufficient to track a TV modulated signal with a peak deviation Δf of 1.1 MHz. The experiments confirmed the observations made in 4.3.5.
- 3) The decreasing TV components at higher frequencies were severely contaminated by noise. This can be explained by the sharply decreasing TV spectrum (see Section 2) and the fact that flat noise added at RF is giving rise to an increasing noise characteristic at baseband. Raising the deviation would improve the SNR, but this was impossible for the reasons mentioned above.
- 4) The narrow bandwidth of the combs severely limits the acquisition and hold-in range.

Several methods to overcome these limitations will be discussed in later sections.

4.3.6.3 Signal-Plus-Noise Waveform Tests

A qualitative estimate of the noise rejection performance was obtained by observing the effect of the PLL on the output signal-plus-noise waveforms as displayed on an oscilloscope. The striking results were identical to those obtained with the equivalent baseband circuit described in 3.3.3 and are, therefore, not repeated here.

4.3.6.4 Signal-to-Noise Ratio Tests

The block diagram of the experimental setup was similar to that shown in Figure 4-3. A 95.11 kHz tone (at a comb peak) was used to simulate the TV signal. Flat narrowband (± 1 MHz) noise was added at 50 MHz. The output signal and signal-plus-noise power were measured both with the combline filter operating and open-circuited. The latter gave rise to a first-order PLL with about 2 MHz bandwidth. The envelope bandwidth of the combline PLL was also 2 MHz. The output data was converted to signal-to-noise ratio. Input noise power was held constant at -31.8 dBm (measured after the summing T in the above-mentioned bandwidth). The carrier-to-noise ratio (CNR) was varied by attenuating the modulated carrier power. For the AGC and limiter action in the upconverter, recall 4.2. The loop gains were adjusted such that the error signals at maximum CNR were identical in both cases.

Figure 4-20 represents the measured data. Curve 1 stands for the first-order loop and curve 2 for the combine PLL. An accepted definition of FM threshold is based on the graphical determination of the input CNR value, whose output SNR occurs 1 dB below an extension of the linear portion of the transfer curve. According to this definition, Figure 4-20 indicates a 16 dB threshold extension of the combine PLL over the first-order loop.

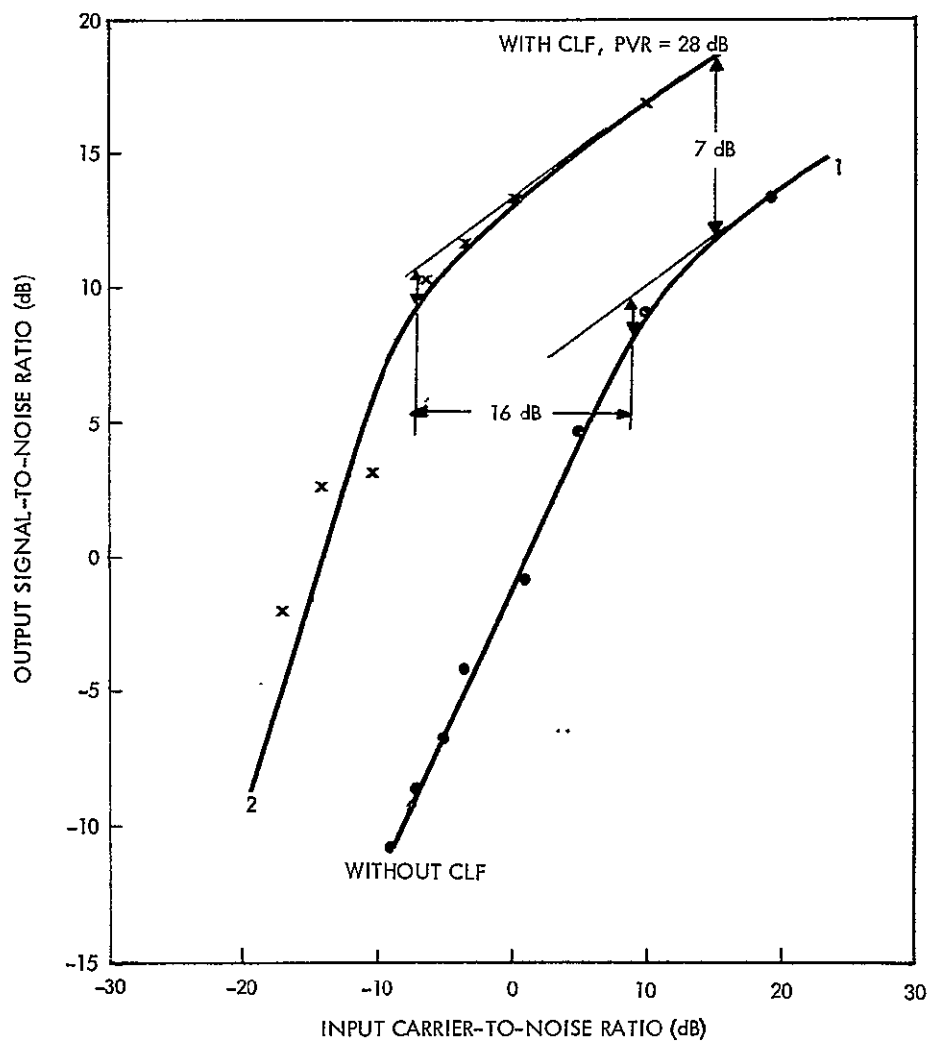


Figure 4-20. SNR of 95.11 kHz Signal vs Input CNR
Narrowband, Additive Noise

A first- and second-order PLL have identical threshold behavior if the IF noise bandwidth is narrow compared to the PLL loop bandwidth.¹ Since this is the case for the measurements in Figure 4-20, curve 1 is also representative for a second-order loop under the same conditions. If the IF noise bandwidth is much larger than the loop bandwidth, the threshold of both first- and second-order loops decreases, but that of an optimal second-order loop is about 4.5 dB below the first-order loop threshold. Thus, even under these conditions, a significant threshold extension of the combine PLL over a second-order PLL can be expected.

Above threshold, the performance of either second- or first-order loop and discriminator are alike. However, according to Figure 4-20, the combine PLL offers a 7 dB SNR improvement.

In concluding this section, it should be remarked that the measured threshold improvement compares favorably with the theoretical predictions made in 4.3.1. The present loop was operated with a peak-to-valley ratio of 28 dB and $K \approx 1$. According to Figure 4-11, this would require G smaller than 0.1. According to Figure 4-12, such a combination of G and K results in a noise bandwidth reduction (and thus a threshold improvement) in the vicinity of 16 dB.

¹ T. F. Haggai, "Reduction of Threshold Carrier Power Requirements in FDM/FM Satellite Communications Systems," Hughes Aircraft Corporation No. CD R-207, April 1963.

5. IMPROVED COMBLINE PLL SYSTEMS

5.1 LOW FREQUENCY MODULATION ERROR REDUCTION

5.1.1 Miscellaneous Methods

It was pointed out in 4.3.5 and verified experimentally in 4.3.6 that it is impossible to achieve high peak-to-valley ratio and high open-loop gain at the same time. The amount of maximum deviation that can be tracked is below the specified values. There are several potential methods to overcome this problem.

First, the gain and bandwidth of the low pass subloop were increased such as to keep the error sufficiently low. The computer calculations for a combline loop mentioned in 4.3.4 were extended for a wide low pass subloop. Severe interference between the two loops was predicted. The comb peaks of the overall response appeared shifted and skewed. This was confirmed in experiments with low pass filters whose closed-loop bandwidth exceeded f_L and no improvement over the basic PLL could be achieved.

Another possibility is to track the signal at low frequency with only the low pass subloop and limit the combline loop to higher frequencies where the amplitude spectrum of the TV signal is low. This was found impossible because the closed-loop bandwidth of a second-order loop is much larger than the bandwidth of the signal to be tracked. For example, in order to reduce the modulation error at the first line harmonic $f_L \approx 15$ kHz to 0.2 radians for a deviation of Δf of 1.1 MHz, the loop natural frequency would have to be about 300 kHz. Under these circumstances, one would run into the same interference problems mentioned before. Experiments were performed with such loops to confirm these results.

The gain can also be increased at low frequency by simply eliminating the differentiator in the combline subloop. Experiments showed that the comb structure disappeared at lower frequencies as expected (high G). As the gain of the VCO decreases, combs start to appear and the peak-to-valley ratio increases toward higher frequencies. However, the combs appeared skewed and shifted away from f_L by several kHz, especially at

lower frequencies. This clearly indicates the need for a constant combline loop gain, i.e., for a differentiator to cancel the $1/S$ gain variation of the VCO.

Based on the above results, it was concluded that preemphasis was the only solution to the tracking problem.

5.1.2 Preemphasis

In a system with preemphasis, the block diagram in Figure 4-3 has to be modified slightly. A preemphasizing network is added between the signal source and the modulator, and the output of the PLL is moved between the combline filter and the differentiator. This eliminates the need for a deemphasizing network.

Tests were run on such a system to investigate its feasibility. A simple 6 dB/octave preemphasizer was implemented with an RC network and used to process a TV spectrum. As expected, the resultant output was essentially flat. At the receiver end, the deemphasized signal was recovered undistorted. Although preliminary and incomplete, these tests nevertheless indicated that preemphasis is a promising method to overcome the gain problems of the combline phase-lock loop.

5.2 AUTOMATIC FREQUENCY CONTROL

Due to the narrow comb bandwidth, acquisition and hold-in ranges are limited to several kHz. It was experimentally demonstrated that frequency offsets in the predetection filter degrade the demodulator output signal-to-noise ratio even when the predetection filter is wide enough to handle the modulation sidebands.

The performance degradation can be eliminated by using an AFC system with the phase-locked demodulator. The AFC centers the incoming carrier in the predetection filter by comparing the carrier to a frequency reference and using the error signal to control the frequency of a local oscillator ahead of the predetection filters. TRW has previously made an exhaustive study of this method and obtained excellent experimental

results^{1,2}. The incoming carrier could be transformed to within a few kHz of the local loop VCO even for low carrier-to-noise ratios; i.e., to well within the acquisition and hold-in range of a combine PLL. Thus, this method is believed to eliminate the acquisition and tracking problems inherent to a combine PLL.

5.3 PREDISTORTION AND POSTDETECTION FILTERING

An attempt to resolve the distortion problem inherent to combine filtering was discussed in 3.3.4, but was found ineffective. Another possibility is to process the TV signal either before modulation (pre-distortion filter) or after detection (postdetection equalization filter) in order to compensate for the distortion. This could be achieved with an inverse combine filter based on Figure 5-1 where $K(s)$ is assumed to be a low pass filter. The transfer function of this circuit is given by

$$H_1(s) = 1 - Ke^{-s\tau} = 1 - K \cos s\tau + jK \sin s\tau \quad (5-1)$$

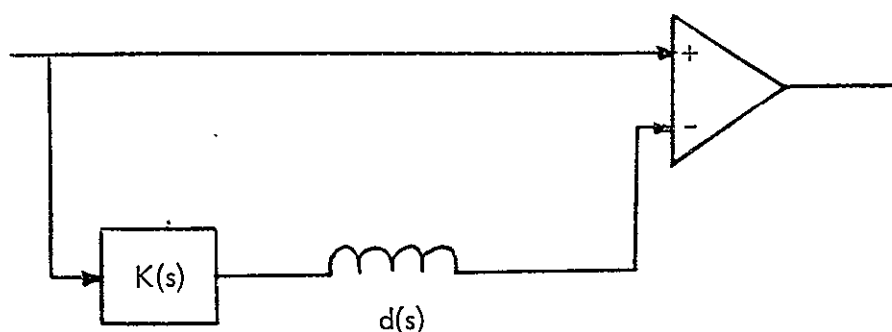


Figure 5-1. Inverse Combine Filter

¹"Signal Data Demodulation System (SDDS) FM Demodulator Modifications Study," TRW Systems Report for NASA under Contract No. NAS9-4810.

²"Preliminary Design Report for Modification of the FM Demodulator of the Signal Data Demodulation System (SDDS)," TRW Systems Report for NASA under Contract No. NAS9-7968.

For simplicity, assume $K = 1$. Then the amplitude response becomes

$$|H_1(j\omega)| = 2[1 - \cos \omega\tau] \quad (5-2)$$

This is sketched in Figure 5-2. Clearly this is the inverse of the response of a filter based on the same delay line having maxima at multiples of f_L and a transfer function

$$H_2(s) = \frac{K}{1 - K^{-s}\tau} \quad (5-3)$$

A signal processed by H_1 and H_2 is subject to the overall transfer function

$$H_1(s) \times H_2(s) \text{ or } H_2(s) \times H_1(s) = K(s) \quad (5-4)$$

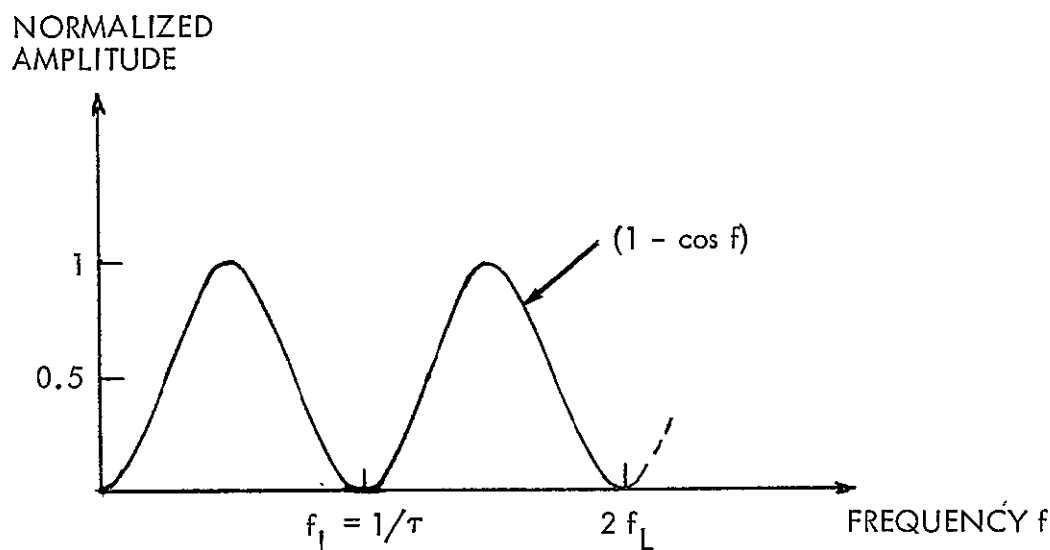


Figure 5-2. Amplitude Response of Inverse Combline Filter

Thus the net effect is simply due to $K(s)$ (i.e., low pass filtering in our case) and the distortion caused by the combine filter is compensated for.

Undoubtedly, using the inverse combine filter as a predistortion filter would result in a better net SNR than if it were used as a post-detection filter. Postdetection filtering may have the advantage of eliminating the noise-smearing effect (3.4.1) which is subjectively annoying despite obvious SNR improvement. A combination of predistortion, post-detection filtering may be the best compromise; additional experimentation is needed to substantiate this point.

A preliminary implementation of an inverse combine filter according to Figure 5-1 was realized to show its feasibility, but no attempts were made to match it to the existing combine filters.

APPENDIX A
ANALYSIS AND CHARACTERISTICS OF
THE DIGITAL FILTER

APPENDIX A

ANALYSIS AND CHARACTERISTICS OF THE DIGITAL FILTER

The principal portion of the digital filter is a sampler, which is composed of a set of N identical low pass filters with their inputs and outputs synchronously commutated into and out of the signal path. Typically, each low pass filter is a simple RC lag circuit. In the conventional application, the sampler is prefiltered by a low pass filter, passing ω_s and rejecting all frequencies above $N\omega_s/2$, where ω_s is the switching frequency. It is also postfiltered by a broad bandpass filter centered about ω_s (or by a low pass filter with dc blocking). Thus all filter elements can be realized without the use of inductors.

The composite filter behaves as a single-pole bandpass filter centered about ω_s (and thus tunable), with a 3-dB bandwidth (for the case of single RC filter sections) of $2/N\tau$ rad/sec, where $\tau = RC$. The circuit $Q, \omega_s N\tau/2$, can exceed that of quartz crystals.

In summary, the principal advantages of the DBF are:

- It is tunable, since the passband is centered about ω_s
- It is capable of extremely small relative bandwidths (high Q)
- It can be realized with RC elements and digital logic and is thus amenable to integrated circuitry techniques.

Its major disadvantages are:

- Tuning range is restricted because of the pre- and post-filtering requirements
- There is feedthrough of switching frequency ω_s in the center of the passband as a result of imperfect balance and of leakage of the gating signal through the switches
- Attenuation (for noncascaded filter sections) is limited by the finite switch resistance
- The operating frequency is restricted to a few tens of megahertz because of constraints on switching speed
- There may be isolation problems, since the switching signal is centered in the output band.

SAMPLER ANALYSIS

The following analysis pertains to the sampler in which a set of single-section RC filters is employed. It follows those of Kaufman¹ and Thompson², but is somewhat more generalized.

The generalized configuration is shown in Figure 1, illustrated for $N = 4$. The initial phase angles of the switches with respect to the centers of commutator segments number one are α_1 and α_2 , respectively. Both switches rotate synchronously at ω_s rad/sec. The angular widths of the segments are θ_1 and θ_2 , respectively. Thus, their respective duty cycles ("on" time to period ratio) are $h_1 = \theta_1/2\pi$ and $h_2 = \theta_2/2\pi$.

Since the switches are symmetrical and the low pass filters are identical, the initial analysis can be confined to a single section, as shown in a) of Figure 1. The switches have a duty cycle and phase angle corresponding to their respective commutator segments. They are represented by squarewave gating functions which have values only of 0 or 1, and are

$$g_1(t) = \sum_{m=-\infty}^{\infty} h_1 \operatorname{sinc} m h_1 e^{jm(\omega_s t + \alpha_1)} \quad (1)$$

and

$$g_2(t) = \sum_{n=-\infty}^{\infty} h_2 \operatorname{sinc} n h_2 e^{jn(\omega_s t + \alpha_2)} \quad (2)$$

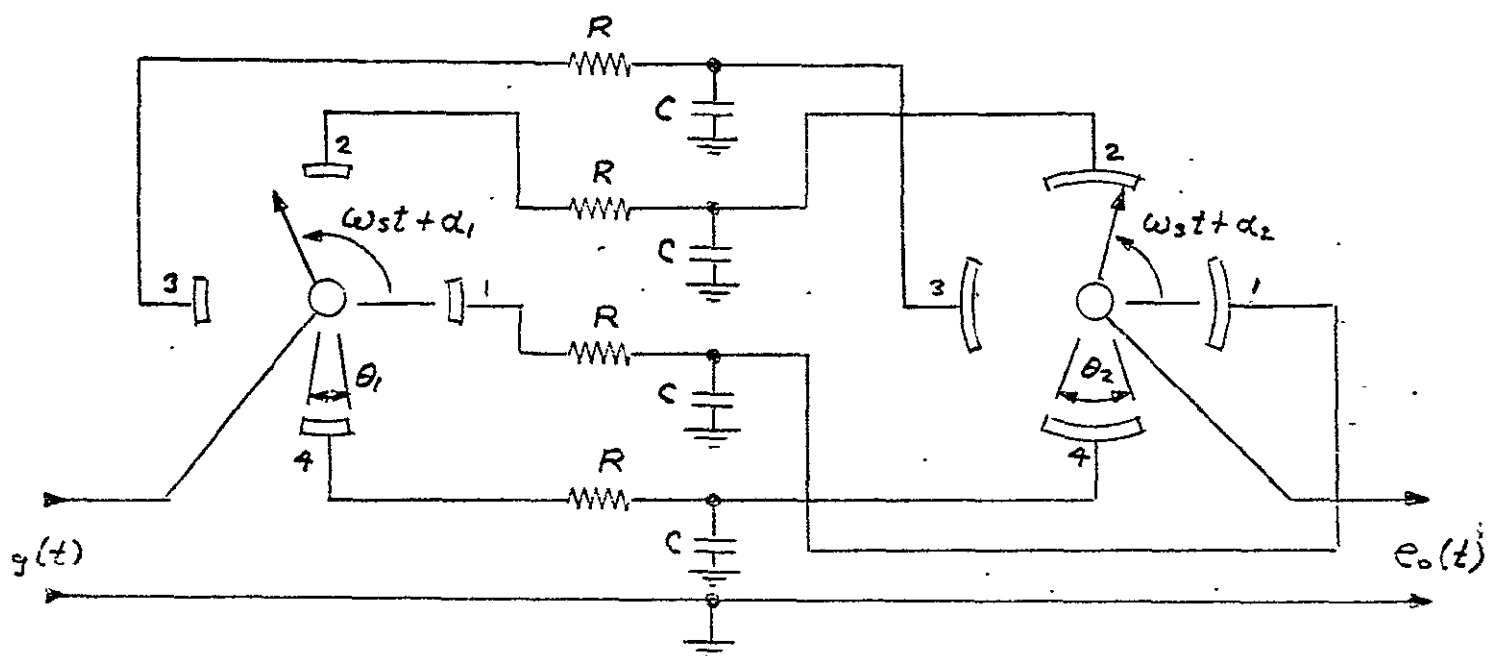
where

$$\operatorname{sinc} x \triangleq \frac{\sin \pi x}{\pi x}$$

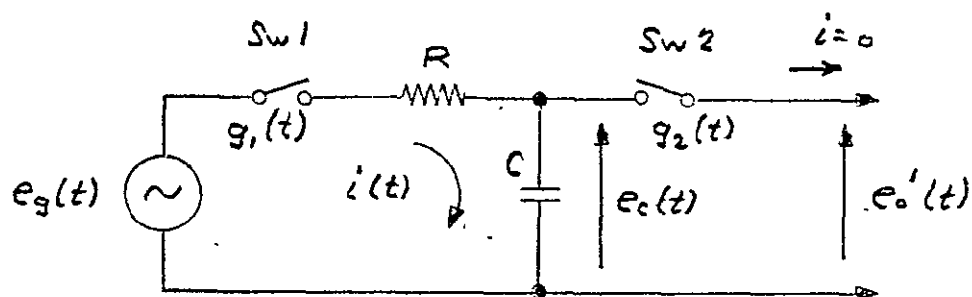
The current, $i(t)$, is the difference between generator and capacitor voltage, divided by R , when Sw_1 is closed, and is zero when the switch is open. Since this current flows into the capacitor, it is also equal to the capacitance times the rate of change of voltage across it. Thus

¹"Theory and Synthesis of the Digitalized Bandpass Filter," a thesis by M. A. Kaufman, submitted to UCLA, 1966.

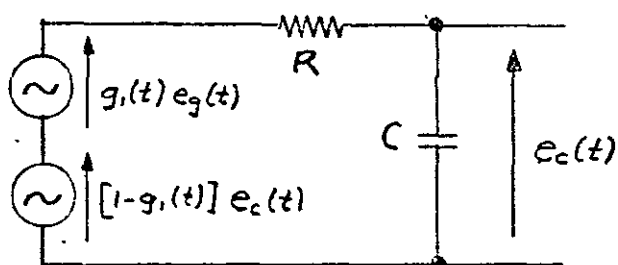
²J. Thompson, "RC Digital Filters for Microcircuit Bandpass Amplifiers," EEE, March 1964, pp. 45-108.



a) Generalized Sampler Configuration
(Four Single-Section RC Filters)



b) Circuit of Single Commutated Section



c) Equivalent Input Circuit

Figure 1. Sampler

$$i(t) = g_1(t) \frac{e_g(t) - e_c(t)}{R} = C \dot{e}_c(t) \quad (3)$$

or

$$\sum_{m=-\infty}^{\infty} \left(h_1 e^{jma_1} \text{sinc } mh_1 \right) e^{jm\omega_s t} \left[e_g(t) - e_c(t) \right] = \tau \dot{e}_c(t) \quad (4)$$

where

$$\tau \triangleq RC$$

It is seen from (3) that the current may be written as

$$i(t) = \frac{g_1(t) e_g(t) + [1 - g_1(t)] e_c(t) - e_c(t)}{R}$$

giving an equivalent input circuit shown in c) of Figure 1 showing two generators in series across the input to the low pass filter. By the principle of superposition, the voltage $e_c(t)$ is the sum of the voltage across the capacitor resulting from either generator above, the other being shorted. Since we choose to make $1/\tau < \omega_s$, it is apparent that the $[1 - g_1(t)] e_c(t)$ generator will develop negligible voltage across the capacitor for all frequencies except near zero. Hence, the $g_1(t)$ series pertaining to this generator has effectively only its zero-order term ($m = 0$). Thus, (3) becomes

$$\sum_{m=-\infty}^{\infty} \left(h_1 e^{jma_1} \text{sinc } mh_1 \right) e^{jm\omega_s t} e_g(t) - h_1 e_c(t) = \tau \dot{e}_c(t) \quad (5)$$

since

$$\sum_{m=0}^0 \left(h_1 e^{jma_1} \text{sinc } mh_1 \right) e^{jm\omega_s t} = h_1$$

Since $\mathcal{L}[e^{jat}f(t)] = F(s - ja)$, where $\mathcal{L}[f(t)] = F(s)$, the transform of (5) is

$$\sum_{m=-\infty}^{\infty} \left(h_1 e^{jma_1} \text{sinc } mh_1 \right) E_g(s - jm\omega_s) = (h_1 + \tau s) E_c(s) \quad (6)$$

or

$$E_c(s) = \frac{\sum_{m=-\infty}^{\infty} \left(e^{jma_1} \text{sinc } mh_1 \right) E_g(s - jm\omega_s)}{1 + \frac{\tau}{h_1} s} \quad (7)$$

From b) of Figure 1,

$$\begin{aligned} e'_0(t) &= g_2(t) e_c(t) \\ &= \sum_{n=-\infty}^{\infty} \left(h_2 e^{jna_2} \text{sinc } nh_2 \right) e^{jn\omega_s t} e_c(t) \end{aligned} \quad (8)$$

and

$$\begin{aligned} E'_0(s) &= \sum_{n=-\infty}^{\infty} \left(h_2 e^{jna_2} \text{sinc } nh_2 \right) E_c(s - jn\omega_s) \\ &= \sum_{m=-\infty}^{\infty} \sum_{n=-\infty}^{\infty} \frac{h_2 e^{j(ma_1 + na_2)} \text{sinc } mh_1 \text{sinc } nh_2}{1 + \frac{\tau}{h_1} (s - jn\omega_s)} E_g[s - j(m+n)\omega_s] \end{aligned} \quad (9)$$

Now, having derived the response transform for a single switched section, it is apparent from a) of Figure 1 that the overall sampler response is the sum of the responses of b), given by (9), where the phase angles are suitably adjusted for each successive section.

The resultant output is

$$E_0(s) = \sum_{p=1}^N E'_0(s, a_1, a_2) \quad (10)$$

where $a_1 \triangleq \beta_1 + 2\pi p/N$, $a_2 \triangleq \beta_2 + 2\pi p/N$, and the β are initial phase angles; $E'_0(s, a_1, a_2)$ is a function of a only in the $e^{j(ma_1 + na_2)}$ term, and since the summations may be taken in any order, consider

$$\begin{aligned}
& \sum_{p=1}^N e^{j(m\alpha_1 + n\alpha_2)} \\
& = e^{j(m\beta_1 + n\beta_2)} \sum_{p=1}^N e^{j2\pi p \frac{m+n}{N}} = \begin{cases} N e^{j(m\beta_1 + n\beta_2)}, & \frac{m+n}{N} = k \\ 0, & \frac{m+n}{N} \neq k \end{cases}
\end{aligned} \tag{11}$$

where k is any integer. It is apparent that

$$\sum_{p=1}^N e^{j2\pi pk} = N$$

if k is an integer. While not obvious, it can be demonstrated that the function vanishes for nonintegral values of $m+n/N$.

Thus, the overall sampler response is, from (9) and (11)

$$E_o(s) = Nh_2 \sum_{m=-\infty}^{\infty} \sum_{n=-\infty}^{\infty} \frac{e^{j(m\beta_1 + n\beta_2)} \text{sinc} mh_1 \text{sinc} nh_2}{1 + \frac{\tau}{h_1} (s - jn\omega_s)} E_g[s - j(m+n)\omega_s] \tag{12}$$

subject to the constraint, $m+n = kN$, or in steady state

$$E_o(j\omega) = Nh_2 \sum_{k=-\infty}^{\infty} \sum_{n=-\infty}^{\infty} \frac{e^{j[(kN-n)\beta_1 + n\beta_2]} \text{sinc}(kN-n)h_1 \text{sinc} nh_2}{1 + j \frac{\tau}{h_1} (\omega - n\omega_s)} E_g[j(\omega - kN\omega_s)] \tag{13}$$

DISCUSSION

Equation (13) states that the output voltage approaches zero if $|\omega - n\omega_s| \tau/h_1 \gg 1$; i.e., responses can occur only in a comb spectrum for input frequencies within the comb-tooth bandwidth centered about an integral multiple of the switching frequency, ω_s . The tooth 3-dB bandwidth is $2h_1/\tau$ and is constrained to be much less than ω_s .

Further, an output response can be produced only by an input signal differing in frequency from that of the response by $kN\omega_s$. Thus, a response

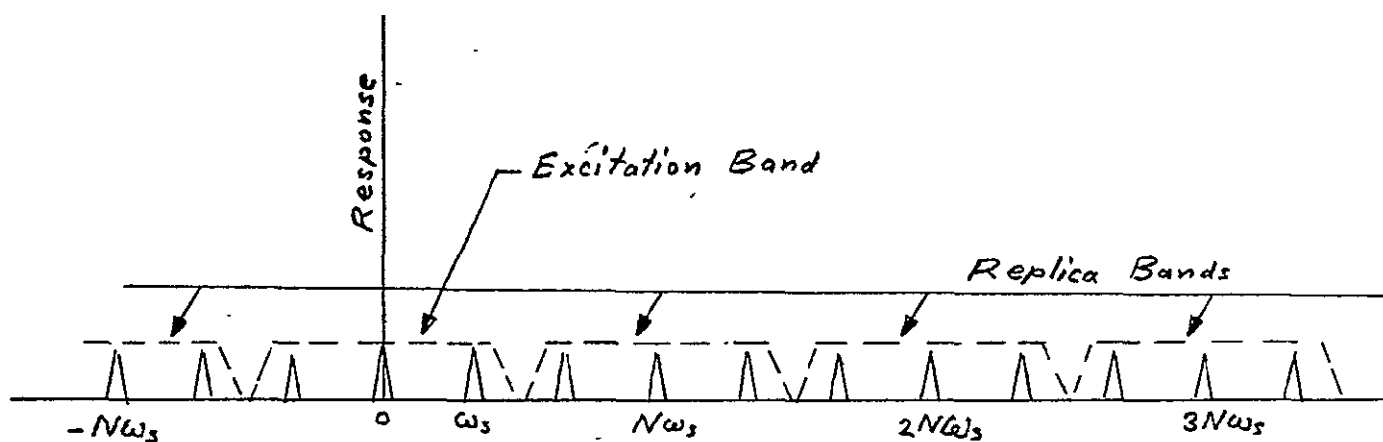
of order n ; i. e., $\omega \approx n\omega_s$ can be produced only by an input of order $(n - kN)$; i. e., $\omega_{in} \approx (n - kN)\omega_s$, or $\omega_{out} = \omega_{in} + kN\omega_s$. Hence, ω_{in} is replicated in the output at intervals of $kN\omega_s$, and conversely, a given output response is excited by a multiplicity of input frequencies.

Figure 2 illustrates the comb response of the sampler. (The attenuation characteristic of the sinc functions has been omitted for simplicity.) The critical requirement in the application of the sampler is the prevention of spectrum foldover at the desired response (i. e., equal output frequency responses from a multiplicity of input frequencies).

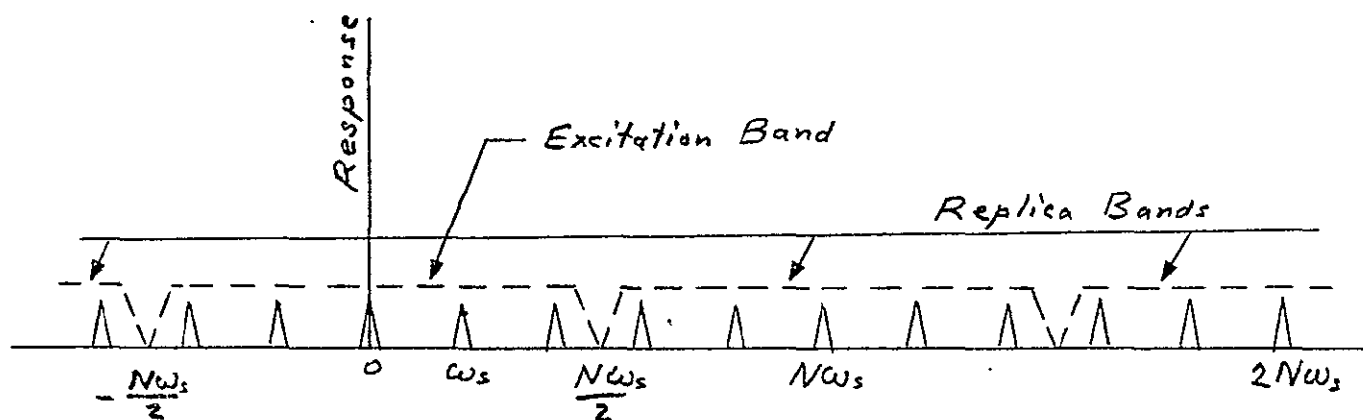
If the input frequency is considered to be within a band of width $N\omega_s$ centered about an integral multiple of $N\omega_s$, as in a) of Figure 2, then it is replicated in the output both in the corresponding position in each replica band and also as an image response symmetrically opposite the center to its band. Specifically, any input at a given frequency, $(k_1N + n_1)\omega_s$, gives rise to a set of responses of frequency $(kN + n_1)\omega_s$, where k includes all integers, positive and negative. Thus, in order to prevent spurious responses at the desired comb $(k_2N + n_1)\omega_s$, it is necessary to prefilter the sampler to eliminate all inputs of the set $(kN + n_1)\omega_s$, except for the one at the desired input frequency. This does not require that other input frequencies be rejected, however, for only an input in that set of frequencies can produce a response in that set.

There must be at least three commutated filter sections employed, as shown in a) of Figure 2, or else spectrum overlap occurs in all bands. Excitations of frequency in the $kN\omega_s$ tooth bands are unusable in any event, since the image and desired response are within the same comb-tooth bandwidth. Since the prefilter must pass one tooth band of the set $(kN + n)\omega_s$ and reject all others, it is necessary that $(kN + n)\omega_s < [(kN + 1) - n]\omega_s$, or $2n < N$. Hence, $N_{min} = 3$, and $n_{min} = \pm 1$.

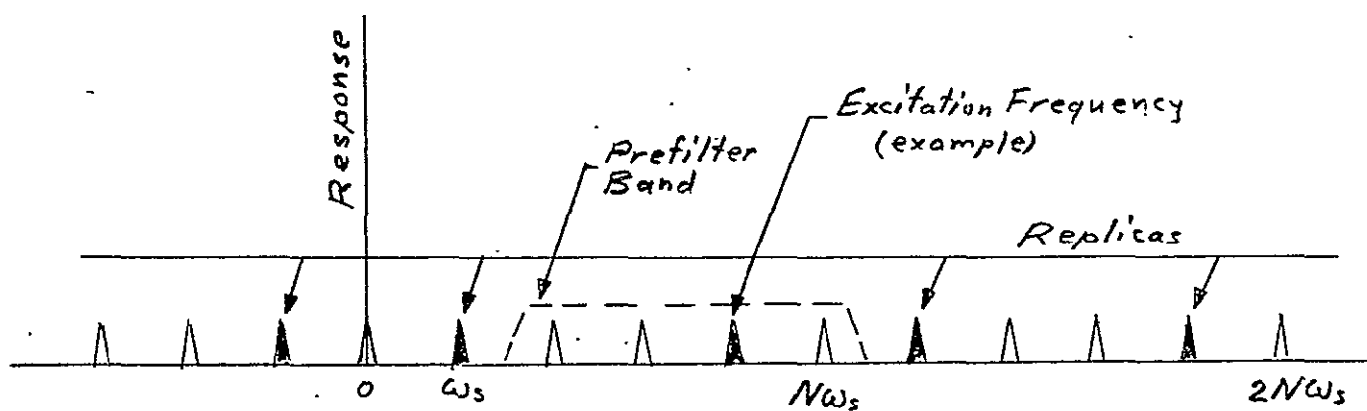
If the excitation frequency lies between zero and $N\omega_s/2$, then this entire band may be admitted to the sampler since no response frequency is produced by more than one excitation frequency, as shown in a) and b) of Figure 2. If the excitation frequency is greater than $N\omega_s/2$, however, all other excitations in its set $(kN + n)\omega_s$ must be suppressed in the prefilter as discussed above in order to avoid creating the same response frequency from a multiplicity of input frequencies. Thus, in c) of Figure 2,



a) $N_{\min} = 3$



b) $N = 5$



c) $N = 5$

Figure 2. Sampler Spectra

if, for example, the desired excitation frequency is $(N - 1)\omega_s$, the desired response can be this or any of its replicas. In this example the minimum prefiltering requirement is to pass only frequencies between, but not including, ω_s and $(N + 1)\omega_s$. Other frequencies in the prefilter passband can excite other responses, but none will coincide with those produced by the example excitation frequency.

Perhaps a clearer indication of the relation between sampler excitation and response frequencies can be had by plotting the expression $\omega_{out}/\omega_s = \omega_{in}/\omega_s + kN$, shown for various values of N in Figures 3, 4, 5, and 6. It should be noted that responses occur only near integral coordinates and that crossed lines at such points indicate image responses. It is verified from Figure 3 that $N = 2$ is unusable, since all responses have images.

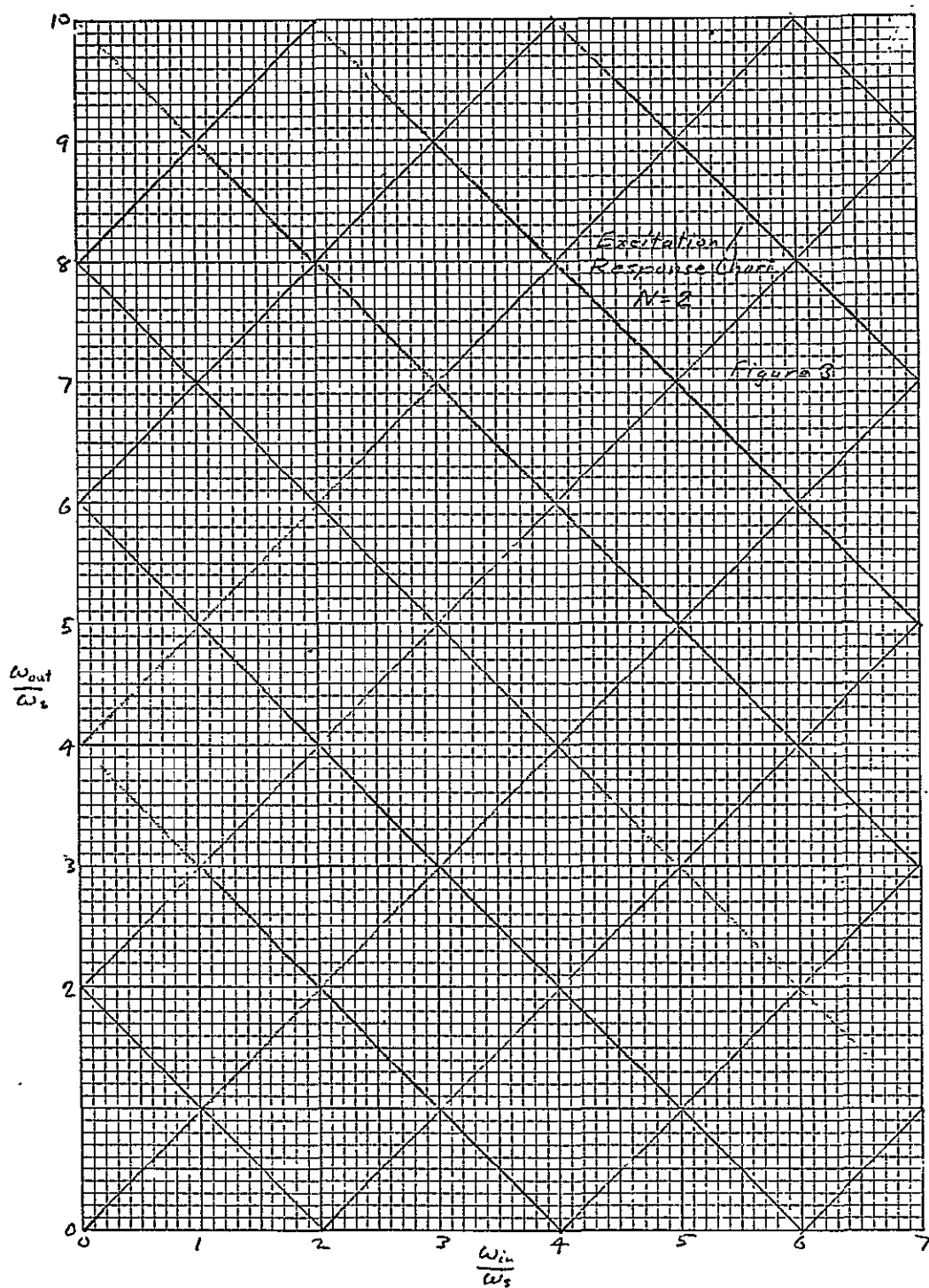


Figure 3. Excitation/Response Chart
N = 2

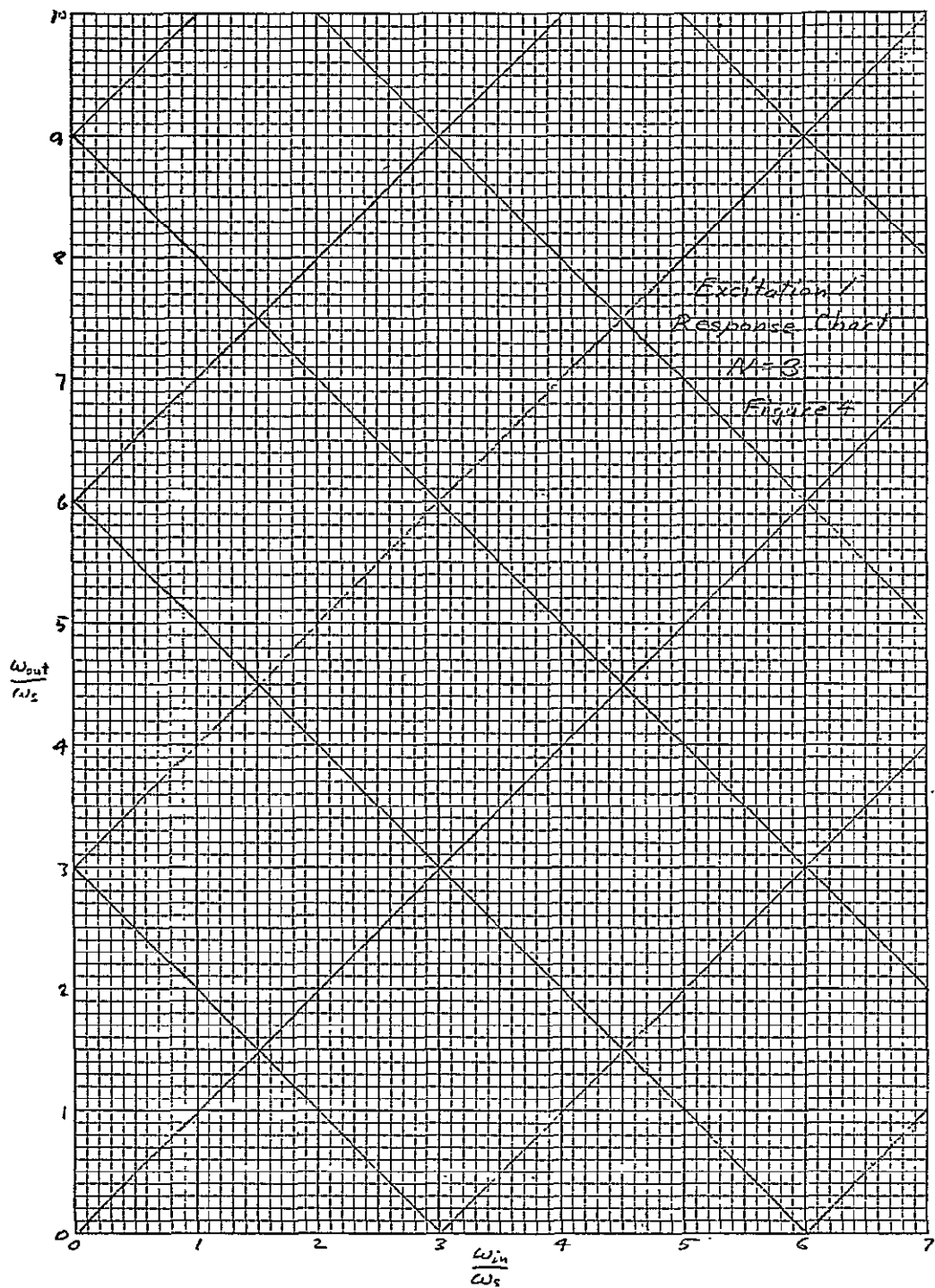


Figure 4. Excitation/Response Chart
 N = 3

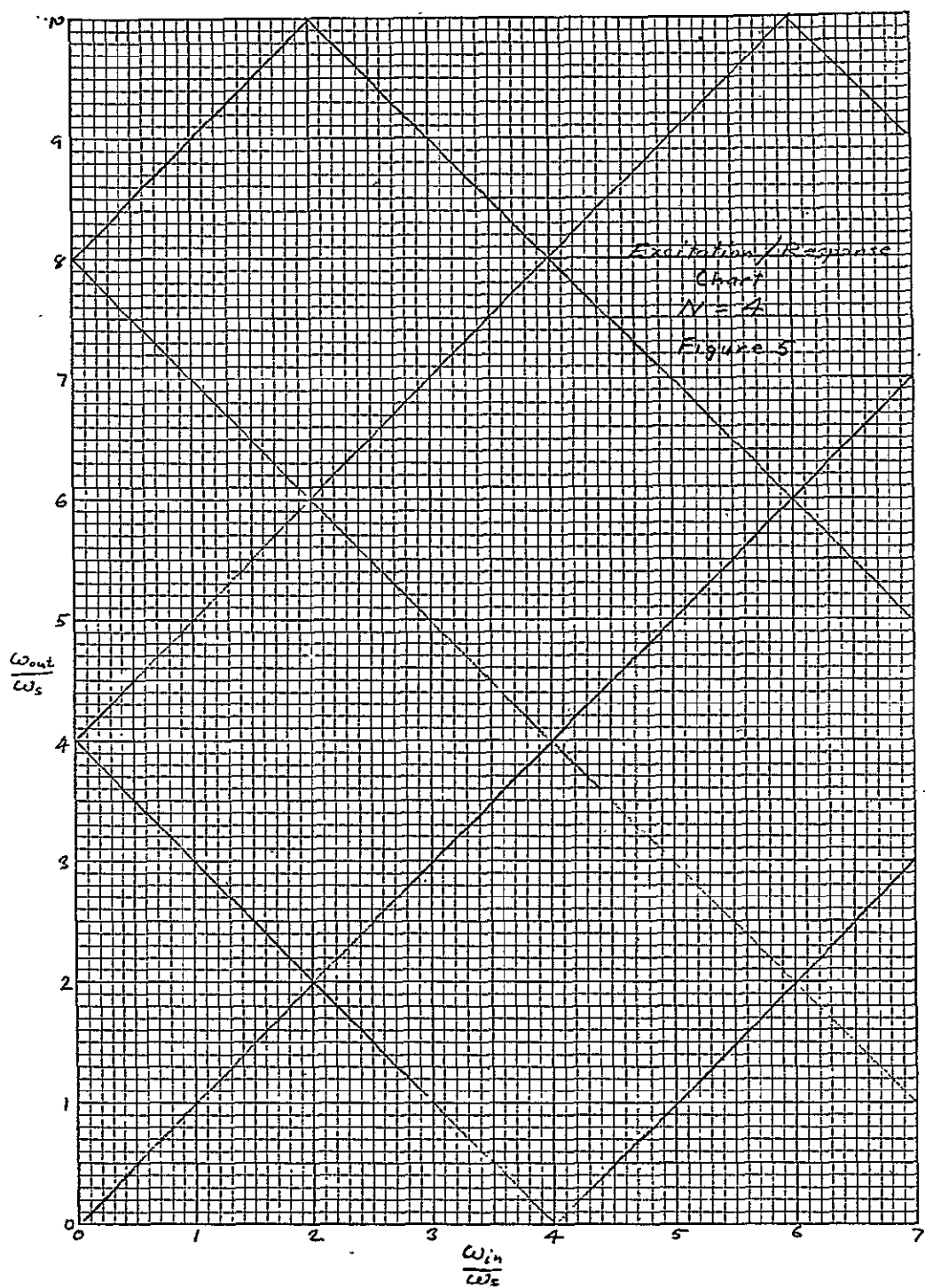


Figure 5. Excitation/Response Chart
 $N = 4$

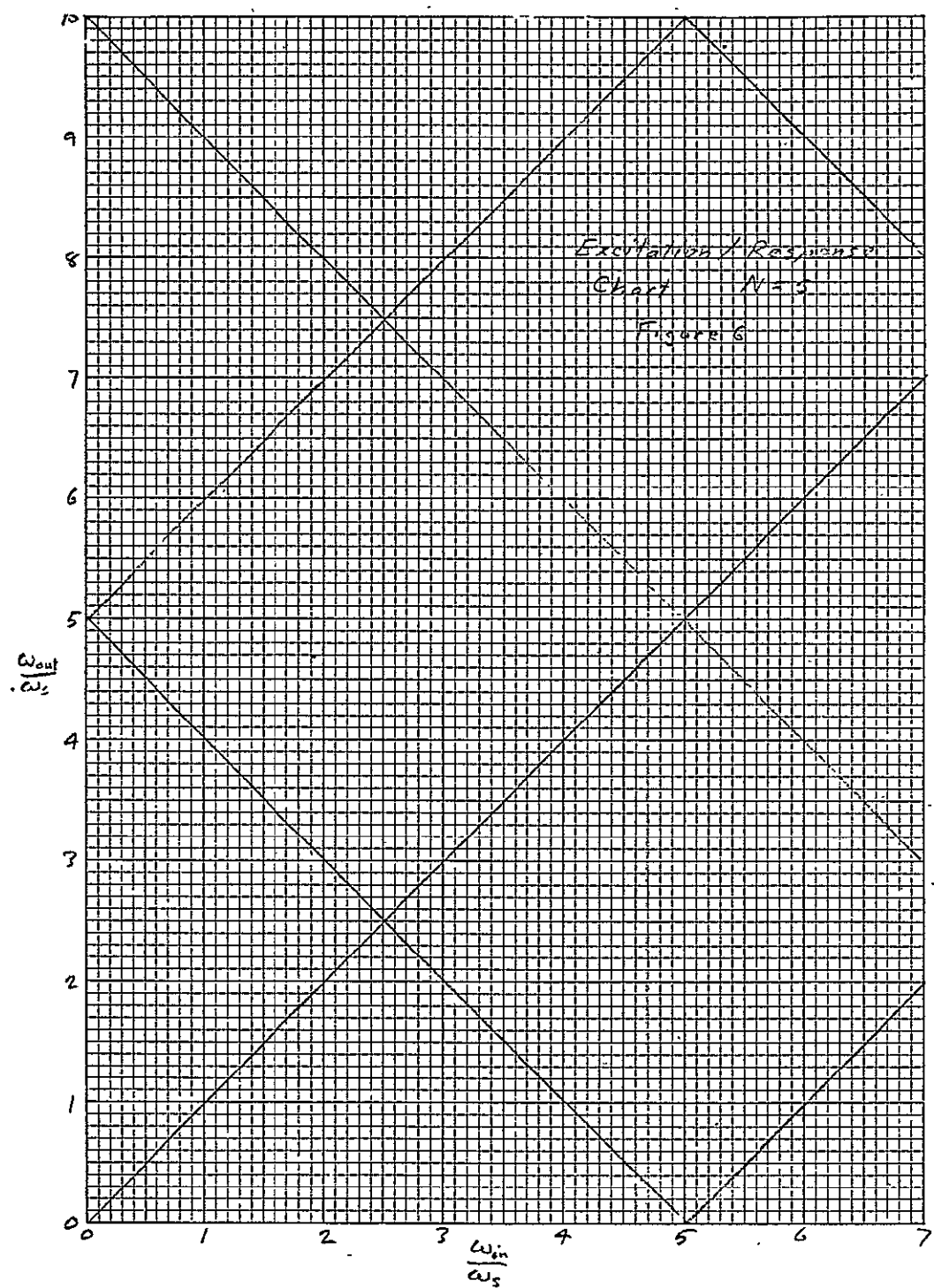


Figure 6. Excitation/Response Chart
 $N = 5$

APPENDIX B
COMPUTER PROGRAMS

APPENDIX B

COMPUTER PROGRAMS

The computer programs listed in this appendix comprise the majority of the programs generated on the TV improvement project. The other programs not listed fall into two categories:

- 1) Variations in the programs contained in this report. These include corrections of an earlier version of the listed programs, which contained logic errors, and changes made to facilitate input or printout.
- 2) Adaptations of the listed programs to (a) account for changes in gain, bandwidths, and/or delays (as indicated in this writeup), or (b) make the programs compatible with MINMAX, which includes changing variable names to avoid ambiguities in their definition and renumbering their line numbers to fit the required MINMAX format.

All programs were written for use with the Tymeshare language Super Basic.

1. Comblane Filter

The first program (CLFF) solves for the amplitude response of the comb filter in the frequency domain. The variables asked for are W, T, K, Epsilon, N and Step N

where W = low pass bandwidth (3-dB point in radians/sec)

T = loop delay in seconds

K = loop gain

Epsilon = Accuracy desired in solution of peaks

N and Step N specify the harmonics of interest.

If one is interested in solving only for the peaks and valleys, the following changes can be made:

```
30  PRINT "TYPE IN EPSILØN FØR FINDING MAXIMUM":
41  INPUT E1
70  FØR N=1,2 TO 10 STEP 2,50,100
210 IF N=1 THEN H5=H
220 PRINT "PEAK RESPONSE IS": 20*LGT(H5/H):" DB"
230 X=X+PI
240 GØSUB 600
250 IF N=1 THEN PRINT "PEAK TO VALLEY=": 20*LGT(H5/H):" DB"
```

The peak to valley ratios are solved at the comb harmonics defined by Step 70. The second program (CLFT) solves for the CLF response in the time domain. Variable names used are the same as CLFF. Note that the solutions are normalized by the response at $t=0$.

CLFF

```
5   VAR = ZERO
10  PRINT "WHAT ARE THE VALUES FOR W,T AND K":
20  INPUT W,T,K
30  PRINT "TYPE IN EPSILONS FOR FINDING MAXIMUM N AND STEP N"
41  INPUT E1, N1,N$
50  B1=1/(1+W*T)
60  A1=B1/(K*W*T)
70  FOR N=0 TO N1 STEP N$
80  F=1E10
90  X=2*PI*N
100 P=A1*X+B1*X*COS(X)+SIN(X)
102 IF ABS(P)<ABS(F) THEN 115
103 X=L-(F/(2+S))
104 S=S+1
105 GO TO 100
115 F=P,S=1
117 L=X
120 IF ABS(P)<E1 THEN 150
130 X=X-P
140 GO TO 100
150 D$=X-(2*PI*N)
160 PRINT "FOR THE":N:" HARMONIC, MAXIMUM OCCURS AT":X/(2*PI*T):" HZ"
170 PRINT "SHIFT =" :D$*180/PI,"EPSILON =" :P,"(X GIVEN IN DEGREES)"
180 C=1/(W*T)
200 GOSUB 600 !SUBROUTINE AT 600 SOLVES FOR AMPLITUDE WHEN GIVEN X
210 FOR Ø=-.5,-.2,.05 TO .65 STEP .2,1
220 X=(2*N+Ø)*PI
230 GOSUB 600
240 NEXT Ø
270 PRINT
280 NEXT N
300 STOP ! MAIN PROGRAM ENDS HERE
600 COMPLEX Y
610 R=1-K*COS(X)
620 S=C*X*K*XIN(X)
630 Y=CMPLX (R,S)
640 Y1=ABS(Y)
650 H=K/Y1
660 PRINT "FOR X =" :X*180/PI,"AMPLITUDE =" :H
670 RETURN
```

CLFT

```
10  PRINT "WHAT ARE THE VALUES FOR W AND K":
20  INPUT W,K
30  PRINT "WHAT WINDOWS DO YOU WANT (N AND STEP N)":
40  INPUT N1,N2
50  FOR N=0 TO N1 STEP N2
60  E=N/W
70  PRINT
80  PRINT N:"WINDOW, MAXIMUM AT NT+":E
85  M=SQRT(N)
90  PRINT "INFLECTION POINTS AT":(N+M)/W:" AND":(N-M)/W
100 PRINT "TIME","AMPLITUDE NORMALIZED BY":K*W
110 IF E=0 THEN 130 ELSE GOSUB 500
120 GO TO 150
130 Y=1
140 GOSUB 560
150 E=(N-M)/W
160 IF E=0 THEN 190 ELSE GOSUB 500
170 E=(N+M)/W
180 GOSUB 500
185 GO TO 200
190 E=2/W
200 E1=E
210 FOR P=-1.5 TO 1.5 STEP 1
220 E = E1*(10+P)
230 GOSUB 500
240 NEXT P
250 NEXT N
260 STOP
500 N$=1
510 FOR N9=1 TO N
520 N$=N$*N9
530 NEXT N9
540 R=EXP(-W*E)
550 Y=(K*W*E)^(N*R/N$) !NORMALIZED BY MAGNITUDE AT T=0
560 PRINT E,Y
570 RETURN
```

2. Combine Filter in Phase Lock Loop

The computer programs for the comb filter in the phase lock loop are PLLF and PLLT corresponding to the solution in the frequency and time domain respectively. Remembering that W is in radians/sec, the programs should be self explanatory. The program entitled BANDWIDTH solves

$$\int_{C1}^C \left| \frac{\phi_o}{\phi_i} \right|^2 d(w\tau)$$

where $C1$ and C are the comb harmonic numbers over which the integration is to be taken and compares this integral to the integral of the square of the comb envelope. The integral is done using Simpson's Rule, hence the requirement of solving over an even number of combs.

The program PVR solves for peak to valley ratios and the envelope 3-db point for various parameters (W , K and G) which are specified in steps 20, 30 and 40. Epsilon (for solving peaks) and the loop delay are specified in step 10.

The last program in this section titled RESPONSE solves for the response of the phase lock loop to any picture described in the DATA. In the program listed, the data represents 10 white lines followed by 10 black lines. By specifying any other limits, one can solve for the response to blocks of white and black.

Lines 11 and 41 allow for minor loop delays which may be different from the horizontal sync period. It has been suggested that this program can be expanded to account for an intermediate shade of grey and consider the effects of noise on the response by introducing between steps 130 and 140 a weighting factor to account for "greyness" and a random number generator to add "noise" to the system.

PLLF

```
5   VAR = ZERO
10  PRINT "TYPE IN VALUES FØR W, T, K, AND EG"
20  INPUT W, T, K, G
30  PRINT "TYPE IN EPSILØNS FØR FINDING MAXIMUM AND WIDTH, N AND STEP N"
40  INPUT E1, E2, N1, N$
41  PRINT
45  A=K*G
50  B1=1/(1+W*T*(1+A))
60  A1=B1/(K*W*T)
70  FØR N=0 TØ N1 STEP N$
80  F=1E10
90  X=2*PI*N
100 P=A1*X+B1*X*CØS(X)+SIN(X)
102 IF ABS(P)<ABS(F) THEN 115
103 X=L-(F/(2+S))
104 S=S+1
105 GØ TØ 100
115 F=P, S=1
117 L=X
120 IF ABS(P)<E1 THEN 150
130 X=X-P
140 GØ TØ 100
150 D$=X-(2*PI*N)
160 PRINT "FØR THE":N:" HARMØNIC, MAXIMUM ØCCURS AT":X*180/PI:" DEGREES"
170 PRINT "SHIFT =":D$*180/PI, "EPSILØN =":P
180 C=1/(W*T)
190 B=1+A
200 GØSUB 600 !SUBROUTINE AT 600 SØLVES FØR AMPLITUDE WHEN GIVEN X
210 H1=H
220 X=(2*N+1)*PI
230 GØSUB 600
240 H2=H
250 H3=(H1+H2)/2
260 GØSUB 800 !SUBROUTINE AT 800 SØLVES FØR X AT HALF HEIGHT
270 PRINT
280 NEXT N
300 STOP ! MAIN PRØGRAM ENDS HERE
600 CØMPLEX Y
610 R=B-K*CØS(X)
620 S=C*X+K*SIN(X)
630 Y=CMPLX (R,S)
640 Y1=ABS(Y)
650 H=A/Y1
655 IF X=L ØR X=(2*N+1)*PI THEN 660 ELSE RETURN
660 PRINT "FØR X=":X*180/PI,"AMPLITUDE =":H
670 RETURN
```

```

800 X=L+.5
820 D1=1E50
840 P1=1
850 GOSUB 600
860 D=H3-H
870 IF ABS(D)<E2 THEN 950
875 IF ABS(D)<D1 THEN 900 ELSE 880
880 P1=P1+1
890 GOTO 905
900 D1=ABS(D)
901 X$=X
905 IF D<0 THEN 910 ELSE 930
910 X=X$+(10+(-P1))
920 GOTO 850
930 X=X$-(10+(-P1))
940 GOTO 850
950 M=(X-L)*180/PI
960 PRINT "X AT HALF HEIGHT =":X*180/PI;"HALF WIDTH =":M;"EPS=":D
1000 RETURN

```

PLLT

```
10 PRINT "WHAT ARE THE VALUES FOR W,K AND EG":
20 INPUT W,K,G
30 PRINT "WHAT WINDOWS DO YOU WANT (N AND STEP N)":
40 INPUT N1,N2
45 A=G*K
46 B=1+A
50 FOR N=0 TO N1 STEP N2
60 E=N/(B*W)
70 PRINT
80 PRINT N:" WINDOW, MAXIMUM AT NT+":E
85 M=SQRT(N)
90 PRINT "INFLECTION POINTS AT":(N+M)/(B*W):" AND":(N-M)/(B*W)
100 PRINT "TIME","AMPLITUDE NORMALIZED BY":A*W
110 IF E=0 THEN 130 ELSE GOSUB 500
120 GO TO 150
130 Y=1
140 GOSUB 560
150 E=(N-M)/(W*B)
160 IF E=0 THEN 190 ELSE GOSUB 500
170 E=(N+M)/(W*B)
180 GOSUB 500
185 GO TO 200
190 E=2/(W*B)
200 E1=E
210 FOR P=-2.1 TO 3.1
220 E=E1*(5+P)
230 GOSUB 500
240 NEXT P
250 NEXT N
260 STOP
500 N$=1
510 FOR N9=1 TO N
520 N$=N$*N9
530 NEXT N9
540 R=EXP(-W*E*B)
550 Y=(K*W*E)+N*R/N$
560 PRINT E,Y
570 RETURN
```

BANDWIDTH

```
10 PRINT "WHAT ARE THE VALUES FOR K,T,WO AND EG":
11 INPUT K,T,W,G
12 PRINT "WHAT IS THE INTEGRATION RANGE IN TERMS OF THE COMBS"
20 PRINT "GIVE LOWER FIRST, WITH EVEN # BETWEEN LIMITS":
21 INPUT C1,C
22 PRINT "HOW MANY STEPS PER COMB":
23 INPUT M1
24 PRINT
25 N1=0
30 M=M1*(C-C1)
40 DIM Y(-1:M),Z(0:(C-C1))
41 Y(-1)=1E50
45 Z(C-C1)=0
50 H=2*PI/M1
60 FOR N=0 TO M
70 X=2*PI*C1+N*H
100 Y1=(1+G*K-K*COS(X))+2
110 Y2=(X/(W*T)+K*SIN(X))+2
120 Y=1/(Y1+Y2)
200 Y(N)=Y
210 IF N=0 THEN Z(N1)=Y ELSE 220
215 GO TO 240
220 IF Y(N)<Y(N-1) THEN 230 ELSE 250
230 IF Y(N-2)<=Y(N-1) THEN Z(N1)=Y(N-1) ELSE 250
240 N1=N1+1
250 NEXT N UNLESS N=M
260 IF Z(C-C1)=0 THEN Z(C-C1)=Y(M)
300 P1,P2=0
310 FOR P=2 TO M STEP 2
320 P1=P1+Y(P)
330 P2=P2+Y(P-1)
340 NEXT P
350 P5=H*(Y(0)-Y(M)+2*P1+4*P2)/3
400 R1,R2=0
410 FOR R=2 TO (C-C1) STEP 2
420 R1=R1+Z(R)
430 R2=R2+Z(R-1)
440 NEXT R
450 R5=2*PI*(Z(0)-Z(C-C1)+2*R1+4*R2)/3
500 PRINT "COMB NOISE BANDWIDTH =":(G*K)+2*P5
510 PRINT "ENVELOPE NOISE BANDWIDTH =":(G*K)+2*R5
520 PRINT "REDUCTION =" :P5/R5:" OR ":10*LGT(P5/R5):" DB"
```

PVR

```
5   VAR = ZERO
10  E1=1E-6,T=635E-7
20  FOR W=5E6,8E6,1E7,5E7,1E8
30  FOR G=.5,.7,.8,.9,1
40  FOR K=.5,.9,1,1.5,1.9
41  PRINT
45  A=K*G
50  B1=1/(1+W*T*(1+A))
60  A1=B1/(K*W*T)
65  PRINT W/(2*PI);G;K,
70  FOR N=0 TO 200 STEP 1
80  F=1E10
90  X=2*PI*N
100 P=A1*X+B1*X*COS(X)+SIN(X)
102 IF ABS(P)<ABS(F) THEN 115
103 X=L-(F/2+S))
104 X=X+1
105 GO TO 100
115 F=P,S=1
117 L=X
120 IF ABS(P)<E1 THEN 180
130 X=X-P
140 GO TO 100
180 C=1/(W*T)
190 B=1+A
200 GOSUB 600 !SUBROUTINE AT 600 SOLVES FOR AMPLITUDE WHEN GIVEN X
205 IF N=0 THEN 210 ELSE 240
210 H1=H
220 X=(2*N+1)*PI
230 GOSUB 600
235 PRINT "PVR =":20*LGT(H1/H):" DB"
237 NEXT N
240 IF H<=.707*H1 THEN 250 ELSE NEXT N
250 PRINT "AT ENVELOPE =":20*LGT(H/H1):" DB, X=":N:" HARMONIC OR":
260 PRINT X*7875/PI:" HZ"
270 PRINT
290 NEXT K,G,W
300 STOP ! MAIN PROGRAM ENDS HERE
600 COMPLEX Y
610 R=B-K*COS(X)
620 S=C*X+K*SIN(X)
630 Y=CMPLX (R,S)
640 Y1=ABS(Y)
650 H=A/Y1
655 IF X=L OR X=(2*N+1)+PI THEN 660 ELSE RETURN
660 IF N=0 THEN PRINT H;
670 RETURN
```

RESPONSE

```
10 PRINT "WHAT IS THE FILTER CUTOFF FREQUENCY W AND TIME DELAY T":
11 INPUT W, T1
15 PRINT "WHAT ARE THE GAINS K AND EG":
16 INPUT K, G
20 PRINT "DESCRIBE PICTURE BY SPECIFYING NUMBER OF TV LINES YOUR".
21 PRINT "PICTURE TAKES UP. THEN GIVE DATA LOWER AND UPPER LIMITS OF"
22 PRINT "EACH LINE WHERE PICTURE IS WHITE. LIST ALL LOWER LIMITS TOGET-"
23 PRINT "HER THEN UPPER LIMITS. HOW MANY LINES ARE THERE":
24 INPUT N1
25 PRINT
26 DIM L(1:N1), U(1:N1)
27 MAT READ L, U
28 PRINT
29 PRINT "N-TH LINE", "RESPONSE"
30 A=G*K
31 J=G*K/(1+G*K-K)
40 B=1+A
41 T2=635E-7-T1
49 FOR N2=1 TO N1
50 S=0
60 FOR N3=1 TO N2
65 N=N2-N3
70 X=L(N3)
80 GOSUB 300
90 I1=I
100 X=U(N3)+N*T2
110 GOSUB 300
120 I2=I
130 I3=I1-I2
140 S=S+I3
150 NEXT N3
160 PRINT N2, S/J
162 NEXT N2
170 PRINT
180 STOP ! MAIN PROGRAM ENDS HERE
300 IF X=0 THEN 310 ELSE 330
310 I=G*(K/B)+(N+1)
320 RETURN
330 R=EXP (-W*B*X)
331 IF R=0 THEN I=0 ELSE 335
332 RETURN
335 T=0
340 FOR M=0 TO N
350 IF (N-M)=0 THEN 360 ELSE 380
360 F$=1
370 GO TO 420
380 F$=1
```

510 DATA 1,1,1,1,1,1,1,1,1,1,0,0,0,0,0,0,0,0,0,0

3. Low Pass Filter in Delay Path

The following program was run as a commands file to solve for the effects of placing the low pass in the feedback path of the minor loop.

Line 10 specifies the loop parameters.

Lines 50 and 60 determine the frequency for which the amplitudes are solved.

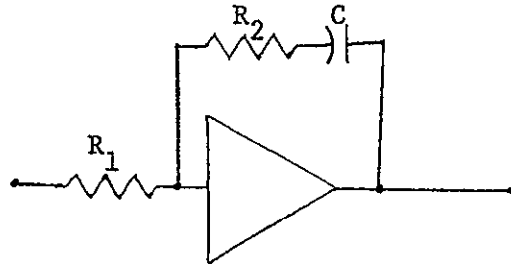
Here ω_0 is the 3-db point of the low pass in radians/sec.

All the other symbols are as defined previously.

```
SBASIC
10 K=.95,G=.68,WO=1E7,T=635E-7
20 PRINT " FREQ","CLF RESPONSE","PLL RESPONSE"
30 CMPLX S,V,H$
40 R=0
50 FOR X1=0 TO 3E6 STEP 5E5
60 FOR X2=0 TO 2E4 STEP 1E3
70 X=X1+X2
80 I=2*PI*X
90 S=CMPLX(R,I)
100 V=CMPLX(COS(I*T),-SIN(I*T))
110 H$=(S+WO)/(S+WO-K*WO*V)
120 Y=ABS(G*H$/(1+G*H$))
130 Y1=ABS(H$)
140 PRINT X,Y1,Y
150 NEXT X2,X1
RUN
QUIT
LØGØUT
```


4. Second Order Low Pass Phase Lock Loop

The response in a phase lock loop of a second order low pass is analyzed in the program LPF. The low pass is



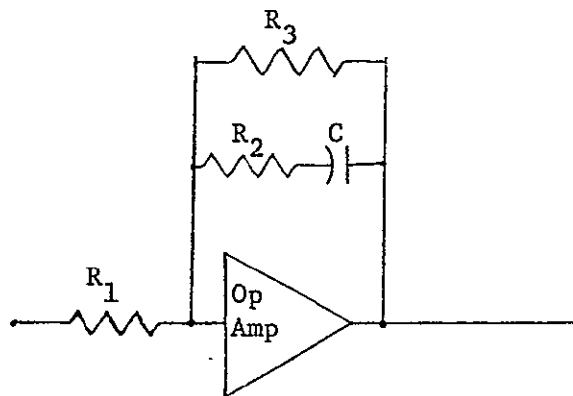
In line 10, $T1 = R_1 C$, $T2 = R_2 C$

$A = (\text{phase detector gain}) \times (\text{VCO gain}) \times (\text{Any other loop gain})$.

These values are related to the natural resonant frequency ω_n and

the damping ξ by $\omega_n = \sqrt{\frac{A}{T1}}$ and $\xi = \frac{T2}{2} \omega_n$.

The response is solved both at the output of the low pass and after a $1/s$ post PLL filtering (or a $1/s$ filtering during the modulation process). The program BREAK POINTS solved for the roots of K (total loop gain) when the second order low pass is realized by the following configuration.



The second part of this program solved for the break points of the denominator of the transfer function of this filter in the closed phase lock loop. The approximation used was that the operational amplifier gain is very large.

LPF

```
10 T1=.44E-2,T2=233E-7,Ø=0,A=1.6E7
20 CØMPLEX S,N,D
30 R=0
39 PRINT "FREQ. ","AMPLITUDE","(IN DB.)"
40 FØR X1=0 TØ 5 STEP .25
45 X=10+X1
50 I=2*PI*X
60 S=CMPLX(R,I)
65 IF Ø=0 THEN 70 ELSE 75
70 N=S*(S*T2+1)*A
71 GØ TØ 80
75 N=A*(S*T2+1)
80 D=S*S*T1+A*(S(T2+1)
90 Y=ABS(N/D)
100 PRINT X,Y,20*LGT(Y)
110 NEXT X1
120 PRINT
121 PRINT
125 IF Ø=1 THEN STØP
130 Ø=1
140 GØ TØ 30
```

BREAK POINTS

```
10 INPUT R1,R2,R3,C,K
20 A1=(R2/R1)+2
30 B1=-2*(2-(R2/R3))/(R1*C)
40 C1=1/(R3*C)+2
50 A2=1
60 B2=1/(R3*C)+K*R2/R1
70 C2=K/(R1*C)
80 PRINT "CØEF ØF K:",A1;B1;C1
90 PRINT "CØEF ØF S:",A2;B2;C2
100 A=A1,B=B1,C=C1
110 PRINT" ***ZERØS ØF K***"
120 GØSUB 500
130 A=A2,B=B2,C=C2
140 PRINT " ***ZERØS ØF S***"
150 GØSUB 500
155 PRINT " ØR";Y1/(2*PI);Y2/(2*PI):" HZ"
160 STØP
500 X=B+2-4*A*C
510 X1=SØRT(ABS(X))
520 IF X<0 THEN 570
530 Y1=(-B+X1)/(2*A)
540 Y2=(-B-X1)/(2*A)
550 PRINT "RØØTS AT";Y1;Y2
560 RETURN
570 PRINT "CØMPLEX RØØTS AT":-B/(2*A):" +-J":X1/(2*A)
580 PRINT "BREAK PØINTS AT":SØRT(B+2+X1+2)/(4*PI*A):" HZ"
590 STØP
```

5. MINMAX

One of the most useful programs from the standpoint of solving for the frequency of the comb. peak and valleys is a TYMSHARE* library program called MINMAX, which solves for the maximum, minimum, and zeros of any function specified by $y = f(x)$ in any given range of x . With some minor revisions, the library program is reproduced on the next page.

Variables used in the library program are:

D, F, F1, I, K, K1, M, Q, Q5, R, T, W, X, X1, Y, Y1

The function $y = f(x)$ must fit between lines 500 and 699 and use none of the above variables. The program listed solves for the peaks and valleys for the combline loop in parallel with the low pass loop.

(See following section).

* TYMSHARE, INC. 334 East Kelso Street, Inglewood, Calif. 90301

MINMAX

```
0 PRINT
2 PRINT "TYPE IN LOWER BOUND OF THE INTERVAL TO BE SEARCHED,"
4 PRINT "FOLLOWED BY A CARRIAGE RETURN":
6 INPUT I
8 PRINT
10 PRINT "TYPE IN UPPER BOUND":
12 INPUT F
14 PRINT
16 PRINT "TYPE IN NUMBER OF SIGNIFICANT FIGURES DESIRED":
18 INPUT Q
20 PRINT
22 PRINT "TYPE IN NUMBER OF INCREMENTS DESIRED FOR INTERVAL":
24 INPUT W
26 PRINT
110 PRINT
115 PRINT "POINT-TYPE", " F(X)", " X"
120 PRINT
130 K=(F-I)/W
135 K1=K
140 Q5=INT(0.4343*LØG(0.5*(ABS(I)+ABS(F))))
145 M=0.5*(10+(Q5-Q))
150 F1=F+K
155 R=0
160 X=I-K
165 T=2
500 T1=.25,T2=.22E-3,W0=1E7
505 G=.5,K5=.95,A=1E7,T0=635E-7
510 CØMPLEX S,V,F5,G$,L$
515 R1=0
520 I1=2*PI*X
525 S=CMPLX(R1,I1)
530 V=CMPLX(CØS(I1*T0),-SIN(I1*T0))
535 G$=G*K5*W0/(W0+S-K5*W0*V)
540 L$=A*(S*T2+1)/(S*T1)
545 F5=(S*G$+L$)/(S+(S*G$+L$))
550 Y=ABS(F5)
700 IF T<2 THEN 3000
800 IF T=3 THEN 1100
900 T=3
1000 GØ TØ 5000
1100 IF Y=Y1 THEN 2400
1200 IF Y<Y1 THEN 2000
1300 D=1
1400 IF Y1<0 THEN 1700
1500 T=-1
1600 GØ TØ 4100
1700 T=1
1800 GØ TØ 3100
2000 D=-1
2100 IF Y1>0 THEN 1700
2200 T=0
```

```

2300 GØ TØ 4500
2400 IF K1<M THEN 2800
2500 K1=K1/2
2600 X=X1+K1
2700 GØ TØ 5600
2800 PRINT
2801 PRINT "NØ CHANGE,..."
2900 STØP
3000 IF T<1 THEN 4000
3050 IF Y=0 THEN 6700
3100 IF D=-1 THEN 3500
3200 IF Y>0 THEN 6000
3300 IF ABS(Y)<ABS(Y1) THEN 5000
3400 T=-1
3450 GØ TØ 4100
3500 IF Y<0 THEN 6000
3600 IF ABS(Y)<ABS(Y1) THEN 5000
3700 T=0
3800 GØ TØ 4500
4000 IF R=1 THEN 8500
4050 IF T=0 THEN 4500
4100 IF Y>Y1 THEN 5000
4200 IF K1<M THEN 7000
4300 GØ TØ 4650
4500 IF Y<Y1 THEN 5000
4600 IF K1<M THEN 8000
4650 X1=X1-K1
4660 R=1
4700 GØ TØ 2500
5000 Y1=Y
5100 X1=X
5500 X=X+K1
5600 IF X<F1 THEN 500
5800 STØP
6000 IF K1<M THEN 6200
6100 GØ TØ 2500
6200 IF ABS(Y)<ABS(Y1) THEN 6700
6300 PRINT "  ZERO", " 0.",X1
6400 K1=K
6500 IF D=1 THEN 6600
6520 T=0
6560 GØ TØ 5000
6600 T=-1
6660 GØ TØ 5000
6700 Y1=Y
6800 X1=X
6900 GØ TØ 6300
7000 PRINT "    MAX",Y1,X1
7050 K1=K
7100 D=-1
7200 IF Y1<0 THEN 7500
7300 T=1
7400 GØ TØ 5000

```

```
7500 T=0
7600 GØ TØ 5000
8000 PRINT "MIN",Y1,X1
8050 K1=K
8100 D=1
8200 IF Y1<0 THEN 7300
8300 T=-1
8400 GØ TØ 5000
8500 R=0
8600 GØ TØ 5000
8999 PRINT
```

6. More Complex Loops

a) The low pass in parallel with the comb filter is solved using lines 500-550 of the previous MINMAX program with the following additions:

```

506 PRINT "INPUT FREQ","OUTPUT W/Ø 1/S","WITH 1/S"
516 FOR X5=1 TO 1E6 STEP 15000
517 FOR X4=0 TO 5E3 STEP 1E3
518 X=X5+X4
560 Y1=ABS(S*F5)
570 PRINT X,Y1,Y
600 NEXT X4,X5

```

T1 and T2 are the time constants in the low pass (as defined previously).

A = low pass PLL gain

W0 = rolloff of the low pass filter in the comb filter in rad/sec

G = CLF PLL open loop gain

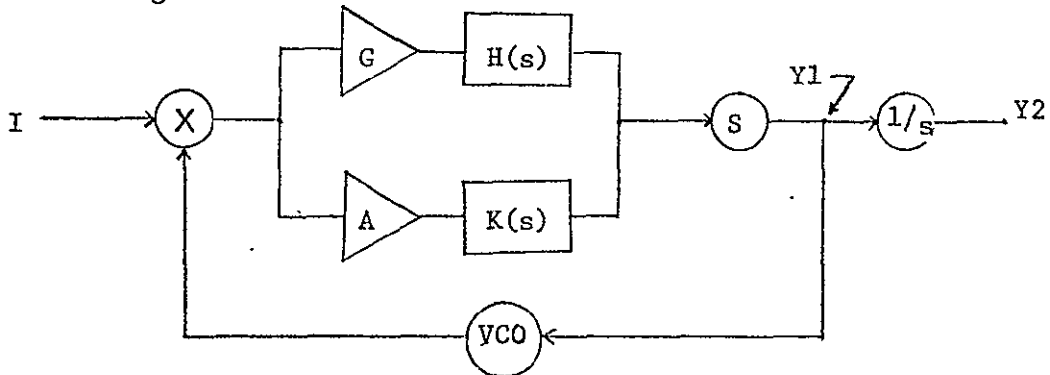
K = CLF open loop gain

T0 = CLF loop delay

On line 535, G\$ = CLF loop transfer function X (G)

On line 540, L\$ = low pass transfer function X (A)

b) The comb filter is parallel with a bandpass. (CLF-BPF) represents the following circuit:



where $K(S) = \frac{AS}{S^2 + S(A1) + (A1)(A2)}$ and $H(S)$ is the comb filter.

On line 10, values for the bandpass are defined.

On line 20, the comb filter parameters are specified.

"Return" and "transmitted" refer to Y2 and Y1 respectively.

Line 120 determines the frequencies of solution.

c) A bandpass with a 12 db/octave rise was tried, i.e. where

$$K(S) = \frac{AS^2}{[(S+A1)^2(S+A2)-S^2(A2)]}$$

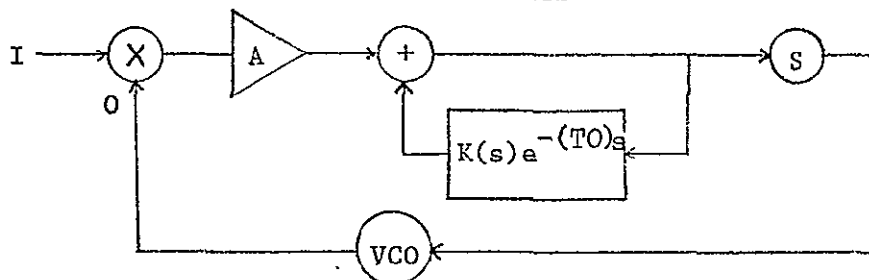
Only changes necessary to the above program are:

```
10 A1=1E7,A2,A=15E6
30 PRINT "FREQ","RETURN","CLF ONLY","BPF ONLY"
160 B$=A*(S+2)/((S+A1)+2*(S+A2)-A2*S+2)
200 Y1=ABS(B$/(1+B$)).
205 Y5=ABS(H$/(1+H$))
```

d) Additive-subtractive CLF (+ - CLF)

Fig. 3.16
See ~~100-7322-03-27~~ for block diagram. All variables used are consistent with terminology used previously.

e) Bandpass combline filter. BPCLF



$$\text{where } K(S) = \frac{(S)(K5)}{(S+A1)(S+A2)}$$

Lines 500 - 600 can be used with the MINMAX program. This program

also compares the response if the minor feedback path loop had no delay.

CLF - BPF

```
10 A1=12E6,A2=15.7E6,A=23E6
20 K=.95,G=.68,WO=8E6,T=635E-7
30 PRINT "INPUT FREQ.", " RETURN", "TRANSMITTED", " W/Ø BPF"
100 CØMPLEX S, V, F, B$, H$
110 R=0
120 FØR X=0 TØ 3E4 STEP 1E3
130 I=2*PI*X
140 S=CMPLX(R, I)
150 V=CMPLX(CØS(I*T), -SIN(I*T))
160 B$=A*S/(S+2+S*A1+A1*A2)
170 H$=G*K*WO/(S+WO-K*WO*V)
180 F=(B$+H$)/(1+B$+H$)
190 Y2=ABS(F)
200 Y1=ABS(S*F)
205 Y5=ABS(H$/(1+H$))
210 PRINT X, Y2, Y1, Y5
300 NEXT X
```

+ - CLF

```
10 K=.95,WO=2E7,T=31.75E-6,G=.5
20 CØMPLEX S, V, H1, H2, H, Z
30 R=0
35 PRINT "INPUT.", "CLF (ADD)", " (SUBTRACT)", " (TØGETHER)", " PLL"
40 FØR X=0 TO 5E4 STEP 1E3, 3E6 TØ 3.05E6 STEP 1E3
50 I=2*PI*X
60 S=CMPLX(R, I)
70 V=CMPLX(CØS(I*T), -SIN(I*T))
80 Z=K*WO*V
90 H1=K*WO/(S+WO-Z)
100 H2=K*WO/(S+WO+Z)
110 Y1=ABS(H1)
120 Y2=ABS(H2)
130 H=G*(H1+H2)
140 Y=ABS(H/(1+H))
150 Y3=ABS(H/G)
160 PRINT X, Y1, Y2, Y3, Y
170 NEXT X
```

BPCLF

```
500 TO=635E-7,K5=12E6,A=15
510 A1=6E6,A2=12E6
520 CØMPLEX S, V, H$, F5, G$
530 R1=0
540 I1=2*PI*X
550 S=CMPLX(R1, I1)
560 V=CMPLX(CØS(I1*TO), -SIN(I1*TO))
570 F5=(S+A1)*(S+A2)
580 H$=F5/(F5-K5*SV)
590 G$=F5/(F5-K5*S)
600 Y=ABS(A*H$/(1+A*H$))
610 Y5=ABS(A*G$/(1+A*G$))
50 PRINT "FREQ", "AMPL W/DELAY W/Ø DELAY"
100 FØR X=1E6 TØ 2E6 STEP 15750
700 PRINT S, Y, Y5
710 NEXT X
```